SOIL MORPHOLOGY, SEASONAL SATURATION, AND HYDROLOGY OF MAFIC LANDSCAPES IN THE PIEDMONT OF GEORGIA

by

KELLI E. COLEMAN

(Under the Direction of Larry T. West)

ABSTRACT

Whereas most soils in the Piedmont of Georgia have formed from saprolite from felsic gneiss or schist, approximately 10% of the soils have formed from saprolite of mafic/ultramafic rocks. Soils developed from these two contrasting parent materials have differing physical and chemical characteristics, thus making the spatial distribution of these soil types a critical factor when examining the interaction between soil and water. The study site had loamy colluvial upper soil horizons overlying residual soil horizons developed from chlorite schist. The objectives were: 1) evaluate depth and distribution of colluvial parent material over the site, and to evaluate the effect of the lithologic discontinuity on seasonal water tables; and 2) relate frequency and duration of saturation and reduction to redoximorphic features in mafic soils in Georgia. This study found that unique soil characteristics have a definite effect on the movement of water on the site. Landscape attributes and soil characteristics strongly affect the frequency and duration of saturation, and the type and abundance of redoximorphic features in mafic soils of Georgia.

INDEX WORDS: Redox potential, E_H, Mafic, Hydraulic Conductivity, K_s

SOIL MORPHOLOGY, SEASONAL SATURATION, AND HYDROLOGY OF MAFIC LANDSCAPES IN THE PIEDMONT OF GEORGIA

by

KELLI E. COLEMAN

B.S., The University of Georgia, 2005

A Thesis Submitted to the Graduate Faculty of The University of Georgia in Partial Fulfillment of The Requirements for the Degree

MASTER OF SCIENCE

ATHENS, GEORGIA

2008

SOIL MORPHOLOGY, SEASONAL SATURATION, AND HYDROLOGY OF MAFIC LANDSCAPES IN THE PIEDMONT OF GEORGIA

by

KELLI E. COLEMAN

Major Professor: Larry T. West

Committee: Miguel Cabrera
Dory Franklin

Electronic Version Approved:

Maureen Grasso
Dean of the Graduate School
The University of Georgia
May 2008

DEDICATION

To my parents – thanks for your infinite love, support, and belief in me.

ACKNOWLEDGEMENTS

I am blessed to have had so many wonderful people come into my life throughout the entirety of this project. A very special debt of thanks is owed to Vicki Hufstetler, the countless hours of hard work she spent in both the laboratory and field with me were an integral part of the research presented in this thesis. I would like to thank Ken Bradshaw for his hard work and dedication to my project when he had so many other things going on. I am also very thankful for the help and assistance of my research assistants Stephen Jones, Gus McCormick, and Frank Cochran. I would like to thank Beth Barton and Dave Butler for their guidance and support. I would also like to extend my gratitude to the staff at the Central Georgia Research and Education Center in Eatonton, Georgia. A very special thanks to Frank Newsome for the inestimable time he spent helping me and collecting the data that made this whole project possible. Thanks also to Chad Westmoreland for all the help and keeping the cows away, Lynn for taking my calls, and Vaughn Calvert for checking on me.

My academic career has been influenced by many people, but without a few, I would not be where I am today. I would like to especially thank, Dr. Gene Cravey because without him I may have never made it out of Middle Georgia College. A special debt of thanks is owed to Dr. Larry West, who will always be my inspiration and by example, makes me want to strive for greatness. I would also like to thank Dr. Dory Franklin for believing in me, encouraging me, and empowering me to take control of any situation. Also, a special thanks to Dr. Miguel Cabrera who provided me with constant guidance and support. Finally, I would like to thank Dr. Bill

Miller, who was my first soil science professor and who helped me find my voice in the classroom by providing me with my first teaching experience.

I am forever indebted to John Bryant, the best officemate and friend a girl could want, for the many, many times he spent at my site in the pouring rain, the one hundred pedons he helped dig and describe, and his never ending support that helped me make it though. I am also thankful for the special friend God provided me in Catie Young, who spent too many hours, nights, and weekends to count hanging out with me while I worked on my thesis. Thanks also to my wonderful friends: Blake and Lindsey Underwood who kept me nourished and sane; James Greco who let me take advantage of his brute strength and kept me smiling; Vivienne Sturgill who was always a pillar of strength, love, and support when I needed it most; and Rita McCranie who never let me lose touch with who I am. I also owe a debt of gratitude too large to ever be repaid to my best friends Annie Vaughn and Robert Collins, who have always supported even the zaniest of my ideas; without their constant encouragement and support I would have never made it this far.

Most importantly, my sincerest gratitude goes to my entire family, who always provide endless love and support no matter what I set my mind to do. I want to especially thank my siblings Carrie, Clint, and Kevin for encouraging me to follow my dreams, for keeping me focused on my goals, and for helping me obtain them. Also, special thanks to my brother Clint for helping me survey my site. To my parents, Hugh and Cathy Coleman, who this thesis is dedicated to, thank you for your love and the sacrifices you have made for me since the day I was born. Thank you also for always believing in me and encouraging me to follow my heart.

Finally, I would like to thank my dear friend Brandon Woods, who loved me unconditionally, who never gave up on me, and who I will always carry in my heart.

TABLE OF CONTENTS

Page

LIST OF TABLES

Page

LIST OF FIGURES

Page

Chapter One

Introduction

The Piedmont in the southern United States has an exposed surface area of 1200 km by 200 km wide running parallel with the Atlantic Coast (Mayne et al., 2000). Both felsic and mafic rocks are found throughout the Piedmont. Although most soils in the Piedmont of Georgia have formed from saprolite of weathered felsic gneiss or schist, there are scattered areas of soils formed from saprolite of weathered mafic rocks (Hamilton–Wood et al., 2002). Mafic rocks are high in ferromagnesian minerals such as pyroxenes, amphiboles, biotite, olivine and hornblende (American Geological Institute, 1976) and soils formed from mafic parent materials have a higher pH, a higher base saturation, and a greater abundance of expandable (2:1) clay minerals than soils formed from felsic parent materials (Ogg and Smith, 1993; Schroeder et al., 2000; Hamilton–Wood et al., 2002). Because of their unique characteristics, mafic parent materials play an important role in determining soil properties and the interaction between soil and water. Understanding the characteristics of mafic-derived soils can help develop more efficient and accurate methods of evaluating soil behavior and best use and management practices.

One of the most commonly studied hydrologic landscape features is the depth of the seasonal water table. A water table is defined as contact point between the zone of saturation (all pores are filled with water) and aeration in an unconfined aquifer (pores contain both water and air). Water tables have also been defined as the depth of water in an unlined bore hole. Water

tables can naturally fluctuate greatly from year to year and throughout the year when measured in the same soil series as well as between soils of different series (Zoebeck and Ritchie, 1984).

More and more, land–use regulations require evaluating seasonal saturation frequency and duration (He et al., 2002). For instance, both Georgia legislative codes 290–5–26–.07 and 290–5–25–.04 state that the installation of on–site sewage systems and land disposal sites, respectively, must be based on soil characteristics as well as groundwater and seasonal saturation determinations (Georgia Secretary of State, 2005). The concurrence of natural and man–induced fluctuations makes it hard to accurately determine the depth and duration of season water tables. Additionally, measuring water tables for the period needed to reflect seasonal and annual fluctuations makes direct monitoring unfeasible in many cases. Thus, morphological indicators of seasonal saturation of soil horizons are vital in evaluating soil suitability for many cases. Presently, soil color is one of the most common soil morphological indicators of seasonal water tables within soil profiles. Soil color patterns that include Munsell chroma ≤ 2, either as mottles or the matrix color, or gray colors can commonly predict where seasonal saturation occurs in soils (He et al., 2003). Extended seasonal saturation of a soil results in the reduction of manganese and iron found in high concentrations in mafic-derived soils, which cause development of redoximorphic features in a horizon. Redox depletions (gray colors) form in areas of the soil where Fe and Mn have been lost and redox concentrations form in areas of the soil when Fe and Mn have concentrated. Saturation alone, however, will not form these redoximorphic features; facultative anaerobic bacteria and organic substrates must also be present for Fe and Mn reduction to occur.

Objectives

Although several studies have quantitatively related presence of redoximorphic features to depth of seasonal saturation (Simonson and Boersma, 1972; Guthrie and Hajek, 1979; Franzmeier et al., 1983; Vepraskas and Wilding, 1983; Pickering and Veneman, 1984; Zobeck and Richie, 1984; Elless et al., 1996; He et al., 2003), few studies have attempted to relate specific redoximorphic features with depth and duration of seasonal saturation, and little data are available for soils in the Piedmont, especially those formed from mafic parent materials. Thus, the objectives of this study are:

1. Relate the frequency and duration of saturation and reduction to type and abundance of redoximorphic features in mafic soils
2. Establish a relationship among the subsurface perching of water, soil parent material, and landscape attributes for a landscape with soils developed from mafic rocks.

Chapter Two

Literature Review

Soil Morphology

Soil color, physical structure, chemical properties, and mineralogical composition define the morphology of soils. Of these, color is the most obvious and revealing soil characteristic. Soil color can be used to detect the Fe and Mn minerals present in the soil, the organic matter content, the stage of soil development, and the depth and duration of seasonal saturation of the soil. Soil color is typically dominated by the color of coatings found on the soil material. Organic matter is brown to black and commonly cause the horizons near the soil surface to be darker–colored than the underlying horizons. In the subsurface horizons, where organic matter is limited, Fe oxide coatings have a more pronounced effect on the soil color (Rabenhorst and Parikh, 2000). Furthermore, an increase in chroma is generally interpreted as an increase in Fe oxides (Scheinost and Schwertmann, 1999). The color reflected in these horizons depends on the type of Fe and Mn oxides present. Mn oxides cause the soil to be dark brown or black, whereas Fe oxides cause soil to be a range of colors including variations of yellow, brown, orange or red. The lack of color can also provide insight to the soil environment. Redoximorphic features such as a matrix with Munsell chroma ≤ 2 and Fe–concentration or depletion areas have become commonly used indicators of seasonal saturation in soils (Jacobs et al., 2002). The seasonal saturation of soils causes the Fe and Mn oxides to become reduced in the soil solution, thereby allowing these elements to be translocated within the soil leaving behind grayish uncoated soil

minerals. These low chroma colors increase in abundance the longer the soil is saturated and chemically reduced (Vepraskas, 1999).

Water serves as one of the primary energy sources for landscape processes, such as erosion, distribution of soluble and mobile compounds, colonization of vegetation, and sequestration of organic carbon (Reuter and Bell, 2001). The movement of water within a soil is dictated by its physical properties, primarily texture and structure. Soil structure is an important soil property to be evaluated because it mediates many biological and physical processes in soils; for instance, it determines the porosity and infiltration of water into soils (Six et al., 2000). Poor soil structure is a major limitation to infiltration, redistribution and storage of water in a soil profile (Connolly, 1998).

Soil properties such as texture, bulk density, and water retention play important roles in soil behavior. Soil texture is one of the most important soil characteristics; it influences many other properties significant to land use and management (Brown, 2003). Surface soil texture, in particular, can control many important ecological, hydrological, and geomorphic processes (Scull et al., 2005). Bulk density can easily be altered by soil disturbing activities, i.e., agricultural practices and urban development. In turn, physical, chemical and biological properties in the soil can be altered by changes in the compactness state of the soil (Håkansson et al., 1988). Because the pores within the soil can contain water, altering the bulk density of the soil can have adverse effects on the soil–water relationship.

Seasonal Saturation

Water tables play an important role in water and solute transport at the landscape scale (Tassinari et al., 2002). The depth to the seasonal high water table is an important factor in many

land use decisions, including the construction of buildings and roads, surface applications of waste, and the use of onsite waste disposal systems (Morgan and Stolt, 2004). Numerous studies have shown a correlation between seasonal water table depths and soil morphology (Simonson and Boersma, 1972; Franzmeier et al., 1983; Tassinari et al., 2002). More specifically, these studies and others explain that redoximorphic features are correlated to the presence and duration seasonal saturation. The presence of redox concentrations is often correlated with the depth of the seasonal high water table, whereas redox depletions often indicate the duration of the seasonal high water table (Jacobs et al., 2002). The depth to seasonal saturation can be estimated by the presence of low Munsell chroma colors at sites where the natural soil hydrology has not been altered (Hayes and Vepraskas, 2000). Consequently, land–disturbing activities alter the relationship between soil morphology and seasonal saturation, making the typical methods of predicting seasonal saturation unreliable. Extracting ground water for a variety of purposes, whether agricultural or not, profoundly changes the natural water–table levels (Bouma et al., 1980). Water tables can also naturally fluctuate greatly from year to year and throughout the year when measured in the same soil series as well as between soil of different series (Zoebeck and Ritchie, 1984). The concurrence of natural and man–induced fluctuations makes it hard to determine the depth and duration of season water tables.

Redox Potential

Redoximorphic features have been used for more than three decades to identify hydrologic and soil wetness conditions; however, the formation of redoximorphic features is often site–specific and not always directly related to the period of saturation (Fiedler and Sommer, 2004). Redox potential measures the soils ability to oxidize or reduce substances.

Gotoh and Patrick (1974) conducted a study on different forms of Fe in a waterlogged soil over a wide range of closely controlled redox potential and pH conditions. They concluded that increases in water soluble and exchangeable Fe were favored by a decrease in both redox potential and pH. The critical redox potentials for Fe reduction and consequent dissolution was between +300 and +100 mv at pH 6 and 7, and –100 mv at pH 8, while at pH 5 appreciable reduction occurred at +300 mv. Redox potential can be measured in the field with a platinum electrode, voltmeter, and reference electrode (Vepraskas, 2002). Many studies show this method as an acceptable means of assessing redox status (Gao et al., 2002; Jenkinson et al., 2002; Fiedler and Sommer, 2004).

The major advantage of the Pt electrode method to measure redox potential is that it is still the most practical and convenient method for most cases. Several disadvantages of the Pt electrode method include: it can be impractical to measure the redox potential in wetlands at all times because of flooding, weather conditions, and sample location; it can be a highly fluctuating value and sensitive to water pressure in the soil; and it can not conveniently record fluctuations in redox conditions on a longer time scale because of changes in flooding, weather conditions, and vegetation type (Vorenhout et al., 2004).

Hydrology

Soil hydrology predicts the location of wet soils in a landscape, how water and sediments move on soil surfaces, and how water and dissolved nutrients move through soils (Jenkinson et al., 2002). Soil hydrology is also the behavior of water in the soil in relation to the earth's atmosphere, surface, and subsurface. Soil hydrology is crucial in identifying wetlands and maintaining the water balance for agricultural productivity. Morphological features can help to

interpret the soil hydrology in landscapes, and the hydraulic conductivity is generally expressed as a measure of a soils capability to transmit water. Saturated hydraulic conductivity can be estimated indirectly from easily measured soil texture data (Rawls et al., 1998). A soil with a coarser texture tends to have higher hydraulic conductivity, allowing it to transmit water more rapidly than a finer textured soil with a lower hydraulic conductivity. Therefore, hydraulic conductivity can partly determine the suitability of a soil for various land uses. For example, a soil with a high hydraulic conductivity, i.e., a coarse sandy soil, would be unsuitable for an onsite drain field because the water would drain too quickly through the soil. Conversely, a soil with a low hydraulic conductivity would also be unsuitable because the water would infiltrate the soil too slowly, causing water to pond at the surface.

Subsurface flow is an important component of the hydrologic cycle and its contribution to stream flow has been the subject of many studies (Shirmohammadi et al., 1984). Piezometers, small diameter wells, aid in the determination of groundwater locations. When placed within a study area, piezometers provide information on the subsurface response to precipitation (Wigmosta and Burges, 1997).

Digital Elevation Model

Soil–landscape modeling provides a means for analyzing and predicting spatial distribution of soil properties (Thompson et al., 2006). Methods for creating a soil–landscape model normally involve (i) characterization of the local physiographic domain through analysis of digital elevation model (DEM) data, (ii) collection of georeferenced soil samples and compiling desired soil property data, and (iii) development of explicit, quantitative, and usually simple empirical models (McSweeney et al., 1994). The term Digital elevation model (DEM) is

widely used in North America to refer to data sets containing regularly spaced elevations in the form of a lattice or square grid (Lo and Yeung, 2002). As with many other forms of raster-based geographic data, DEMs are typically stored as text (ASCII, Dbase IV, etc.) files, making DEM data relatively simple to handle. However, an excessive number of elevation points are needed in order to represent the terrain surface to a specific level of accuracy (Lo and Yeung, 2002), making these files somewhat bulky when working with large areas. Depending on the location and size of the area of interest, DEM data can be obtained in a variety of methods, such as ground survey, photogrammetry, or cartography. Generally, ground survey methods have very high accuracy but are limited to specific sites that typically tend to be small. Conversely, cartographic methods (existing maps) have lower accuracy and nationwide coverage at small scales. The photogrammetric methods have high accuracy if from spot heights or low accuracy if from contours and can cover large-area projects (Lo and Yeung, 2002). Also, many studies have shown the effect of DEM resolution on the spatial pattern of terrain characteristics (Smith et al., 2006). Thus, the proper acquisition of DEM data is crucial to the quality of end product of a study relying on DEM for spatial interpretation and analysis.

DEMs must be obtained from external sources or generated from collected field data. Hydrologic predictions such as runoff peaks, timing, and volume are affected by the resolution of the DEM (Kenward et al., 2000). A finer resolution DEM best matches the observed runoff data (Cochrane and Flanagan, 2004).

Mafic Landscapes

Mafic Landscapes are found scattered throughout the Piedmont region of Georgia (Figure 2.1). Soils derived from mafic parent materials have thinner sola, higher pH, higher base

saturation, and greater abundance of expandable (2:1) clay minerals than saprolitic soils developed from other parent materials (Hamilton–Wood, et al., 2002). Common mafic rocks include basalt (fine-grained), dolerite (medium-grained), gabbro (coarse-grained) and metamorphic derivatives from them (Rice et al., 1985). Pyroxenes, olivines, chlorite, and biotite are the predominant ferromagnesian primary minerals in gabbro and metagabbro (Glentworth, 1944; Craig and Loughnan, 1964; Basham, 1974; DeConinch et al., 1977, Rice et al, 1985). The secondary weathering products of biotite are vermiculite, hydrobiotite, or kaolinite (Rice et al. 1985). Smectite, iron oxides and hydroxides, and kaolinite are weathering products of amphiboles, pyroxenes, and olivine (Butler, 1953; Basham, 1974, Rice et al., 1985). Soils formed over basic parent rocks commonly contain 2:1 clays that expand and contribute to slow vertical percolation of water (Buol and Weed, 1991). These highly expansive 2:1 clays can pose a problem during development and urbanization. Thomas et al. (2000) found that a correlation between shrink–swell potential and parent material along with drainage class could be extrapolated; poorly drained, mafic parent material soils posed a very high shrink–swell risk while well drained, mafic parent material soils posed a moderate shrink–swell risk.

Piedmont Region

Georgia encompasses five geophysical regions: the Ridge and Valley, the Blue Ridge, the Coastal Plain, the Flatwoods, and the Piedmont. Comprising approximately 30% of the land in Georgia, the Piedmont covers ± 4,606.139 ha (Turner, 1987) or ± 46,061.390 km^2 and is an upland sloping region with gently rolling hills. Metamorphic rocks, such as schists, amphibolites, and gneisses, and igneous rocks such as granites define the geological makeup of the Piedmont. Being Georgia's most densely populated region, most important cities and farms

are located in the Piedmont (Britannica, 2005a). The Piedmont region is not exclusively found in Georgia; it stretches some 1200 km by 200 km wide (Mayne et al., 2000) from New Jersey in the north to Alabama in the south (Britannica, 2005b). The topological, geological, and physiological features of the Piedmont region in Georgia are similar to those features found in the other states' Piedmont regions; thus the results from studies in Georgia can be interpolated to fit these other regions.

Land–use Regulations

Many watersheds in the Piedmont have been impacted by extensive pasture-based beef production, forestry, and rapid urban development (Fisher et al., 2000). As land development increases, stricter land–use regulations are necessary to safeguard water sources. Specifically, many rules and regulations regarding the installation of on–site sewage systems have been adopted by the Georgia Legislature. According to the Georgia Legislative code 290–5–26–.07, "No absorption field shall be installed in areas where groundwater, soil characteristics or adverse geological formation may interfere with the absorption or effective treatment of sewage effluent" (Georgia Secretary of State, 2005). Regulations emphasize horizontal separations between drainfields and water supplies. Georgia Legislative code 290–5–26–.07 also states "No absorption field will be constructed less than one hundred feet (100') from existing or proposed wells, springs, or sinkholes (Georgia Secretary of State, 2005). Furthermore, Georgia Legislature set forth similar distance restrictions for land disposal of septage (code 290–5–25, Georgia Secretary of State, 2005). Overall, the basis for many land–use applications in Georgia depends on soil characteristics as well as groundwater and seasonal saturation determinations.

References

Borah, D.K., and M. Bera. 2003. Watershed–scale hydrologic and nonpoint–source pollution models: Review of mathematical bases. Am. Soc. Agric. Eng. 46:1553–1566.

Borah, D.K., M. Bera, and R. Xia. 2004. Storm event flow and sediment simulation in agricultural watersheds using DWSM. Am. Soc. Agric. Eng. 47:1539–1559.

Bouma, J., P.M. de Laat, A.F. van Holst, and T.J. van de Nes. 1980. Predicting the effects of changing water–table levels and associated soil moisture regimes for soil survey interpretations. Soil Sci. Soc. Am. J. 44:797–802.

Britannica Student Encyclopedia. 2005a. Georgia [Online]. Available at http://www.britannica.com/ebi/article–201486/Georgia. (accessed 1 Dec. 2005; verified 24 Feb. 2008) Encyclopedia Britannica Premium Service.

Britannica Student Encyclopedia. 2005b. Piedmont [Online]. Available at http://www.britannica.com/ebi/article–9059956. (accessed 1 Dec. 2005; verified 24 Feb. 2008) Encyclopedia Britannica Premium Service.

Brown, R.B. 2003. Fact Sheet SL–29: Soil texture [Online]. Available at http://edis.ifas.ufl.edu/pdffiles/SS/SS16900.pdf. (assessed 3 Oct. 2005; verified 24 Feb. 2008). Soil and Water Science Department, Florida Cooperative Extension Service, Institute of Food and Agricultural Sciences, University of Florida.

Buol, S.W., and S.B. Weed. 1991. Saprolite–soil transformations in the Piedmont and mountains of North Carolina. Geoderma 51:15–28.

Cochrane, T.A., and D.C. Flanagan. 2004. Effect of DEM resolutions in the runoff and soil loss predictions of the WEPP watershed model. Am. Soc. Agric. Eng. 48:109–120.

Connolly, R.D. 1998. Modeling effects of soil structure on the water balance of soil–crop systems: A review. Soil Tillage Res. 48:1–19.

Feddes, R.A., P. Kabat, P.T. Van Bakel, J.B. Bronswijk, and J. Halbersma. 1988. Modeling soil water dynamics in the unsaturated zone – state of the art. J. Hydrol. 100:69–111.

Fiedler, S., and M. Sommer. 2004. Water and redox conditions in wetland soils – their influence on pedogenic oxides and morphology. Soil Sci. Soc. Am. J. 68:326–335.

Fisher, D.S., J.L. Steiner, D.M. Endale, J.A. Stuedemann, H.H. Schomberg, A.J. Franzluebbers, and S.R.Wilkinson. 2000. The relationship of land use practices to surface water quality in the Upper Oconee Watershed of Georgia. For. Ecol. Manage. 128:39–48.

Franzmeier, J.E., Yahner, G.C.Steinhardt, and H.R. Sinclair, Jr. 1983. Color patterns and water table levels in some Indiana soils. Soil Sci. Soc. Am. J. 47:1196–1202.

Gao, S., K.K. Tanji, S.C. Scardaci, and A.T. Chow. 2002. Comparison of redox indicators in a paddy soil during rice–growing season. Soil Sci. Soc. Am. J. 66:805–817.

Georgia Secretary of State. 2005. Rules and regulations of the State of Georgia [Online]. Available at http://www.sos.state.ga.us/rules_regs.htm. (accessed 17 Oct. 2005; verified 24 Feb. 2008). Georgia Secretary of State.

Gotoh, S., and W.H. Patrick. 1974. Transformation of iron in a waterlogged soil as influenced by redox potential and pH. Soil Sci. Soc. Am. Pro. 38:66–71.

Hamilton–Wood, D.A., L.T. West, and P.A. Schroeder. 2002. Weathering sequences of contrasting mafic and felsic parent materials in the Georgia Piedmont, US. Proc. 17th World Cong. Soil Sci., Aug. 14–21, 2002., Bangkok, Thailand. p. 871–1 – 875–9.

Håkansson, I., W.B. Voorhees, and H. Riley. 1988. Vehicle and wheel factors influencing soil compaction and crop response in different traffic regimes. Soil Tillage Res. 19: 271–278.

Hayes, W.A., Jr., and M.J. Vepraskas. 2000. Morphological changes in soil produced when hydrology is altered by ditching. Soil Sci. Soc. Am. J. 64:1893–1904.

He, X., M.J. Vepraskas, R.W. Skaggs, and D.L. Lindbo. 2002. Adapting a drainage model to simulate water table levels in Coastal Plain soils. Soil Sci. Soc. Am. J. 66:1722–1731.

He, X., M.J. Vepraskas, D.L. Lindbo, and R.W. Skaggs. 2003. A method to predict soil saturation frequency and duration from soil color. Soil Sci. Soc. Am. J. 67:961–969.

Jacobs, P.M., L.T. West, and J.N. Shaw. 2002. Redoximorphic features as indicators of seasonal saturation, Lowndes County, Georgia. Soil Sci. Soc. Am. J. 66:315–323.

Jenkinson, B.J., D.P. Franzmeier, and W.C. Lynn. 2002. Soil hydrology on an end moraine and a dissected till plain in west–central Indiana. Soil Sci. Soc. Am. J. 66:1367–1376.

Kao, J. 1996. Neutral net for determining DEM–based model drainage patterns. J. Irrig. Drain. Eng. 122:112–121.

Kenward, T., D. P. Lettenmaier, E. F. Wood, and E. Fielding. 2000. Effects of digital elevation model accuracy on hydrologic predictions. Remote Sens. Environ. 74:432–444.

Mayne, P.W., D. Brown, J. Vinson, J.A. Schneider, and K.A. Finke. 2000. Site characterization of Piedmont residual soils at the NGES, Opelika, Alabama. Am. Soc. Civil Eng. Geotechnical Spec. Publ. 93:160–185.

Milly, P. C. 1994. Climate, soil water storage, and the average annual water balance. Water Resour. Res. 30:2143–2156.

Morgan, C.P., and M.H. Stolt. 2004. A comparison of several approaches to monitor water–table fluctuations. Soil Sci. Soc. Am. J. 68:562–566.

Ogg, C.M., and B.R. Smith. 1993. Mineral transformation in Carolina Blue Ridge–Piedmont soils weathered from ultramafic rocks. Soil Sci. Soc. Am. J. 57:461–472.

Padmanabhamurty, B., C.V. Satyanarayana Rao, and J. Dakshinamurti. 1970. On the water balances of some Indian stations. J. Hydrol. 11:169–184.

Rabenhorst, M.C., and S. Parikh. 2000. Propensity of soils to develop redoximorphic color changes. Soil Sci. Soc. Am. J. 64:1904–1910.

Rao, N.H. 1987. Field test of a simple soil water balance model for irrigated areas. J. Hydrol. 91:179–186.

Rao, N.H. 1998. Grouping water storage properties of Indian soils for soil water balance model applications. Agric. Water Manage. 36: 99–109.

Rawls, W.J., D. Gimenez, and R. Grossman. 1998. Use of soil texture, bulk density, and slope of the water retention curve to predict saturated hydraulic conductivity. Am. Soc. of Agric. Biol. Eng. 41: 983–988.

Reuter, R.J., and J.C. Bell. 2001. Soils and hydrology of a wet–sandy catena in east–central Minnesota. Soil Sci. Soc. Am. J. 65:1559–1569.

Scheinost, A.C., and U. Schwertmann. 1999. Color identification of iron oxides and hydroxysulfates. Soil Sci. Soc. Am. J. 63:1463–1471.

Schroeder, P.A., N.D. Melear, L.T. West, and D.A. Hamilton. 2000. Meta–gabbro weathering in the Georgia Piedmont, USA: Implications for global silicate weathering rates. Chem. Geol. 163:235–245.

Scull, P., G. Okin, O.A. Chadwick, and J. Franklin. 2005. A comparison of methods to predict soil surface texture in an alluvial basin. Prof. Geogr. 57:423–437.

Shirmohammadi, A., W.G. Knisel, and J.M. Sheridan. 1984. An approximate method for partitioning daily streamflow data. J. Hydrol. 74:335–354.

Simonson, G.H., and L. Boersma. 1972. Soil morphology and water table relations. II. Correlation between annual water table fluctuations and profile features. Soil Sci. Soc. Am. Proc. 36:649–653.

Six, J., E.T. Elliott, and K. Paustian. 2000. Soil structure and soil organic matter II: A normalized stability index and the effect of mineralogy. Soil Sci. Soc. Am. J. 64:1042–1049.

Tassinari, C., P. Lagacherie, R. Bouzigues, and J.P. Legros. 2002. Estimating soil water saturation from morphological soil indicators in a pedologically contrasted Mediterranean region. Geoderma 108:225–235.

Thomas, P.J., J.C. Baker, and L.W. Zelazny. 2000. An expansive soil index for predicting shrink–swell potential. Soil Sci. Soc. Am. J. 64:268–274.

Turner, M.G. 1987. Spatial simulation of landscape changes in Georgia: A comparison of 3 transitional models. Landscape Ecol. 1:29–36.

Van Bochove, E., S. Beauchemin, and G. Thériault. 2002. Continuous multiple measurement of soil redox potential using platinum microelectrodes. Soil Sci. Soc. Am. J. 66:1813–1820.

Vepraskas, M.J. 1999. Redoximorphic features for identifying aquic conditions. Tech. Bull. 301. NC Agric. Exp. Stn., Raleigh, NC.

Vepraskas, M.J. 2002. Redox potential measurements [Online]. Available at http://www.soil.ncsu.edu/wetlands/wetlandsoils/RedoxWriteup.pdf (accessed 9 Sept. 2005; verified 24 Feb. 2008). Dept. of Soil Science at North Carolina State University.

Vorenhout, M., H.G. van der Geest, D. van Marum, K. Wattel, and H.P. Eijsackers. 2004. Automated and continuous redox potential measurements in soil. J. Environ. Qual. 33:1562–1567.

Wigmosta, M.S., and S.J. Burges. 1997. An adaptive modeling and monitoring approach to describe the hydrologic behavior of small catchments. J. Hydrol. 202:48–77.

Zobeck, T.M., and A. Richie, Jr. 1984. Analysis of long–term water table depth records from a hydrosequence of soils in central Ohio. Soil Sci. Soc. Am. J. 48:119–125.

Fig. 2.1 Parent Material Distribution in Georgia; mafic parent materials are concentrated mainly in the Piedmont region.

Chapter Three

Evaluating Soil Saturation Frequency and Duration in Mafic Soils of Georgia

Presently, soil color is one of the most common morphological indicators of seasonal saturation within soils. More specifically, prior studies show that soil color patterns with low Munsell chroma (≤ 2) or gray colors are commonly used to predict the occurrence to seasonal saturation (Daniels et al., 1971, Bouma, 1983, Pickering and Veneman, 1984; Buol and Rebertus, 1988; Veneman et al., 1998, He et al., 2003). Extended seasonal saturation of a soil results in the reduction of manganese and iron found in high concentrations in mafic derived soils, which cause development of redoximorphic features in a horizon. Faulkner and Patrick (1992) concluded that redox features were not always directly related to the period of saturation but were connected through complex interacting soil forming processes dominated by redox chemistry. Saturation alone, however, will not form these redoximorphic features, facultative anaerobic bacteria and organic substrates must also be present for Fe and Mn reduction to occur. The duration of saturation, the amount of Fe and Mn present, the soil temperature, the landscape position, and the nature of flooding events are also variables that control the redox reactions of soils (Faulkner and Patrick, 1992).

The three common types of redoximorphic features studied in the soil are redox concentrations (accumulations of Fe/Mn), redox depletions (zones of low chroma (≤2) where Fe/Mn have been removed, and reduced matrices (horizon matrices that have low chroma (≤2) in situ, but undergo changes in hue or chroma when exposed to air) (Soil Survey Staff, 1999). Of these types, redox concentrations and depletions are of particular interest at our site. Redox

concentrations form when Fe and Mn are oxidized while redox depletions form when Fe and Mn become reduced. Redox concentrations can be nodules or soft masses (concentrations). The form in which a redox concentration is found indicates the time frame in which it was formed; more specifically, the boundaries of nodules and concentrations may be diffuse (faded out) or sharp. The sharp boundaries found on nodules indicate that they were moved and are considered relict, meaning that, unlike nodules with diffuse boundaries, they were not formed under the current hydrologic conditions of the soil. Redox depletions are formed by the reduction and removal of Fe and Mn from the soil. The soil must become reduced not just saturated for redox depletions to form, meaning that saturation must last long enough for anoxic conditions to prevail. Differing lengths of saturation cause redox depletions to form in an array of colors; however, those with low chroma (≤ 2) are of particular interest because they are the most often used to determine seasonal saturation of soils. Although redox depletions are useful in determining if a soil has been saturated, they alone can not be used to interpret the frequency and duration of saturation.

Redox potential is a commonly used method in the quantification of seasonal saturation. By measuring the redox potential, it is possible to determine if the soil is aerobic or anaerobic, or if chemical compounds such as Fe oxides have been chemically reduced or are present in their oxidized forms (Vepraskas, 2002). The assessment of soil redox potential is particularly useful for characterizing the onset of reducing conditions in a soil caused by a lack of oxygen (Van Bochove et al., 2002). A lag time between saturation of a horizon and the threshold redox potential for Fe and Mn reduction occurs because Fe and Mn reduction is a microbial-mediated process. For soils in the southeastern USA, this lag has been reported to be 14 to 30 days and to vary with organic C content as related to depth of the horizon (He et al., 2003). Thus, short

periods of saturation (<14 days) would not be expected to produce redoximorphic features in a horizon.

Jenkinson and Franzmeier (2006) introduced the use of Indicator of Reduction In Soil (IRIS) devices that consist of PVC tubes painted with ferrihydrite (FH) paint as an alternative method of monitoring and quantifying the Fe reduction in soils. The authors conducted laboratory and field studies concluding that IRIS tubes or devices have the potential to help identify hydric soils and the potential for studying redox processes in soils. A significant correlation was found between removal of FH from the IRIS and depth to water table in saturated soils in Indiana, North Dakota, and Minnesota. The FH coating remained undisturbed on the tubes in locations where the soil was unsaturated. Castenson and Rabenhorst (2006) point out that iron paint was removed or translocated in soluble form (Fe^{2+}) from the tube surface due to reducing conditions in the soil. They tested the IRIS tubes to evaluate their suitability for identifying reduced conditions in the Mid-Atlantic region. Castenson and Rabenhorst (2006) concluded that IRIS tubes appear to be useful in the identification of reduced soil conditions, showing that a relationship between the soil redox potential and the amount of FH paint removed from the tubes exists. No studies on the use of IRIS tubes in the Southeastern US were found at the time of this study.

The objective of this study is to relate the frequency and duration of saturation and reduction to the type and abundance of redox features in mafic soils. IRIS tubes were used in conjunction with redox potential measurements, soil analysis, and water table monitoring for this study.

Materials and Methods

Site Selection

The project site is located at the University of Georgia Central Research and Education Center in Putnam County, approximately 15 km northwest of Eatonton, Georgia (Fig 3.1). The site consists of a stream valley and encompasses the total width of the valley (Fig 3.2). Area of the site is 40.5 ha, and current land use is pasture. The site was chosen because previous studies suggested that stream flow varied along the length of the stream dissecting the watershed segment (Matthews, 2003). Soils at the site were fine and fine-loamy, mixed, thermic, Typic Halpudalfs; Typic Paleudalfs; Oxyaquic Hapludalfs; and Udollic Albaqualf. Soils were developed in two parent materials. Lower horizons were formed in residuum from chlorite schist (Hamilton, 2002). Upper horizons were formed in loamy transported materials of unknown origin. Within the study site, 12 sites were chosen for soil description and seasonal saturation monitoring (Fig. 3.2). Moreover, four of these sites were also equipped with IRIS tubes and redox electrodes to evaluate Fe/Mn reduction.

Local Precipitation

Precipitation data were collected from a weather station located at headquarters of the Central Research and Education Center (Eatonton, Georgia), which was 1.50 km from the site. The station was equipped with tipping bucket rain gage. Climate data were used to evaluate precipitation effects on the depth of seasonal saturation and deviation from long-term averages.

Pedon Description and Sampling

An undisturbed core, taken by hydraulic probe, was described at each site (Appendix A), using standard terminology (Soil Survey Staff, 1999). Additionally, two pedons, S03GA237-01 and S03GA237-02, described and sampled from a backhoe to depths of approximately 1 m and 2.5 m, respectively. Pedon S03GA237-01 was described and sampled from the pit wall. Pedon S03GA237-02 was described and sampled from the pit wall and bucket auger samples taken from the pit bottom. Sampling was by horizon and bulk samples were taken for laboratory analysis.

Characterization Analysis:

Bulk samples were air dried for a period of one week and then crushed with a wooden roller and passed through a 2-mm sieve. Particle size distribution of the pedons was determined by the pipette and sieve method (Kilmer and Alexander, 1949). The pH was determined by a 1:1 deionized water to sample suspension after 30-min equilibrium (Soil Survey Staff, 1996). Bulk density (0.33 kPa and oven dried) was determined by the clod method (Soil Survey Staff, 1996). Exchangeable cations were extracted by a mechanical extractor using 1N pH 7 ammonium acetate (Soil Survey Staff, 1996). Ca, Mg, Na, and K concentrations were measured by atomic absorption.

An estimate of shrink-swell potential was derived as the coefficient of linear extensibility (COLE) by the following equation: [COLE = (oven dry bulk density/moist bulk density)$^{1/3}$ -1]. The correlation between K_s and moist and dry bulk density, and COLE was determined and a regression model was fitted with other parameters.

Cation exchange capacity was measured by saturating the exchange sites with Na, using 1N, pH 8.2 sodium acetate. The samples were then washed twice with ethanol to remove any excess sodium. Ammonium acetate was then passed through the samples so that NH_4 replaced the Na on exchange sites. The Na was then measured by atomic absorption (Soil Survey Staff, 1996).

Saturation Events

Piezometers (monitoring wells), above and below the field interpreted restrictive horizons, were installed at the twelve sites to monitor depth to saturation (Figure 3.2). Five piezometers (1, 2, 14, 15, and 17) were equipped with data loggers and transducers, which recorded depth of water in the piezometer daily. At the remaining piezometers, saturation depth was measured manually on a weekly interval. To capture seasonal and annual climatic variations, monitoring was conducted for two years.

Redox Measurements

Pt electrodes were constructed based on the procedure established by Vepraskas (2002). A brief recount of the procedure with modifications from the original method is located in Appendix B.

Electrodes were installed to the depth of extended seasonal saturation to monitor redox potential (E_H) to determine the time interval between onset of saturation and the threshold redox potential for Fe reduction (Mausbach and Richardson, 1994; Hayes and Vepraskas, 2000).

Five replicate platinum electrodes were installed at sites 1 and 11; four replicate platinum electrodes were installed at site 4 (Table 3.1). A pilot hole was made with a push probe to ensure

no damage was made to the Pt tip during insertion. Electrodes were spaced 30.5 centimeters apart. All of the redox data reported were corrected for the standard calomel electrode by adding 244 mV to the field readings (Pruitt, 2001), which were made weekly during periods when the electrode installation depths were saturated. Soil pH was measured periodically in the field to account for changes in the threshold E_H value for Fe reduction due to pH differences (Mausbach and Richardson, 1994).

Preparation of IRIS tubes

IRIS (Indicator of Reduction In Soil) tubes were constructed based on the procedure established by Jenkinson (2002) and modified by Castenson and Rabenhorst (2006). A brief synopsis of the procedure is shown in Appendix C. IRIS tubes were installed at nine sites to the depth of extended seasonal saturation (Table 3.1). A pilot hole was made with a ½" diameter push probe to minimize abrasion during insertion but to maintain maximum contact with the soil.

Results and discussion

Soil Properties and Parent Materials

Selected properties for each horizon in pedons S03GA237-01 and S03GA237-02 are reported in Table 3.2. In pedon S03GA237-01, an abrupt clay increase and decrease in the sand to silt ratio was observed at 25 cm. These changes may indicate the presence of two parent materials at this site; however, the shallow depth at which these changes occur, make it difficult to differentiate between pedogenic processes that may have resulted in these textural differences and textural differences related to parent material change. At pedon S03GA237-02, a lithologic discontinuity was identified in the field at 120 cm and this field-identified discontinuity was

supported by an abrupt clay increase and a decrease in the s:si ratio at this depth. The depth at which these textural changes were observed is deeper than would be expected were they due to pedogenesis. Thus, this pedon is interpreted as being developed in two parent materials. The lower parent material was identified as residuum from the underlying saprolite. The upper material is assumed to have been transported as either colluvium or alluvium.

The depth to the residual parent material varied across the site (Fig. 4.6). Considerable thickness at upper hillslope positions suggests that alluvial deposition was unlikely. Thus, colluvium is the only viable explanation, movement of this parent material onto the site from the wearing down of a past landscape.

Horizons in the lower residual parent material are clayier than the overlying horizons developed in the loamy colluvial parent material. The abrupt clay increase is hypothesized to perch water which would result in seasonal saturation. At the lithologic contact of these two materials, there is an accumulation of black redox concentrations which suggest frequent oscillations of reducing and oxidizing conditions as expected for perched water tables on a sloping landscape.

Water table depths, measured for two years with nested piezometers, support perching water above the discontinuity (Fig 3.2 and Appendix D). Water tables are generally higher in piezometers above the discontinuity than in piezometers below the discontinuity (Fig 3.2 and Appendix D). Also, there is a lag time between the rise of water in the shallow piezometer and the rise of water in the deep piezometer, which supports the presence of perched water tables.

Redox Potentials

Redox potentials were measured from January 2007 to June 2007 to determine the amount of time required for Fe reduction to occur after saturation. Iron must be reduced for it to be soluble and mobile in the soil. Thus, reduction is a prerequisite for the formation of redox depletions and concentrations a soil (Vepraskas, 2000). The E_H values at which Fe reduction commences were estimated from an E_H – pH relationship for the mineral goethite (FeOOH) given in equation 1 (He et al., 2003).

$$E_H (Fe^{2+}) = 1235 - 177pH \text{ (for } pH < 7.5) \quad [1]$$

The pH values determined for each site were used for the estimation of E_H (Fe^{2+}). The soil pH values ranged from 5.3 to 6.8 across all the sites. Thus, measured E_H values lower than the threshold value calculated for each site were interpreted as being reduced with respect to Fe. These data, along with piezometer data (Fig 3.2 and Appendix D), were used to determine the lag time between the onset of saturation and reduction of Fe for each site.

The water table at site 1 rose abruptly on December 25, 2006 saturating the Bt horizon containing the redox electrodes. For the first redox measurements, taken on January 9, 2007, all five electrodes showed that Fe was reduced and E_H remained low throughout the period the horizon was saturated (Fig. 3.3). Therefore, the time between the onset of saturation and Fe reduction was less than 14 days at this site. If the period a horizon was saturated was less than 14 days, the E_H measurements generally indicated Fe was oxidized. For example, the water table at site 4 rose above the depth of the redox electrodes for brief periods (< 10 days) on four occasions, but E_H data indicated Fe was oxidized throughout the monitoring period (Fig 3.4).

Data loss hampered evaluation of the reduction lag at site 11 (Fig 3.5). However, five days after initial saturation at the redox electrode depth, four of the five electrodes indicated

oxidizing conditions. After equipment repair in February, the water table remained above or slightly below the redox electrodes until mid March. During this period, two of the redox electrodes indicated Fe reduction while the E_H at the other three hovered around the reduced/oxidized Fe threshold. After the water table depth decreased to below the redox electrodes, four of the five electrodes indicated oxidized Fe.

Saturation Events

The number of saturation events (NSE) was proposed by He et al. (2003) as a method to normalize saturation frequency and duration during a particular time interval. A single long period of saturation and reduction may be as effective in producing redoximorphic features as multiple shorter periods of saturation (He et al., 2003). The number of saturation events (NSE) is defined as:

$$NSE = (LDS/LAG) + (NPS - 1) \quad [2]$$

where NSE is the number of saturation events in a given time interval, LDS is the integer of the longest duration of a single period of saturation during the period of interest, LAG is the number of days between onset of saturation and the beginning of Fe reduction, and NPS is the number of times the soil was saturated for periods of longer than LAG time during the time interval. The use of 21 days for NPS in equation 1 was the average time lag between saturation and the drop in redox potential (E_H) to the point of Fe reduction for a site in North Carolina (He et al., 2003). The data from our site, however, support the use of 14 days for the LAG in equation 2.

During the two year monitoring period, seasonal water tables were higher and lasted longer in 2005-2006 than in 2006-2007 (Fig. 3.2 and Appendix D). Significant differences between 2005-2006 and 2006-2007 measurements were not observed in the perched water tables.

Sprecher and Warne (2000) proposed the direct antecedent rainfall method to evaluate the normalcy of monthly rainfall amounts based on rainfall for the three months prior to the month of interest. For our site, the direct antecedent rainfall method was used to evaluate the rainfall normalcy during the two years in which the piezometers were measured. These rainfall data show that five of the eleven months during which the IRIS tubes were in situ were drier than normal (Table 3.3). During the typically wet months (January thru April), January and February exhibited normal rainfall conditions while March and April exhibited drier than normal rainfall conditions. Even though rainfall was normal during six of the eleven months evaluated, it was not enough to replenish the deficit from drier-than-normal summer and fall. Thus, the seasonal high water tables during this time were lower than previous years (2005-2006). These drought-like conditions had an effect on the saturation events observed on our site.

The NSE for each site was calculated per horizon using Eq. [2] for the entire two year period of water table monitoring (February 2005 – April 2007) and for the period during which IRIS tubes were installed (June 2006 – April 2007) (Table 3.4). Since the June 2006 – April 2007 period is a subset of the two year period, the NSE for the two year period are greater. Additionally, the NSE data do not distinguish between perched water tables and seasonal water tables; thus the differences noted in graphical water table data (Fig 3.2 and Appendix D) were not apparent when the NES data were examined numerically.

Correlation of FH depletion with Saturation Events

Once the number of saturation events were determined for the horizons of interest these values were then correlated with the percentage of FH depletion from the IRIS tubes (Table 3.4). The period of interest ranged from June 29, 2006 when IRIS tubes were installed to April 27,

2007 when the IRIS tubes were removed. The percentage of Fe loss from the tubes ranged from 6% to 40%. The amount of Fe loss from tubes tended to increase with increasing depth. Correlations between the percentage of FH loss and saturation events within this period were determined using the simple regression model:

% FH loss from IRIS = Slope x NSE [3]

When considering all horizons, the percentage of FH loss from IRIS tubes was poorly correlated with the number of saturation events ($r^2 = 0.40$) (Fig. 3.8A). Although, no saturation events were measured for the horizons close to the surface and few redox features were observed in the upper 30 cm of the sites, the IRIS tubes showed appreciable amounts of FH depletion. This discrepancy could be caused by greater exposure to rainfall events, greater amounts of organic matter thereby causing greater microbial activity, or the impendence of water by restrictive Bt horizons directly below these horizons (perched water tables). In addition, bentonite was applied to the annular space around the IRIS tubes to prevent infiltration of surface water. Consequently, the surface horizons in contact with the bentonite may have had greater FH loss from the IRIS tubes that was not representative of the natural redox status of the horizons. Thus, correlations were recomputed only for horizons below 30 cm.

Evaluation of only horizons below 30 cm resulted in an increased correlation between FH loss and NSE (Fig 3.8B). However, several horizons had appreciable FH loss with no saturation events. Reasons for FH loss without saturation are unknown but may, in part, be due to perching of water at a deeper depth than interpreted in the field (saturation below base of the shallow piezometer that would not be measured) periods of saturation shorter than 14 days that resulted in FH loss, and/or longer retention of water in the void between the IRIS tube and surrounding soul than was measured with the piezometers.

When FH loss for only those horizons with NSE > 0 were evaluated, the correlation between percentage FH loss and NSE improved (Fig 3.8C). This suggests that IRIS tubes are a valid technique for evaluating reduction in mafic soils of the Piedmont and amount of FH loss may be a reasonable indicator of length of the period(s) of saturation and reduction.

Relation of Redox Features to Saturation and Reduction

For mafic soils in the Piedmont region of Georgia, occurrence of various types of redoximorphic features was associated with the different times of saturation (Table 3.5). Horizons without redox features were shown to be saturated a mean of 4% of the monitoring period and showed a mean NSE of 1.8. Horizons with redox concentrations only were saturated a mean of 11% of the monitoring period and showed a mean NSE of 3.9. Horizons with redox depletions (Munsell chroma ≤2) were saturated a mean of 10% of the monitoring period and showed a mean NSE of 7.6. Horizons with low Munsell chroma (≤2) matrices were saturated a mean of 58% of the monitoring period and showed a mean NSE of 24.

There was no statistical difference between time of saturation for horizons with redox concentrations and those with redox depletions (P=0.8432). The difference between the means for no redox features and the presence of redox concentrations was statistically significant (P=0.0120), as was the difference between the mean for low Munsell chroma (≤2) matrix and all other means (P=0.001). The NSE for no redox features and redox concentrations were not statistically different (P=0.1062). Also, the difference in NSE for redox concentration and redox depletions was not statistically significant (P=0.0999). The difference in NSE for horizons with no redox features and those with redox depletions was statistically different (P=0.0009). Similarly, the difference in NSE for low Munsell chroma (≤2) matrix and other types

redoximorphic features was statistically different (P=0.0001 and P=0.0009). The lengths of the period of saturation associated with no redox features present and horizons with low-chroma matrix are similar to those reported by West et al. (1998) and Jacobs et al. (2002) for lower clay soils in the Coastal Plain. Similar to this study, Jacobs et al., 2002, reported no statistical difference between saturation associated with concentrations and depletions. West et al., 1998, however, reported differences in periods of saturation for redox concentrations and depletions that were not observed in this study.

Many of the upper horizons had appreciable amount of Fe and Mn concentrations and no Fe depletions; however, the IRIS tubes indicated that Fe reduction should be taking place (Fig. 3.6 and Fig 3.8). When looking at horizons with 20% or greater loss of FH from IRIS tubes, redox features found during field classification indicated that saturation is occurring, however, in many cases, redox features found in these horizons were concentrations rather than depletions. Horizons with greater than 30 % reduction of FH from IRIS tubes were found to have redox depletions or reduced matrices during field description. Castenson and Rabenhorst (2006) found similar results; if 30% of the FH was removed, then they concluded that the soil is reducing. Further studies are needed to set a threshold limit of the amount of FH removed to be considered seasonal saturation. While IRIS tubes are good indicators of the presence of saturation, it is difficult to quantify the duration of saturation with them if only one wet season is monitored. He et al. (2003) points out short-term (<3 yr) studies cannot adequately determine the relationship between saturation duration and redoximorphic features. Thus, to relate the saturation duration and redoximorphic features of this site, further study is needed.

Conclusions

1. The lower clayey residual horizons are causing water to perch in the colluvial horizons. An accumulation of black redox concentrations at the lithologic contact of the two parent materials suggests frequent oscillations of reducing and oxidizing conditions as expected for perched water tables. Also, there is a lag time between the rise of water in the shallow piezometer and the rise of water in the deep piezometer, again, supporting the presence of perched water tables (Fig 3.2 and Appendix D).
2. Redox data suggest ≤ 14 day lag between saturation and Fe reduction. The water table at site 1 rose abruptly on December 24, 2006, and the first redox measurements, taken on January 9, 2007, showed that Fe was reduced. E_H data for sites 4 and 11 showed that Fe remained oxidized during brief rises in the water table (≤ 10 days).
3. This study found when FH loss for subsurface horizons with NSE > 0 were evaluated, a strong correlation between percentage of FH loss and NSE is shown ($r^2 = 0.9$). This relationship suggests that IRIS tubes are reliable indicators of reduction in mafic soils.
4. Differences are shown between the percentage of time saturated and NSE for horizons with no redox features, [concentrations, depletions], and low Munsell chroma (≤2) matrices. There are no differences in the percentage of time saturated and NSE for horizons with concentrations and depletions.

References

Bouma, J. 1983. Hydrology and soil genesis of soils with aquic moisture regimes. p. 253–281. In L.P. Wilding et al. (ed.) Pedogenesis and soil taxonomy. I. Concepts and interactions. Elsevier, Amsterdam, the Netherlands.

Buol, S.W., and R.A. Rebertus. 1988. Soil formation under hydromorphic conditions. p. 253–262. In D.D. Hook et al. (ed.) The ecology and management of wetlands. Vol. 1: Ecology of Wetlands. Timber Press, Portland, OR.

Castenson, K.L., and M.C. Rabenhorst. 2006. Indicator of reduction in soil (IRIS): Evaluation of a new approach for assessing reduced conditions in soil. Soil Sci. Soc. Am. J. 70:1222–1226.

Daniels, R.B., E.E. Gamble, and L.A. Nelson. 1971. Relations between soil morphology and water-table levels on dissected North Carolina Coastal Plain Surface. Soil Sci. Soc. Am. Proc. 35:781–784.

Faulkner, S.P., and W.H. Patrick. 1992. Redox processes and diagnostic wetland indicators in bottomland hardwood forests. Soil Sci. Soc. Am. J 56:856–865.

Hamilton, D.A. 2002. Mafic and felsic derived soils in the Georgia Piedmont: Parent material uniformity, reconstruction, and trace metal contents. M.S. thesis Univ. Georgia, Athens, GA.

Hayes, W.A., and M.J. Vepraskas. 2000. Morphological changes in soils produced when hydrology is altered by ditching. Soil Sci. Soc. Am. J. 64:1893–1904.

He, X., M.J. Vepraskas, D.L. Lindbo, and R.W. Skaggs. 2003. A method to predict soil saturation frequency and duration from soil color. Soil Sci. Soc. Am. J. 67:961–969.

Jacobs, P.M., L.T. West, and J.N. Shaw. 2002. Redoximorphic features as indicators of seasonal saturation, Lowndes County, Georgia. Soil Sci. Soc. Am. J. 66:315–323.

Jenkinson, B. 2002. Indicators of reduction in soils (IRIS): A visual method for the identification of hydric soils. Ph.D. dis. Purdue Univ., West Lafayette, IN.

Jenkinson, B.J., and D.P. Franzmeier. 2006. Development and evaluation of Fe-coated tubes that indicate reduction in soils. Soil Sci. Soc. Am. J. 70:183–191.

Kilmer, V.J., and L.T. Alexander. 1949. Methods of making mechanical analysis of soils. Soil Sci. 68:15-24.

Matthews, M. 2003. Water quality in fenced and unfenced stream reaches flowing through grazing pastures in the southern Piedmont. M.S. thesis Univ. Georgia, Athens, GA.

Mausbach, M.J., and J.L. Richardson. 1994. Biogeochemical processes in hydric soil formation. Curr. Topics Wetland Biogeochem. 1:68–127.

Pickering, E.W., and P.L.M. Veneman. 1984. Moisture regimes and morphological characteristics in a hydrosequence in Central Massachusetts. Soil Sci. Soc. Am. J. 48:113–118.

Pruitt, B.A. 2001. Hydrological and soil conditions across hydrogeomorphic settings. Ph.D. dis. Univ. Georgia, Athens, GA.

Soil Survey Staff. 1996. Soil survey laboratory methods manual. Soil Surv. Invest. Rep. 42. USDA_SCS, Natl. Soil Survey Center, Lincoln, NE.

Soil Survey Staff. 1999. Soil Taxonomy. A basic system of soil classification for making and interpreting soil surveys. 2nd Ed. USDA-NRCS. U.S. Government Print. Office, Washington, D.C.

Sprecher, S.W. and A.G. Warne. 2000. Accessing and using meteorological data to evaluate wetland hydrology. ERDC/EL TR-WRAP-00-1, U.S. Army Engineer Research and Develop. Center, Vicksburg, MS.

Van Bochove, E., S. Beauchemin, and G. Thériault. 2002. Continuous multiple measurement of soil redox potential using platinum microelectrodes. Soil Sci. Soc. Am. J. 66:1813–1820.

Veneman, P.L.M., L.A. Spokas, and D.L. Lindbo. 1998. Soil moisture and redoximorphic features: a historical perspective. p. 1–23. In M.C. Rabenhorst et al. (ed.) Quantifying soil hydromorphology. SSSA Special Publ. No. 54. SSSA, Madison, WI.

Vepraskas, M.J. 2000. Morphological features of seasonally reduced soils. p. 163–182. In J.L. Richardson and M.J. Vepraskas (ed.) Wetland soils: Genesis, hydrology, landscapes, and classification. Lewis Publ., Boca Raton, FL.

Vepraskas, M.J. 2002. Redox potential measurements [Online]. Available at http://www.soil.ncsu.edu/wetlands/wetlandsoils/RedoxWriteup.pdf (accessed 9 Sept. 2005; verified 24 Feb. 2008). Dept. of Soil Science at North Carolina State University.

West, L.T., J.N. Shaw, E.R. Blood, and L.K. Kirkman. 1998. Correlation of water tables to redoximorphic features in the Dougherty Plain, Southwest Georgia. p. 247–258. In M.C. Rabenhorst et al. (ed.) Quantifying soil hydromorphology. SSSA Special Publ. No. 54. SSSA, Madison, WI.

Table 3.1. Landscape attributes and equipment installation depths per site

Site	Landscape Position	Soil Class	Piezometer Depth (cm)	Automated	Electrode Depth (cm)	IRIS Depth (cm)
1	Upper Backslope	Typic Paleudalf	Deep – 199 Shallow – 117	Yes	75	100
2	Backslope	Typic Paleudalf	134	No	---	---
3	Footslope	Typic Hapludalf	Deep – 236 Shallow – 62	No	---	110
4	Footslope	Oxyaquic Hapludalf	110	Yes	80	79
5	Shoulder	Typic Paleudalf	229	No	---	---
6	Backslope	Typic Hapludalf	Deep – 214 Shallow – 80	No	---	124
7	Toeslope	Aquic Paleudalf	Deep – 124 Shallow – 61	No	---	104
8	Upper Backslope	Typic Paleudalf	Deep – 100 Shallow – 66	No	---	62
9	Toeslope	Udollic Albaqualf	113	No	---	---
10	Backslope	Oxyaquic Halpudalf	143	Yes	77	95
11	Footslope	Typic Hapludalf	115	Yes	57	80
12	Backslope	Typic Paleudalf	123	No	---	125

Table 3.2. Selected properties for the pedons sampled.

							Bulk Density			Particle Size Distribution								
										Sand								
Hor.	Depth		pH 1:1 H_2O	Ex. Bases	CEC	Base Sat.	0.33 kPa	O.D.	COLE	vcs	cs	ms	fs	vfs	Ts	Silt	Clay	S:Si Ratio
	---cm---			cmol(+) kg^{-1}		%	-----g/cm3-----		m m^{-1}	----------%----------								
S03GA237-01																		
Ap1	0	12	5.4	4.9	9.7	50	---	---	---	4.4	6.9	10.8	25.6	18.0	65.7	23.6	10.7	2.78
Ap2	12	25	5.3	4.6	9.7	47	1.50	1.58	0.017	5.6	6.9	10.3	24.8	16.4	64.0	23.5	12.6	2.72
Bt	25	50	5.5	10.4	19.0	55	1.26	1.43	0.043	3.8	3.9	6.2	13.4	10.3	37.7	26.2	36.1	1.44
Btss1	50	63	5.5	14.8	23.5	63	1.15	1.39	0.065	1.7	2.9	4.6	9.9	9.6	28.7	29.0	42.3	0.99
Btss2	63	89	5.7	26.5	34.0	78	1.21	1.68	0.116	0.6	1.9	4.3	7.1	8.2	22.1	28.5	49.4	0.78
CB	89	107	5.9	12.3	17.2	71	1.61	1.67	0.013	0.9	8.3	22.9	30.3	14.3	76.7	13.4	9.9	5.72
S03GA237-02																		
Ap	0	12	5.0	7.0	16.8	41	---	---	---	6.6	7.4	11.8	16.2	9.5	51.5	32.1	16.5	1.60
Bw	12	37	5.7	5.1	11.0	46	1.63	1.67	0.009	9.5	9.5	11.2	16.4	9.9	56.5	25.6	17.9	2.21
Ab	37	50	5.8	3.6	10.5	34	1.70	1.78	0.015	18.2	13.7	11.6	16.6	9.7	69.8	19.7	10.5	3.54
B'w1	50	78	5.6	3.5	8.1	43	1.66	1.74	0.015	12.1	12.7	13.1	16.3	9.6	63.9	22.6	13.5	2.83
B'w2	78	96	5.8	4.7	13.3	35	1.65	1.79	0.027	21.9	14.0	11.4	12.7	7.2	67.1	19.2	13.7	3.49
Bsm	96	120	5.9	7.0	18.7	37	1.72	1.80	0.016	30.7	16.9	11.3	8.8	5.6	73.3	13.6	13.1	5.39
2Bss	120	160	6.0	13.4	33.8	40	1.13	1.73	0.157	2.6	3.4	6.3	8.7	6.5	27.5	16.2	56.3	1.70
2C	160	226	6.5	24.7	34.9	71	---	---	---	5.3	7.4	10.4	17.8	15.1	56.0	24.8	19.2	2.26
2Cr	226	246	6.8	17.4	22.3	78	---	---	---	17.5	17.0	15.6	15.1	9.7	74.9	16.7	8.4	4.49

Table 3.3. Direct Antecedent Rainfall Method

Month	WETS Rainfall Percentile 30th	70th	Rainfall	Condition of Period
	---------- inches ----------			
February-05	2.82	5.37	4.63	Drier than normal
March-05	3.50	6.37	5.93	Drier than normal
April-05	1.90	4.18	5.13	Normal
May-05	1.93	3.89	2.55	Wetter than normal
June-05	2.14	4.39	5.33	Normal
July-05	3.26	5.12	7.84	Wetter than normal
August-05	2.95	5.30	6.52	Wetter than normal
September-05	1.81	4.15	0.01	Wetter than normal
October-05	1.56	3.67	2.13	Normal
November-05	2.21	4.22	2.76	Normal
December-05	2.5	4.42	2.77	Normal
January-06	3.62	5.67	2.98	Normal
February-06	2.82	5.37	3.95	Normal
March-06	3.50	6.37	2.03	Normal
April-06	1.90	4.18	1.59	Drier than normal
May-06	1.93	3.89	1.77	Drier than normal
June-06	2.14	4.39	3.75	Drier than normal
July-06	3.26	5.12	1.98	Drier than normal
August-06	2.95	5.30	4.71	Drier than normal
September-06	1.81	4.15	1.69	Normal
October-06	1.56	3.67	2.04	Normal
November-06	2.21	4.22	3.25	Normal
December-06	2.5	4.42	3.73	Normal
January-07	3.62	5.67	4.35	Normal
February-07	2.82	5.37	2.70	Normal
March-07	3.50	6.37	2.92	Drier than normal
April-07	1.90	4.18	0.93	Drier than normal
May-07	1.93	3.89	0.17	Drier than normal
June-07	2.14	4.39	3.37	Drier than normal

Table 3.4. Estimation of FH depletion on IRIS tubes and NSE per horizon.

Horizon	Lower Boundary	FH Loss	LDS (Jun 06 – Apr 07)	Number Saturation Events (Feb 05 – Apr 07)	Number Saturation Events (Jun 06 – Apr 07)
	Cm	%	Days	NSE yr-1	NSE yr-1
Site 1					
Ap	13	N/A	0	0.0	0.0
Btc1	35	14	0	2.5	0.0
Btc2	60	23	40	8.5	2.9
Btcg1	88	15	75	11.5	5.4
Btcg2	100	25	94	19.5	6.7
Site 3					
Ap	6	N/A	0	0.0	0.0
BAc	42	22	21	7.0	3.5
Btc	73	21	70	8.0	5.0
Btssc	110	25	0	10.0	0.0
Site 4					
Ap	8	N/A	0	0.0	0.0
ABc	23	40	0	0.0	0.0
Btc	49	15	0	0.0	0.0
BC	74	16	2	6.7	0.0
Site 6					
Ap	6	N/A	0	0.0	0.0
Ac	24	38	0	0.0	0.0
BAc	50	9	7	0.0	0.0
Btc	66	19	14	5.5	2.0
Cr	125	20	77	10.5	5.5
Site 7					
Ap	8	N/A	0	0.0	0.0
Ac	42	40	7	6.0	0.0
BA	60	10	28	20.5	6.0
Btg	74	29	63	20.0	5.5
Ccg	83	22	77	34.5	6.5
Cr	109	38	112	36.5	9.0
Site 8					

Ap	6	N/A	7	0.0	0.0
Ac	23	6	7	1.5	0.0
Btc1	44	13	21	7.0	3.5
Btc2	55	25	63	7.5	4.5
2Btss	62	28	70	9.0	5.0
Site 10					
Ap	6	N/A	0	0.0	0.0
Ac	19	26	0	1.5	0.0
BA	33	17	0	3.0	0.0
2Btc1	50	12	0	4.0	0.0
2Btc2	62	9	14	8.5	1.0
2Btssc	87	10	50	10.5	3.6
Site 11					
Ap	5	N/A	0	0.0	0.0
BA	12	25	0	0.0	0.0
2Btc1	29	9	1	0.0	0.0
2Btc2	50	16	9	5.1	0.0
2Cc	80	26	104	14.1	7.4
Site 12					
Ap	5	N/A	0	0.0	0.0
Ac	18	25	0	0.0	0.0
2Btc	53	36	0	0.0	0.0
2BCc	104	22	0	2.5	0.0

Table 3.5. Mean percentage time of saturation and number of saturation events for horizons with various redoximorphic features

		Time Saturated			Number of Saturation Events		
Redoximorphic Feature	Number of Horizons	Mean	Range	SE[†]	Mean	Range	SE[†]
		%	%		NSE yr^{-1}	NSE yr^{-1}	
None	28	4 A[*]	0 - 37	1.3	1.8 A[*]	0 - 14.1	0.7
Redox concentrations	20	11 B	0 - 36	2.5	3.9 A,B	0 - 10.5	1.2
Redox depletions (chroma ≤2)	7	10 B	0 - 33	6.0	7.6 B	1 - 14.3	1.6
Low chroma (≤2) matrix	15	58 C	25 - 100	5.5	24 C	11.5 - 40.1	2.7

[†]SE = standard error of the mean.

[*]Means with the same letter within the same column showed no statistical difference (multiple t-test adjusted for heterogeneous variances, $\alpha = 0.05$).

Fig. 3.1. Site Map

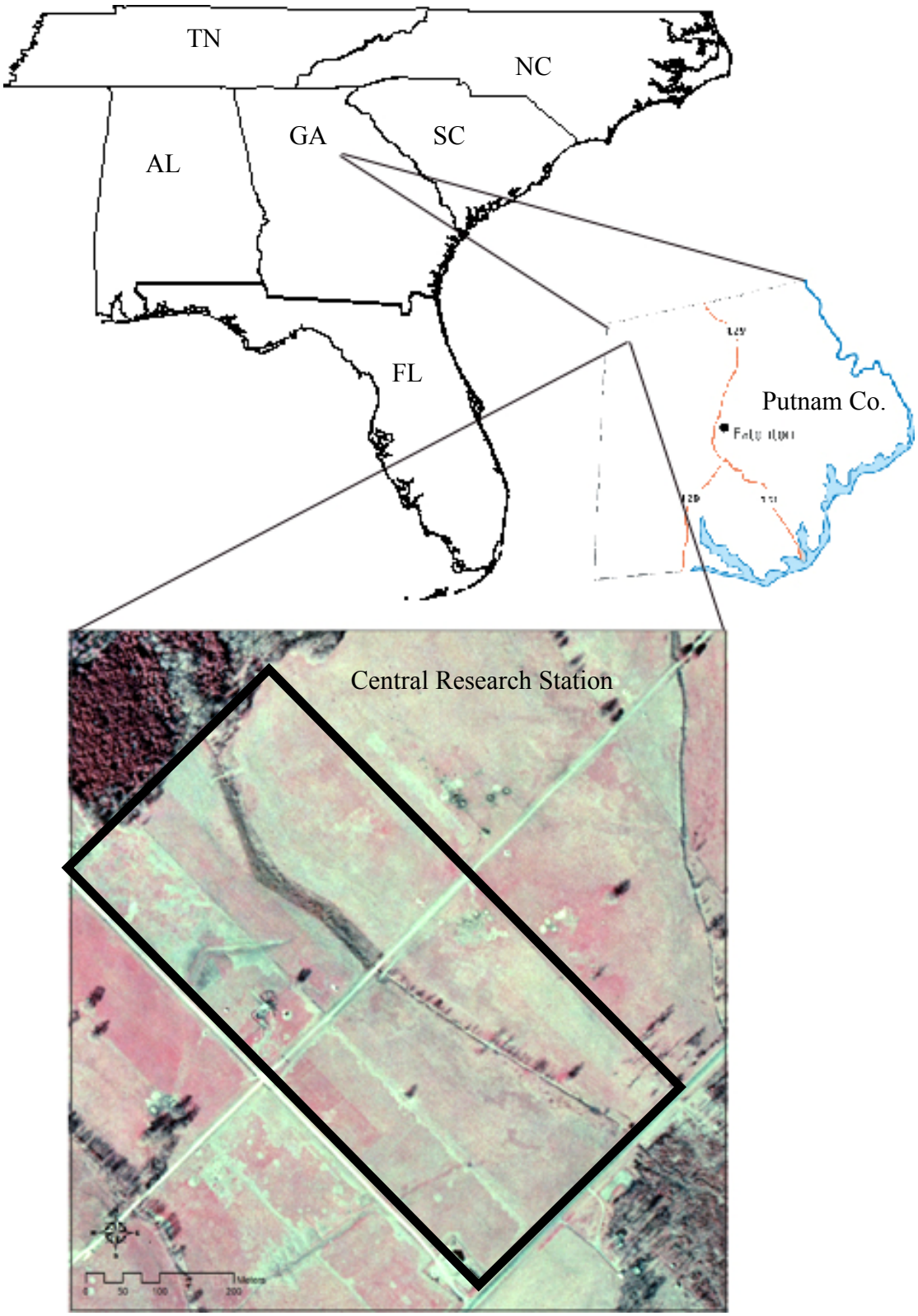

Fig. 3.2. Piezometer locations on project site. Sites 1, 4, and 11 were equipped with well dataloggers, Pt electrodes, and IRIS tubes. Additionally, sites 3, 6, 7, 9, 10, and 12 were equipped with IRIS tubes.

Fig 3.3. Saturation depths measured with piezometers for site 1.

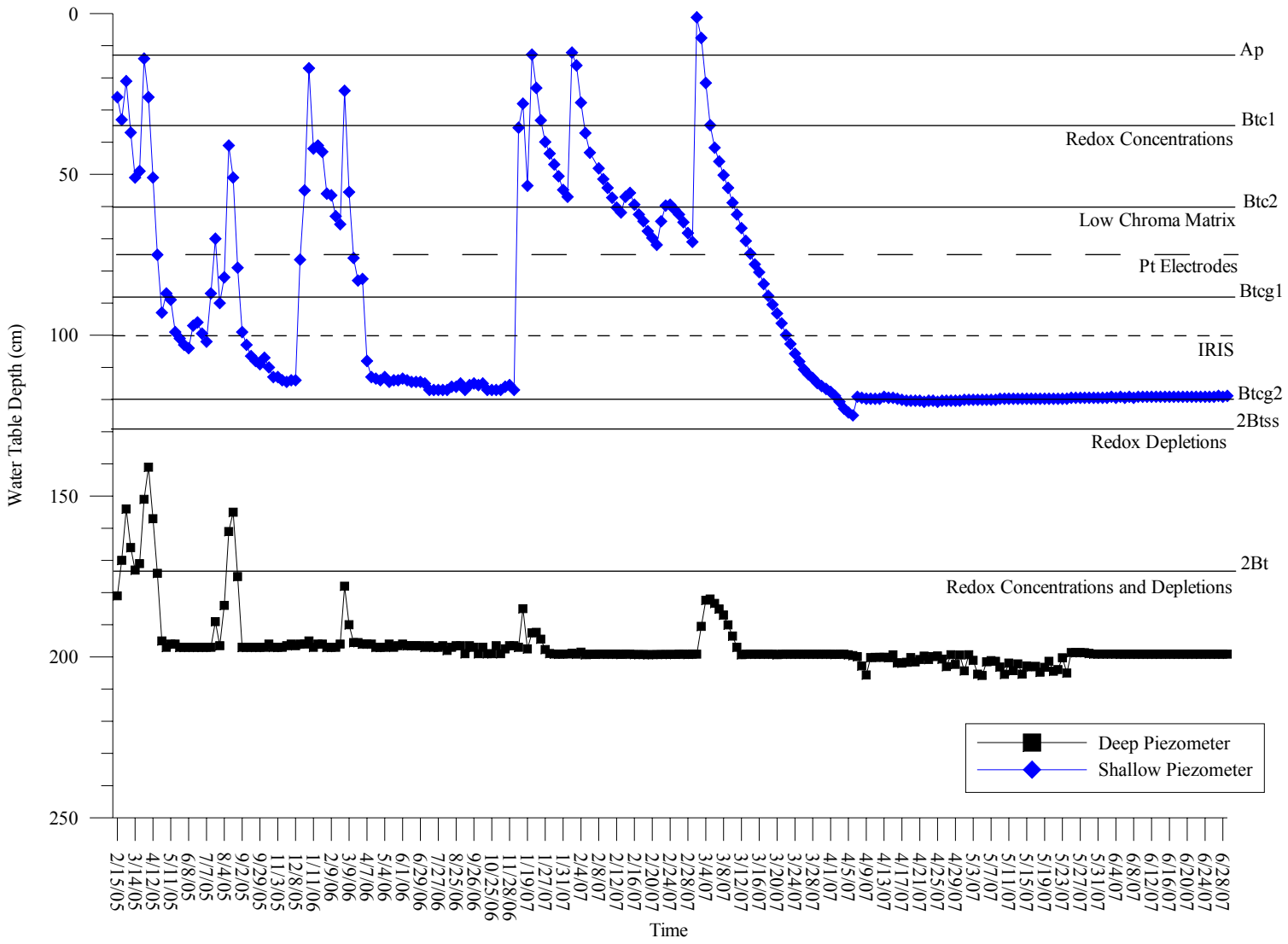

Fig 3.4. Redox potential (E_H) over time for Site 1. E_H is shown for all five electrodes at this site. In this example, the horizon became saturated on December 25, 2006, and 14 days later the initial E_H measurements indicated Fe was reduced.

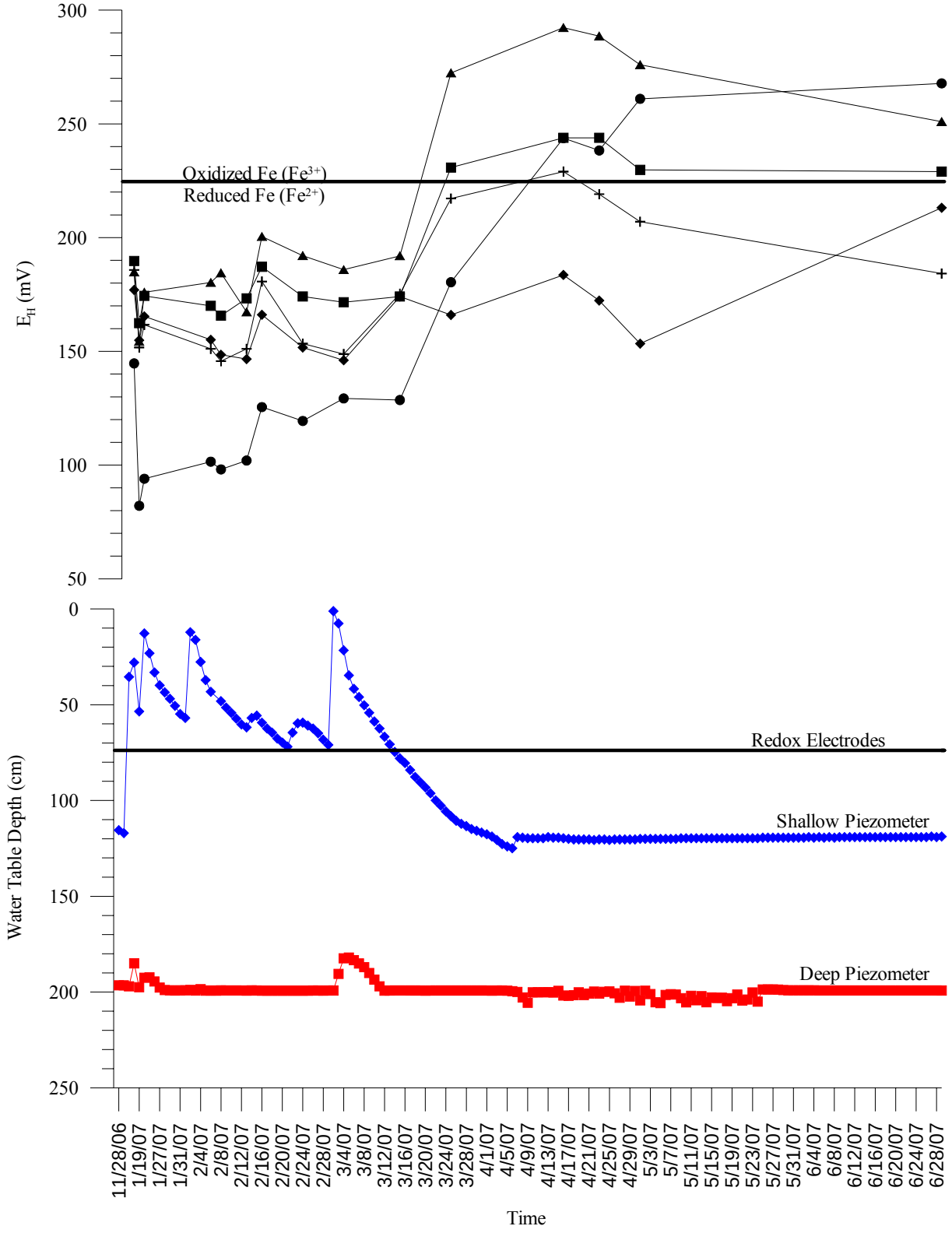

Fig 3.5. Redox potential (E_H) over time for Site 4. E_H is shown for all four electrodes at this site. The horizon became saturated on January 8, 2007, for 5 days. Site had no saturation periods lasting longer than five days. E_H measurements indicated Fe was not reduced.

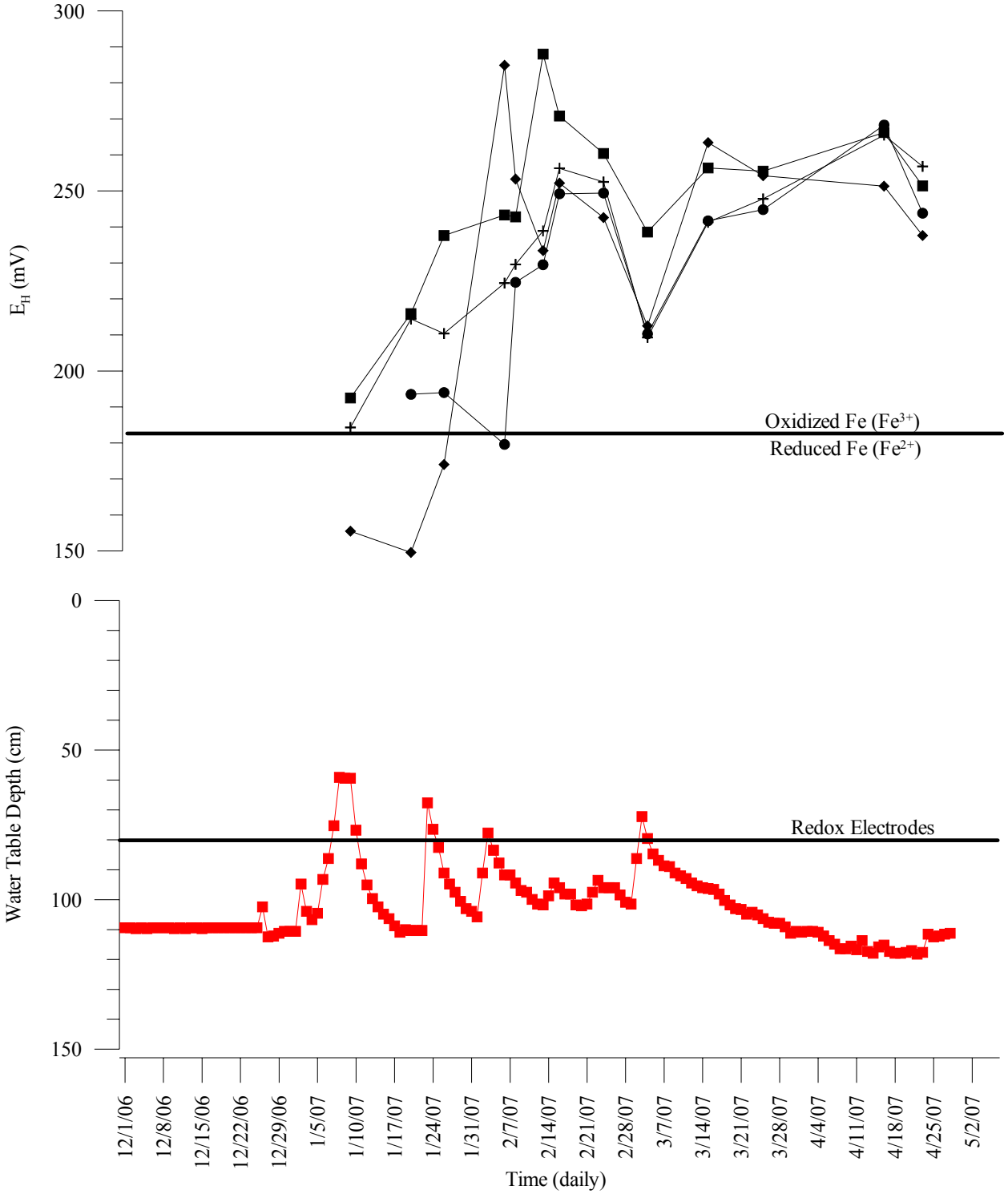

Fig 3.6. Redox potential (E_H) over time for Site 11. E_H is shown for all five electrodes at this site. The horizon became saturated on January 5, 2007, and 4 days later the initial E_H measurements indicated Fe was not reduced.

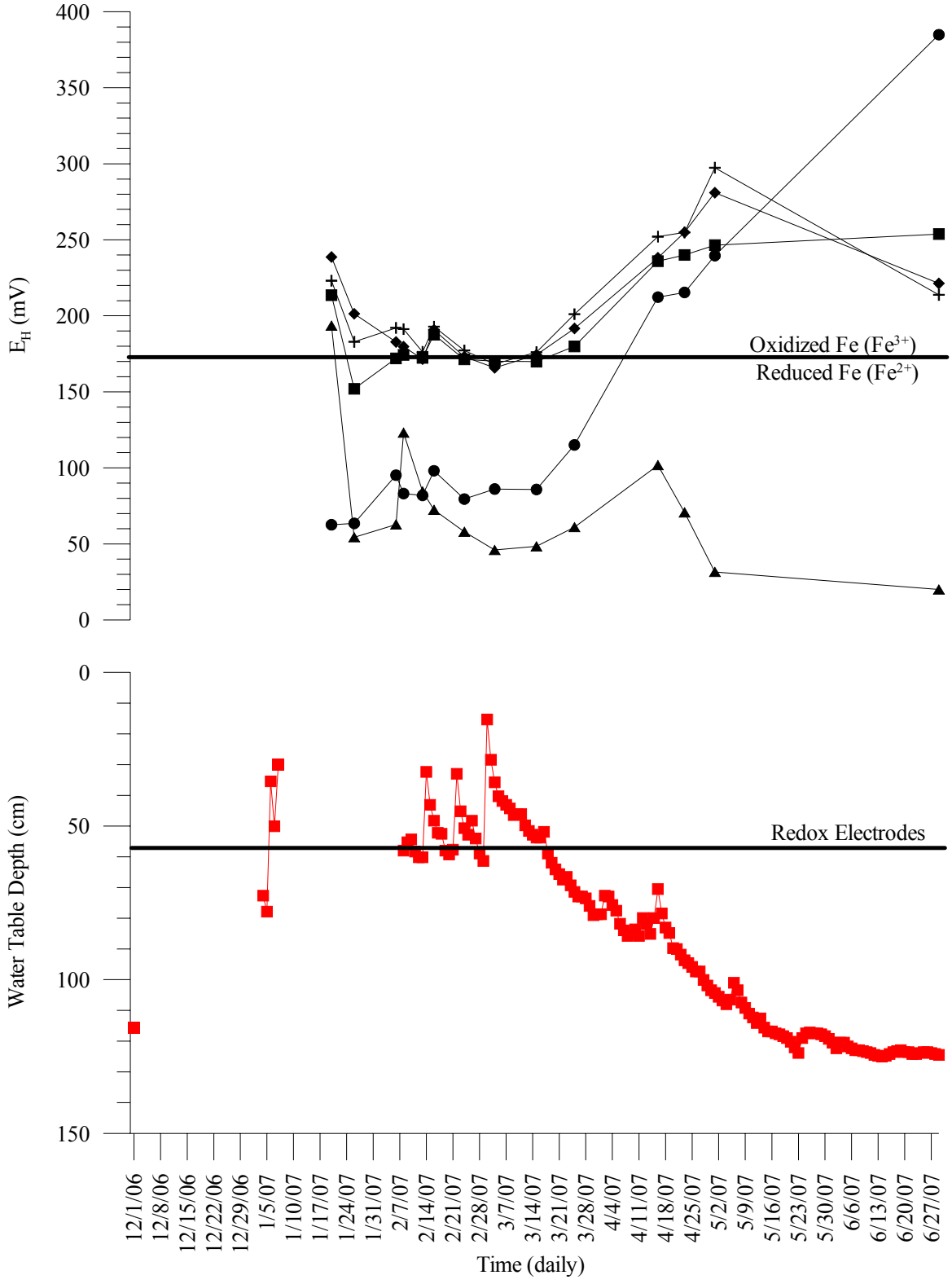

Fig 3.7. Percentage of FH loss from IRIS per horizon for each site. Loss of FH from Ap horizons could not accurately be analyzed because of the effects of bentonite applied around tubes at ground surface; thus data here are not representative of Fe loss in the soil at these depths.

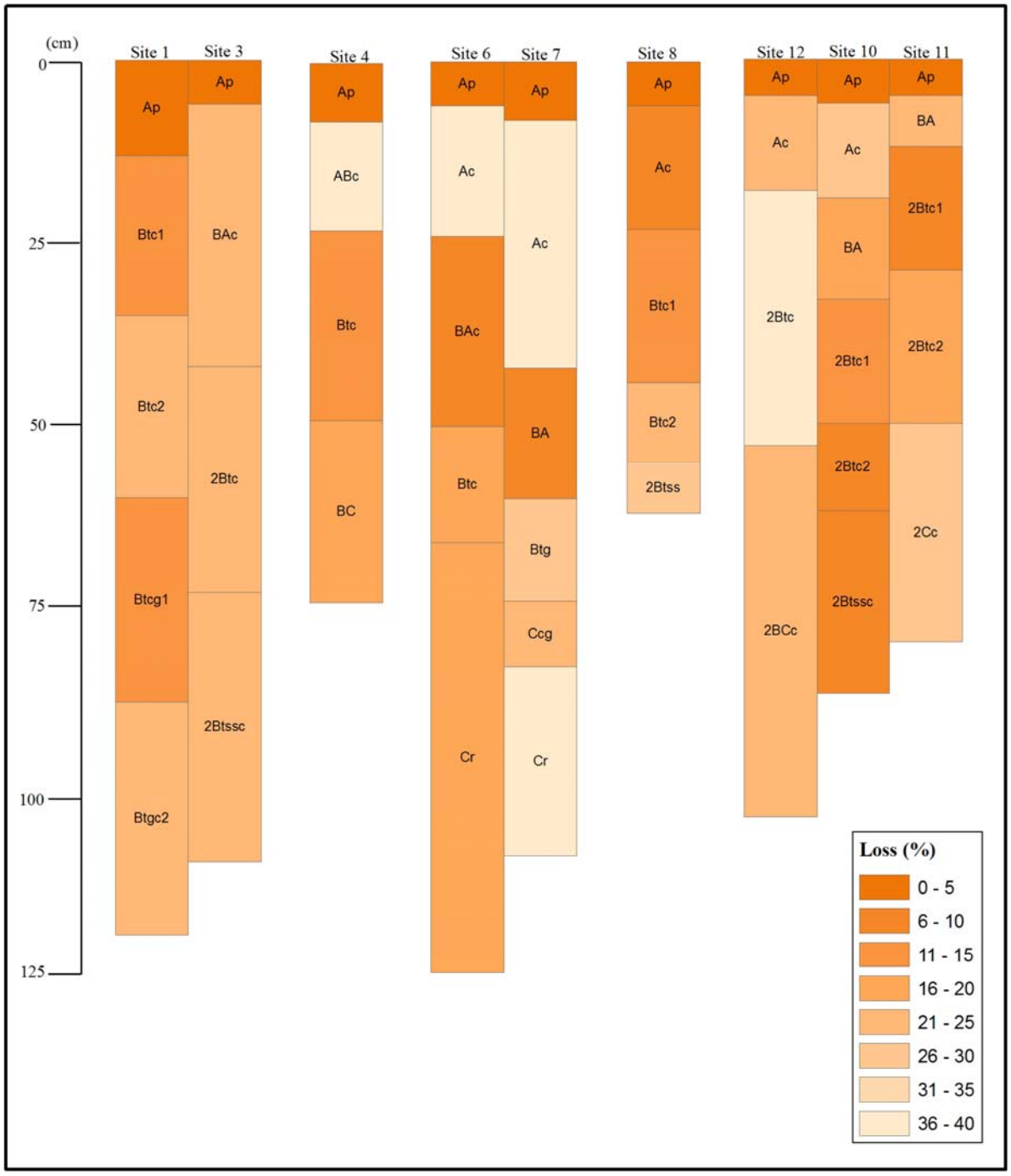

Fig 3.8. Relationships between average number of saturation events (NSEs) and the percentage of FH loss from IRIS tubes per horizon. (A) No correlation shown when comparing NSE to the percentage of FH loss from IRIS for all horizons within the sites (r^2=0.40). Upper horizons show a significant loss of FH even though no saturation events were recorded during the period of interest (June 2006 – April 2007). (B) Data plot for horizons greater than 30 cm show some correlation (r^2 =0. 64) (C) The data for the subhorizons with saturation events (NSE ≠ 0) show that linear relationships are justified (r^2 =0.90).

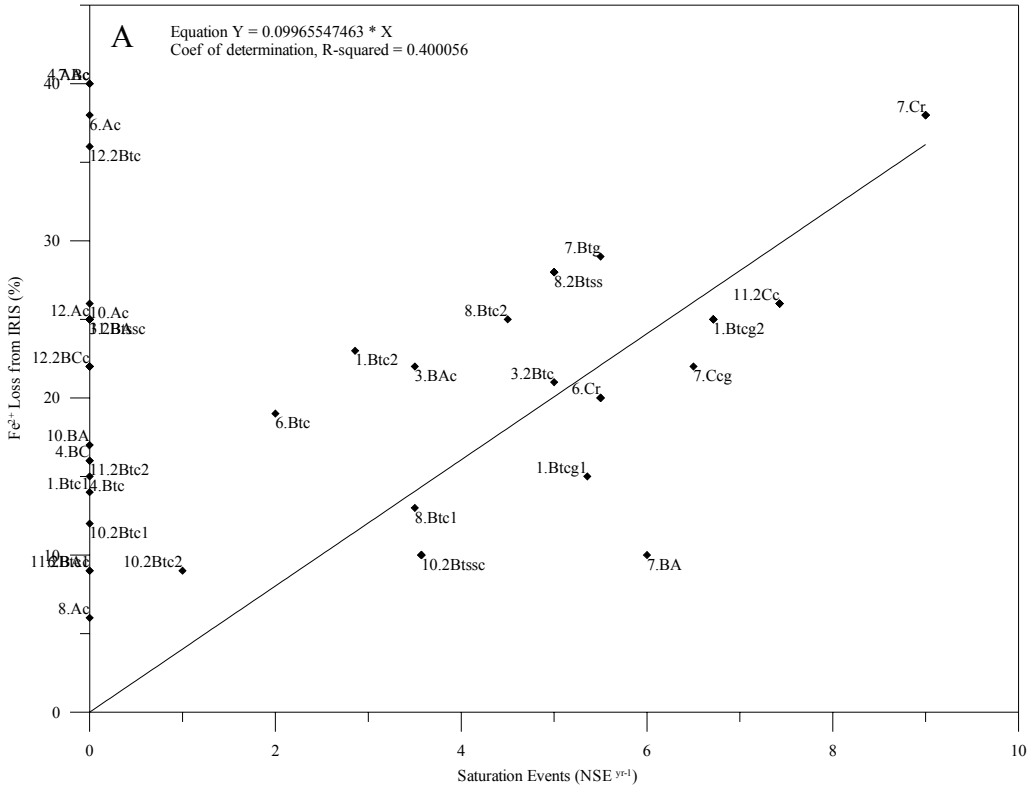

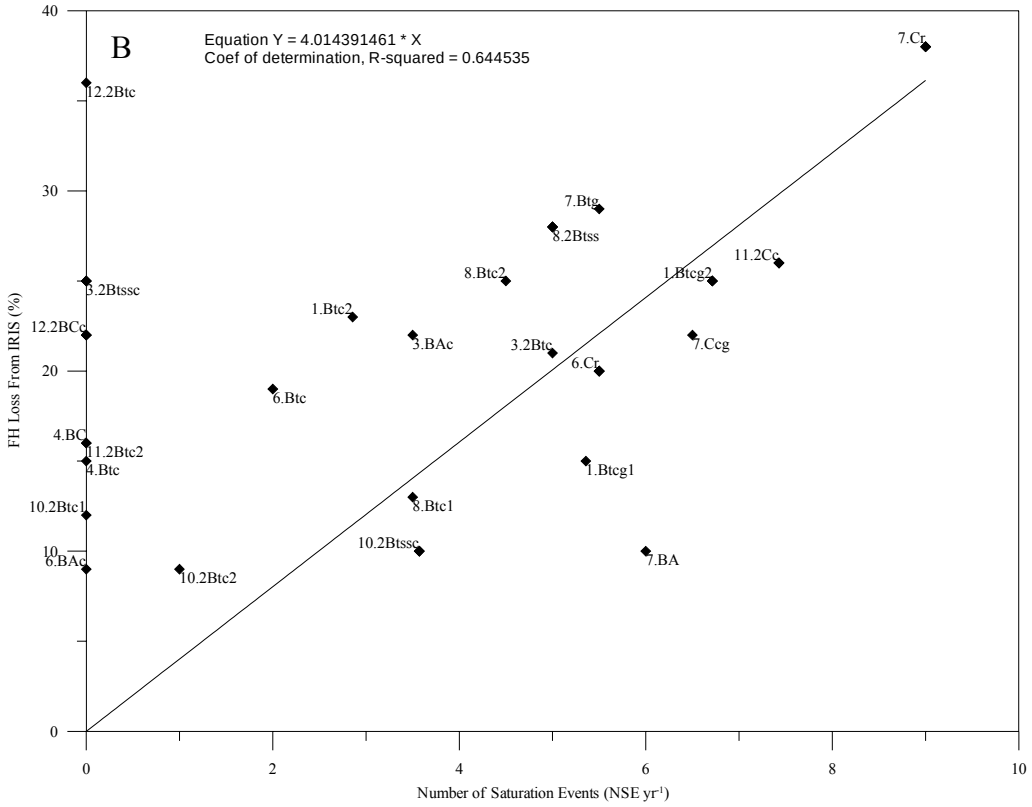
B
Equation Y = 4.014391461 * X
Coef of determination, R-squared = 0.644535
FH Loss From IRIS (%)
Number of Saturation Events (NSE yr-1)
7.Cr
12.2Btc
7.Btg
8.2Btss
11.2Cc
8.Btc2
1.Btcg2
3.2Btssc
1.Btc2
12.2BCc
3.BAc
3.2Btc
7.Ccg
6.Cr
6.Btc
4.BC
11.2Btc2
4.Btc
1.Btcg1
8.Btc1
10.2Btc1
10.2Btssc
6.BAc
7.BA
10.2Btc2
0
2
4
6
8
10
20
30
40

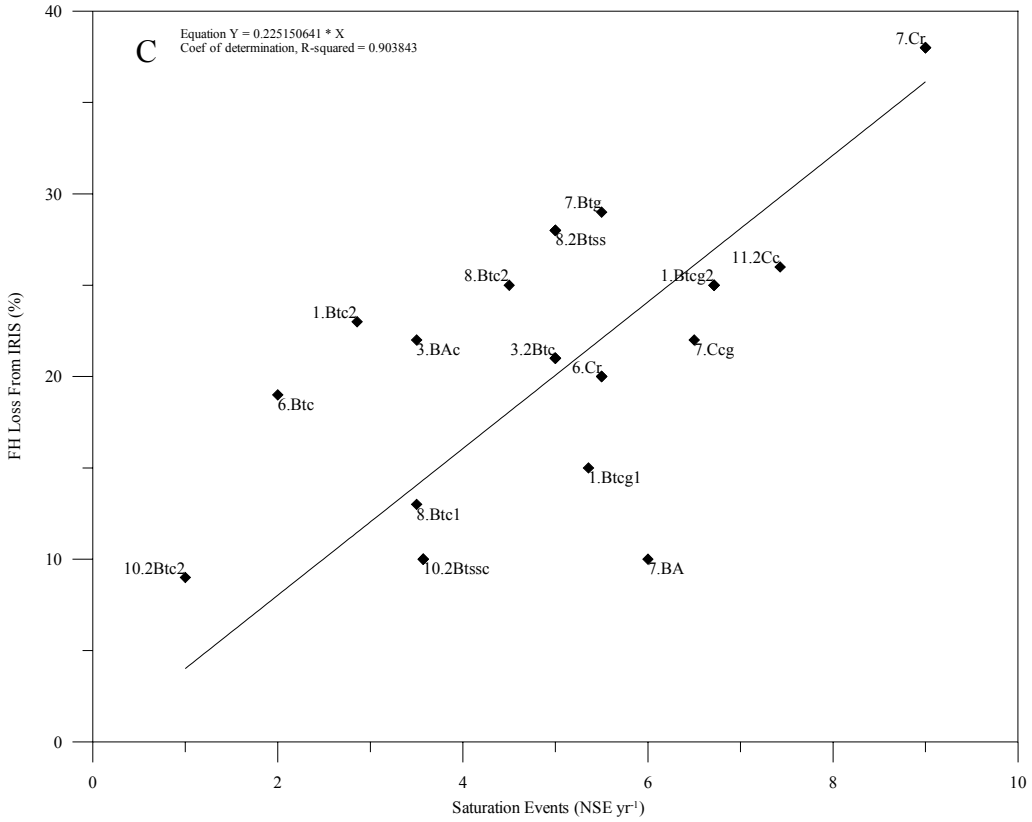
C
Equation Y = 0.225150641 * X
Coef of determination, R-squared = 0.903843
FH Loss From IRIS (%)
Saturation Events (NSE yr-1)
7.Cr
7.Btg
8.2Btss
11.2Cc
8.Btc2
1.Btcg2
1.Btc2
3.BAc
3.2Btc
7.Ccg
6.Cr
6.Btc
1.Btcg1
8.Btc1
10.2Btc2
10.2Btssc
7.BA
0
2
4
6
8
10
20
30
40

Fig 3.9 Presence of redox features (Fe) per horizon at each site corresponding with the IRIS depths. The upper horizons show little correlation between the presence of depletions (chroma ≤2) and the loss of FH from IRIS tubes. This is not taking into account the appreciable accumulation of Mn in the upper horizons.

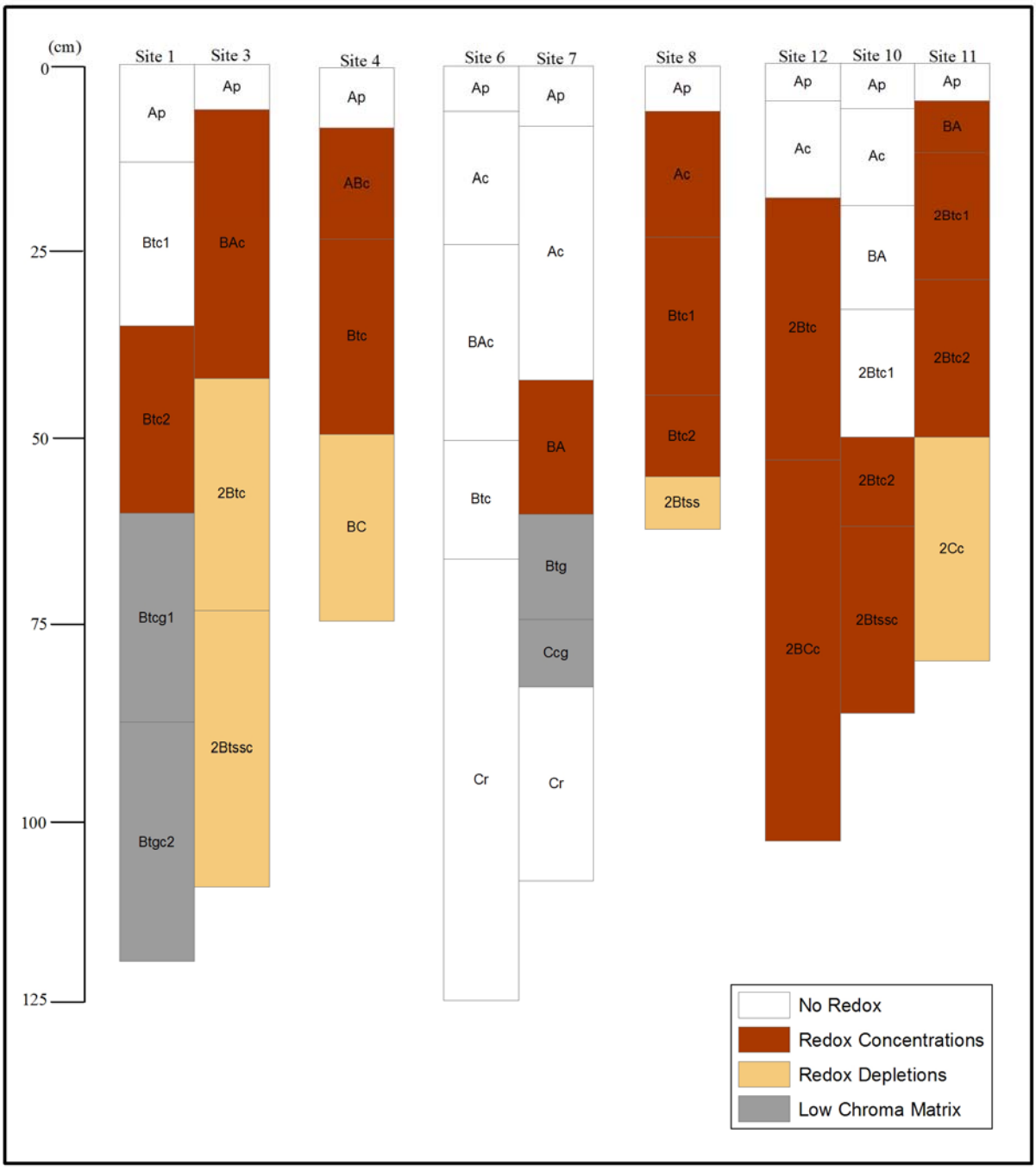

Chapter Four

Subsurface water flow and landscape attributes as related to soil developed from mafic rocks in the Piedmont of Georgia, USA

Depth of weathering, texture, structure, mineralogy of the soil separates, soil reaction, base saturation, and nutrient levels may be influenced strongly by parent material (Rabenhorst and Foss, 1981). Although most soils in the Piedmont of Georgia have formed from saprolite of weathered felsic gneiss or schist, there are scattered areas of soils formed from saprolite of weathered mafic and ultramafic rocks (Hamilton–Wood et al., 2002). The term "mafic" describes igneous rocks composed of higher amounts of minerals containing Mg and Fe such as pyroxenes, amphiboles, biotite, olivine and hornblende (American Geological Institute, 1976). As compared to felsic derived soils, soils formed from mafic and ultramafic parent materials have a loam to clay loam topsoil, a higher pH, a higher base saturation, and a greater abundance of expandable (2:1) clay minerals (Ogg and Smith, 1993; Schroeder et al., 2000; Hamilton–Wood et al., 2002). Because of their unique characteristics, the spatial distribution of mafic parent materials is important when examining the interaction between soil and water.

One of the most important of these characteristics that leads to the effective management of soil is its texture. The water holding capacity and hydraulic properties (Frenkel et al., 1978; Bresler et al., 1984; Jabro, 1992), the cation exchange capacity (Russell, 1973) and the influence on the fertility and productivity (Davey, 1990) are all important attributes affected by the texture of the topsoil. Thus from a hydrologic standpoint, the more loamy soils derived from mafic parent materials affect soil hydrology differently than soils derived from other parent materials. Likewise, subsurface soil textures, especially for horizons with 2:1 clay minerals, of mafic

derived soils impact subsurface flow of water differently than soils derived from felsic parent materials. Understanding the characteristics of mafic derived soils can help develop more efficient methods of determining the suitability of land for various uses.

Measuring a soil's saturated hydraulic conductivity (K_s) is essential for understanding soil water movement. Due to its ease of measurement and field estimation, soil texture is generally given the most weight when measuring K_s; however it alone can not accurately predict K_s (Lin et al., 1999). Clay mineralogy, bulk density, pedogenic structure, and cementation also influence a horizon's K_s (West et al., 2007). Some studies show that clayey horizons typically have low K_s values (Jamison and Peters, 1967; Bouma, 1980). However, other studies have shown that clayey upper Bt horizons have a higher K_s than subadjacent BC horizons, attributing the rapid movement of water through the Bt to well-developed pedogenic structure that from a network of stable macropores in kaolinitic soils with low shrink-swell potential (Bruce et al., 1983; O'Brien and Buol, 1984; Schoeneberger and Amoozegar, 1990; Schoenenberger et al., 1995; Vepraskas et al., 1996; West et al, 2007). Conversely, soils formed over basic parent rocks commonly contain 2:1 clays that expand and contribute to slow vertical percolation of water or low K_s values (Buol and Weed, 1991).

Thomas et al. (2000) found a correlation between shrink–swell potential and parent material along with drainage class; poorly drained, mafic parent material soils posed a very high shrink–swell risk while well drained, mafic parent material soils posed a moderate shrink–swell risk. Thus, soil horizons with a high to moderate shrink-swell risk will have low K_s due to the closing of pores during soil swelling, thereby affecting soil water movement. Blanco-Canqui et al. (2002), studied the K_s on claypan Alfisols in Missouri; finding that 98.5% of applied water moved laterally through the soil horizon above restrictive argillic horizons. These results suggest

that the argillic horizon acted as a barrier directing the vertical flow horizontally above the clay pan as lateral flow. The authors concluded that a perched water table is likely as these soils were saturated for several hours (Blanco-Canqui et al., 2002). Jamison and Peters (1967), and Saxton and Whitaker (1970), also reported the occurrence of lateral flow in similar clay pan soils.

The objective of this study is to establish a relationship among the subsurface perching of water, soil parent material, and landscape attributes for a landscape with soils developed from mafic rocks.

Materials and Methods

Study Area

The project site is located at the University of Georgia Central Research and Education Center in Putnam County, approximately 15 km northwest of Eatonton, Georgia (Fig 3.1). The site consists of a stream valley and encompasses the total width of the valley (Fig 3.2). Area of the site is 40.5 ha, and current land use is pasture. The site was chosen because previous studies suggested that stream flow varied along the length of the stream dissecting the watershed segment (Matthews, 2003). Soils at the site were fine and coarse-loamy, mixed, thermic, Typic Halpudalfs; Typic Paleudalfs; Oxyaquic Hapludalfs; and Uollic Albaqualfs. Soils were developed in two parent materials. Lower horizons were formed in residuum from chlorite schist (Hamilton, 2002). Upper horizons were formed in loamy transported materials deposited as colluvium (Chapter 3).

Digital Elevation Model (DEM) Generation

The first step in creating the DEM is acquiring data. For this project, data were collected in the field using the ground survey method. A CR333 Leica GPS-System was used to collect data in the field terrain, instrument parameters shown in Table 4.1. The projection for the project was set as WGS83_NAD84_UTM_zone_17N. A reference point was established at a USGS benchmark 32. Points were collected every 2 m and were only kept if they met the quality control standard of a ≤0.04 m variance from the accepted value. Once collected, points were all compiled into an ASCII text file using the SKI software package included with the GPS system. Stream elevation data were collected using the Topcon Total Station GTS 211D with a Micro Survey Tracker Extreme data collector. This is a five-second instrument meaning that the error in the angel can be within 5 seconds of the actual value. Points were collected every 6 m, on the top of each bank, mid-bank, and mid-stream. Table 4.2 shows an example of these data entries.

The XYZ file was converted into a grid file (.grd) with Surfer 7.0. The gridding methods within Surfer produce a regularly spaced array of Z values from irregularly spaced XYZ data. The first step to creating a grid within Surfer 7.0 is to set the grid line geometry which defines the grid limits and grid density, following the steps as set out by Keckler (1995) in the Surfer User's Guide. The grid limits are the maximum and minimum X and Y coordinates for the grid. The grid density is defined as the number of columns and rows within the grid. Typically, by defining the grid limits and grid density, the spacing, or size of each grid cell, is automatically determined. In this case, however, the cell size was set to 2 m in both directions and the grid density was automatically determined. Kriging generates the best overall interpretation of most

data sets (Keckler, 1995; Thompson, 2001), thus it was selected as the gridding method for this project.

Post maps, generated in Surfer 7.0, show XY locations; these maps can be useful for examining the distribution and density of the data (Keckler, 1995). Thus, a post map of the all the data collected in the field was generated (Fig. 4.2). The post map shows that there are places in the field that were not sufficiently covered, due to obstacles such as feeders, barns, trees, and roads.

Contour maps are two-dimensional representations of three-dimensional data. The first two dimensions are the XY coordinates, and the third (Z) is represented by contour lines on the map–lines of equal value (Keckler, 1995). The slope of the surface is indicated by the relative spacing between the contour lines, know as contour intervals. The narrower spacing between the contour lines would represent a steeper slope than areas were the contour lines were more widely spaced. A contour map for the ground elevations of the site was created using the initial grid file (Fig 4.3). The elevations of the site range from 166.75 m to 184.40 m, and the contour interval was set to 0.5 m. The elevations decrease as the stream is approached.

Lastly, a three-dimensional surface plot was generated in Surfer 7.0 (Fig. 4.4). On the surface plot, the X lines correspond to the columns in the grid and the Y lines correspond to the rows in the grid file (Keckler, 1995). The Z coordinates are represented by contours, drawn at the appropriate elevation on the surface; this type of surface plot is often referred to as a stacked contour plot. The surface plot is a stacked contour plot viewed with a orthographic projection. The contour interval is set to 0.25 m.

Soil Mapping

Initially, forty pedons were observed from relatively undisturbed hydraulic probe cores. Depth of observation was to probe refusal by dense saprolite (Cr horizon) which ranged from 0.5 m to 1 m deep. The locations of these pedons were determined with a Garmin 76S global positioning system (GPS) (Fig. 4.5). These pedons were observed on a grid with spacing of approximately 100 m North-South and 50 m East-West. All pedon samples were described using standard terminology (Soil Survey Staff, 1999). Horizon characteristics (texture, color, abundance of Fe/Mn nodules) were used to visually identify the depth of the discontinuity between the two parent materials. Abundance and type of redoximorphic features were also estimated. An additional forty-nine pedons located in areas with rapid changes in depth to the parent material discontinuity were described using this same process as previously described (Fig. 4.5). These additional samples were collected to narrow the grid spacing to approximately 50 m North-South and 30 m East-West and give a smoother boundary surface.

A contour map of the depth to the discontinuity was created with in Surfer 7.0 (Fig 4.6a). The boundary depths range from 0 m to 0.9 m; the contour interval is set to 0.05 m.

The elevations for each pedon described were extracted from the surface grid using the residuals function in Surfer 7.0. The depth of the lithologic discontinuity was then subtracted from these elevations and a contour map of the surface of the lower residual parent material was generated (Fig. 4.6b). This map has the same parameters as the previous map; the data ranged from 166.68 m to 184.05 m, with a contour interval of 0.5 m.

Seasonal Saturation Evaluations

Seventeen piezometers, above and below the field interpreted lithologic discontinuity, were installed throughout the site to monitor depth to the water table (Fig. 4.7). Five of the piezometers were equipped with data loggers and transducers, which record daily saturation depth measurements. At the remaining piezometers, saturation depth was measured manually on a weekly interval. To capture seasonal and annual climatic variations, monitoring continued for two years. Data collected on February 2, 2007, represent the highest water table levels observed. Data collected on August 25, 2006, represent the lowest water table levels observed. Data collected on March 15, 2006, represent intermediate water table levels. These data were subtracted from the surface elevation and then a Surfer grid file and Surfer contour map of the upper limits of water for each date was generated, using the previously described steps within Surfer 7.0 (Fig. 4.8).

K_s Measurements

K_s was measured for horizons in the colluvial parent material, the lower residual parent material, and at the boundary between these two layers. A Compact Constant Head Permeameter (CCHP) was used to measure K_s in situ (Amoozegar, 1989a). The Glover solution (Amoozegar, 1989b) was used to convert percolation rate to K_s. After saturation, measurements were taken every 5 minutes at for the upper parent material and at the lithologic discontinuity and every 30 min for the lower parent material horizons with a head of approximately 15 cm.

Results and discussion

Saturated Hydraulic Conductivity

The site had a well established fescue cover, and surface horizons were loam to clay loam textured, relatively dark, and well structured (Appendix A). Thus, rainfall infiltration would be expected to be moderate to high with minimal physical impediment to infiltration.

Field descriptions and pedon data, i.e. abrupt changes in the clay content, S:Si ratios, and COLE measurements, provided sufficient evidence of two parent materials for the soils on our project site, an upper colluvial material underlain by residuum (Table 3.2). Horizons developed in the upper parent material were loam, friable, and had weak to moderate structure, allowing water to move through these horizons relatively quickly. The residual parent material has more clay and greater shrink/swell potential than the colluvial parent material (Table 3.2, Appendix A). As water moves into the clayey horizons derived from the residual parent material, swelling will restrict water movement, and water is forced to flow laterally above these restrictive horizons. Saturated hydraulic conductivity (K_s) measurements support the hypothesized restrictive nature of the clayey residual horizons. Mean K_s of horizons in the upper colluvial parent material were similar at both depths evaluated with a mean of 0.2 cm/hr (Table 3.3). Mean K_s of horizons in the residual parent material was 0.02 cm/hr which was significantly lower than K_s of the horizons in the colluvial material (Table 3.3). Vepraskas suggested that flow is dominantly lateral in a horizon of higher K_s if the K_s values differ by 10 fold or more. The mean K_s of horizons developed inthe residual parent material (0.02 cm/hr) was 10 fold lower than the mean K_s (0.2 cm/hr) of the upper colluvial parent material (Fig 4.9). This data suggests that water is perching at the lithologic discontinuity and moving laterally downslope.

Parent Material Thickness and Distribution

Thickness of the loamy colluvial parent material ranged from 10 to 120 cm across the study site (Fig 4.6A). For this discussion, all non-clayey surficial horizons are considered to be developed in colluvial materials although for thin (< 30 cm) A and E horizons overlying residual Bt horizons it is not possible to differentiate textural differences due to parent material differences from those resulting from pedogenic processes. The downstream (SE) half of the watershed segment generally had colluvial material less than 30 cm thick although colluvial materials were up to 50 cm thick in a few small areas (Fig 4.6A).

The upstream (NW) portion of the watershed segment had thickness of colluvial materials that ranged from 10 to 120 cm (Fig 4.6A). Thickness of the colluvial materials was irregular and the thicker areas appear on the figure as pockets. A portion of the irregular thickness shown on the map, however, may be related to the limited data upon which the map was generated. The deep pockets are generally along lines roughly normal to the stream, and may represent erosion features in the residuum surface. These linear features are visible on the map of the residuum surface although they are subdued (Fig 4.6B).

The colluvial material in the downstream half of the site has a volume of 49,000 m^3, while the colluvium volume on the upstream half of the site was 90,000 m^3. Assuming the restrictive residual horizon allows little to no water to penetrate through, the colluvial horizon, based on bulk density measurements (Table 3.2), the upstream half of the site has 34,000 m^3 of potential water storage. In contrast, potential water storage in the colluvium in the downstream half of the site is 18,000 m^3, a difference of 16,000 m^3. The lower potential storage capacity of the downstream half of the site, results in relatively quick saturation of the colluvial parent

material and greater amounts of saturation induced runoff as compared to the upstream watershed segment with thicker colluvium.

In a prior study at this site, the reach of stream flowing through the downstream half of the site received more water from the surrounding area than reach of stream flowing through the upstream half of the site (Matthews, 2003). The area of both halves is approximately the same area, 710,932 m^2. The stream data fluctuated with rainfall events in both halves of the site. However, the downstream watershed segment had appreciably more flow from runoff than the upstream segment (Fig 4.7)

Since the contributing areas of both stream segments are roughly the same area (710,932 m^2) the flow volumes in the upstream and downstream segments should be similar. We hypothesize that the difference in water delivered to the stream (stream flow) is related to the thickness and potential water storage of the loamy colluvial materials at the site. In the upstream segment, the net flow volume for the three year period of measurement is -6,966,757 m^3, whereas the net flow volume for the three year period was 95,252,389 m^3 for the downstream segment. The upstream segment is adjacent to a forested area, which may account for some of the loss due to evapotranspiration (ET). Also, the thicker, more extensive colluvium in the upstream segment allows for greater infiltration (less runoff). The thinness of the colluvium in the downstream segment causes saturated induced runoff sooner than the thicker colluvium in the upstream segment. This runoff, in addition to subsurface lateral flow above residuum, causes the net flow volume for the downstream segment to be much greater than the net flow volume for the upstream segment.

Water table elevations for three piezometer transects (Fig. 4.8) on three dates were used to evaluate interflow through the colluvium. Water was measured in all piezometers on February

2, 2007 which represent the highest water table levels for our site. Our site received 3.07 cm rain in the week prior to this date; overall, the rainfall for February 2007 was normal based on the direct antecedent rainfall method (Table 3.4). Piezometers 11, 12, and 16 were all dry on March 15, 2006, representing intermediate water table levels for our site. Rainfall for the prior week was 1.6 cm; overall, the rainfall for March 2006 was normal (Table 3.4). Piezometers 3, 4, 7, 8, 10, 11, 12, and 16 were all dry on August 25, 2006, representing lowest water table levels on our site. Rainfall for the prior week was 2.2 cm. Overall, the rainfall for August 2006 was drier than normal (Table 3.4)

Transect 1 cross-section, running from site 1 down slope to site 3, represents the upper half of the site. The upper colluvial parent material is thickest in this upstream half of the project site, meaning that more water is being stored in this area and less water is flowing into the stream (Fig. 4.11). The colluvial parent material is nearly 1 m thick at the beginning of the transect, thinning to 0.5 meter, then thickening again to 1.1 m before thinning out to 0.3 m near the stream. The high water levels on February 2, 2007, show perching of the water in the upper parent material. Water flows down slope towards the stream, thus the water table levels are closer to the ground surface in the lower elevations near the stream (Site 3) than the higher elevations (Site 1). The intermediate water table levels are still in the colluvial parent material at the upper end of the transect (Fig 4.11). Water is closer to the ground surface at the lower elevations, near the stream, although it is now below the lithologic discontinuity. The piezometers at Sites 2 and 3 were below measurable limits on August 25, 2006 (Fig 4.11). Although water was measured in the piezometer at Site 1, the level indicates that water during dry periods, the water table was below the colluvial parent material and any lateral movement through horizons in the residuum would be slow.

Transect 2 cross-section, running from site 5 downslope to site 7, represents the middle portion of the site (Fig. 4.12). The colluvial parent material is thinner here than it was at Transect 1. The colluvial parent material at this transect is also thickest in the lower hillslope positions (middle and lower backslope, footslope), and thinner on the shoulder because the colluvium was thin. Only one piezometer was placed at Site 5 instead of nesting a deep and shallow piezometer. Therefore, the water levels do not represent any perching of water above the lower residual parent material. On February 2, 2007, the high water table levels were at the colluvium-residuum interface at Site 6 and within the colluvial parent material at Site 7. Again, water moving downhill causes water table levels to be closer to the ground surface in the elevations near the stream. The intermediate water table levels were below the surface of the lower residual parent material except near the stream at Site 7. When water table levels are low, the measurements showed water levels only in the lower residual parent materials at downslope parts of the transect. The piezometers at site 6 and 7 were below the limit of measurement on August 25, 2006.

Transect 3 cross-section running from site 12 to site 10 then to site 11 is shown in Figs. 4.13. This transect is representative of the downstream half of the site. The colluvial parent material is thinnest on this portion of the project site, ranging from 0 cm to 35 cm. Also due to the thinness of the colluvium, any perching occurring here is not evident with the piezometer data because wells were only installed below the loamy colluvial parent material. The high water table measurements taken on February 2, 2007, show the water level gets closer to the surface downslope. The piezometer at site 12 was below the limit of measurement on March 15, 2006 and August 25, 2006. Site 10 is located near a small ditch that runs perpendicular to the stream, causing an upward jump in the water table data between 60 and 80 m on the transect.

Overall, the water tables at this transect show similarities to those of the other transects, the water table levels in the lower hillslope positions are closer to the ground surface. Water is moving downhill, towards the stream and drainage ditch.

Conclusions

1. The mean K_s of the horizons developed in the residual parent material (0.02 cm/hr) was 10 fold lower than the mean K_s (0.2 cm/hr) of the upper colluvial parent material. This data suggest that water is perching at the lithologic discontinuity and moving laterally downslope.
2. The depth to this lithologic discontinuity on our site is not uniform. However, certain trends can be noted. The backslope and footslope positions have the thickest capping of colluvial parent material. Also, a perched water table above the restrictive residual parent material can be observed when the colluvial parent material is found in appreciable amounts (> 0.5 m).
3. The water storing capacity of the site is dictated by the thickness of this colluvium. The upstream half of the site, with twice the amount of colluvial parent material, has nearly twice the water storing capacity of the downstream half, allowing less flow into the stream.
4. The thinner colluvium on the downstream half causes saturated induced flow to occur sooner than on the upstream half, thereby increasing the amount of runoff and decreasing the amount of infiltration and potential for evapotranspiration. This runoff, in combination with subsurface lateral flow above residuum, results in a much greater net flow volume for the downstream segment than for the upstream segment.

References

American Geological Institute. 1976. Dictionary of Geologic Terms. Anchor Press/Doubleday, Garden City, NY.

Amoozegar, A. 1989a. A compact constant-head permeameter for measuring saturated hydraulic conductivity of the vadose zone. Soil Sci. Soc. Am. J. 53:1356-1361.

Amoozegar, A. 1989b. Comparison of the Glover solution with the simultaneous-equations approach for measuring hydraulic conductivity. Soil Sci. Soc. Am J. 53:1362-1367.

Blanco-Canqui, H., C.J. Gantzer, S.H. Anderson, E.E. Alberts, and F. Ghidey. 2002. Saturated hydraulic conductivity and its impact on simulated runoff for claypan soils. Soil Sci. Soc. Am. J. 66:1596-1602.

Bouma, J., P.M. de Laat, A.F. van Holst, and T.J. van de Nes. 1980. Predicting the effects of changing water–table levels and associated soil moisture regimes for soil survey interpretations. Soil Sci. Soc. Am. J. 44:797–802.

Bresler, E., Dagan, G.,Wagenet, R.J., Laufer, A., 1984. Statistical analysis of salinity and texture effects on spatial variability of soil hydraulic properties. Soil Sci. Soc. Am. J. 48, 16–25.

Bruce, R.R., J.J. Dane, V.L. Quisenberry, N.L. Powell, and A.W. Thomas. 1983. Physical characteristics of soils in the Southern Region: Cecil. Southern Coop. Series Bull. p. 267

Buol, S.W., and S.B. Weed. 1991. Saprolite–soil transformations in the Piedmont and mountains of North Carolina. Geoderma 51:15–28.

Davey, B.G., 1990. The chemical properties of soils. In: Campbell, K.O., Bowyer, J.W. (Eds.), Scientific Basis of Modern Agriculture. Sydney University Press, Sydney, Australia (Ch. 4).

Frenkel, H., Goertzen, J.O., Rhoades, J.D. 1978. Effects of clay type and content, exchangeable sodium percentage, and electrolyte concentration on clay dispersion and soil hydraulic conductivity. Soil Sci. Soc. Am. J. 42, 32–39.

Hamilton, D.A. 2002. Mafic and felsic derived soils in the Georgia Piedmont: Parent material uniformity, reconstruction, and trace metal contents. M.S. thesis Univ. Georgia, Athens, GA.

Hamilton–Wood, D.A., L.T. West, and P.A. Schroeder. 2002. Weathering sequences of contrasting mafic and felsic parent materials in the Georgia Piedmont, US. Proc. 17th World Cong. Soil Sci., Aug. 14–21, 2002., Bangkok, Thailand. p. 871–1 – 875–9

Jabro, J.D., 1992. Estimation of saturated hydraulic conductivity of soils from particle size distribution and bulk density data. Trans. ASAE 35, 557–560.

Jamison, V.C. and D.B. Peters. 1967. Slope length of claypan soil affects on runoff. Water Resour. Res. 3:471-480.

Keckler, D. 1995. Surfer for Windows user's guide: contouring and 3D surface mapping. Version 6. Golden Software, Inc.

Lin, H.S., K.J. McInnes, L.P. Wilding, and C.T. Hallmark. 1999. Effects of soil morphology on hydraulic properties: I. Quantification of soil morphology. Soil Sci. Soc. Am. J 63:948-954.

Matthews, M. 2003. Water quality in fenced and unfenced stream reaches flowing through grazing pastures in the southern Piedmont. M.S. thesis Univ. Georgia, Athens, GA.

O'Brien, E.L., and S.W. Boul. 1984. Physical transformations in a vertical soil-saprolite sequence. Soil Sci. Soc. Am. J. 48:354-357.

Ogg, C.M., and B.R. Smith. 1993. Mineral transformation in Carolina Blue Ridge–Piedmont soils weathered from ultramafic rocks. Soil Sci. Soc. Am. J. 57:461–472.

Rabenhorst, M.C., and J.E. Foss. 1981. Soil and geologic mapping over mafic and ultramafic parent materials in Maryland. Soil Sci. Soc. Am. J. 45:1156-1160.

Rice, Jr., T.J., S.W. Boul, and S.B. Weed. 1985. Soil-saprolite profiles derived from mafic rocks in the North Carolina piedmont: I. Chemical, morphological, and mineralogical characteristics and transformations. Soil Sci. Soc. Am. J. 49:171–178.

Saxton, K.E., and F.D. Whitaker. 1970. Hydrology of a claypan watershed. Res. Bull. 974, Missouri Agric. Exp. Stn., Columbia, MO.

Schoeneberger, P.J., and A. Amoozegar. 1990. Directional saturated hydraulic conductivity and macropore morphology of a soil-saprolite sequence. Geoderma 46:31-49.

Schoeneberger, P.J., A. Amoozegar, and S.W. Boul. 1995. Physical property variation of soil and saprolite continuum at three geomorphic positions. Soil Sci. Soc. Am. J. 59:1389-1397.

Schroeder, P.A., N.D. Melear, L.T. West, and D.A. Hamilton. 2000. Meta–gabbro weathering in the Georgia Piedmont, USA: Implications for global silicate weathering rates. Chem. Geol. 163:235–245.

Soil Survey Staff. 1999. Soil Taxonomy. A basic system of soil classification for making and interpreting soil surveys. 2nd Ed. USDA-NRCS. U.S. Government Print. Office, Washington, D.C.

Thomas, P.J., J.C. Baker, and L.W. Zelanzy. 2000. An expansive soil index for predicting shrink-swell potential. Soil Sci. Soc. Am. J. 64:268-274.

Thompson, J.A., J.C. Bell, and C.A. Butler. 2001. Digital elevation model resolution: effects on terrain attribute calculation and quantitative soil-landscape modeling. Geoderma 100:67-89.

Vepraskas, M.J., W.R. Guertal, H.J. Kleiss, and A. Amoozegar. 1996. Porosity factors that control the hydraulic conductivity of soil-saprolite transition zones. Soil Sci. Soc. Am. J. 60:192-199.

West, L.T., M.A. Abreu, and J.P. Bishop. 2007. Saturated hydraulic conductivity of soils in the Southern Piedmont of Georgia, USA: Field evaluation and relation to horizon and landscape properties. Catena. Available online.

Table 4.1. Leica GPS-system parameters

	Reference	Rover
Health/L2 mode	AUTO	AUTO
Minimum elevation	15°	15°
Operation type	Static	Kinematic on the fly
Compacted/Sampled	Compacted	Compacted
Obs. rec–rate static	2 sec	2 sec
Obs. rec–rate moving	Does not apply	2 sec

Table 4.2. Sample entries for elevation data

Point ID	X Coordinates	Y Coordinates	Z Coordinates	CQ
		Meters		
1	272445.1576	3698022.641	178.7165	0.023
2	272443.2737	3698014.125	176.6107	0.028
3	272443.47	3698020.51	178.5413	0.023
4	272442.9603	3698020.376	178.5289	0.023
5	272445.417	3698023.307	178.7299	0.023
6	272447.5903	3698025.052	178.8747	0.023
7	272451.3627	3698028.641	178.9426	0.023
8	272453.7414	3698030.893	178.9573	0.023
9	272456.4031	3698033.672	178.9824	0.023
10	272457.9202	3698035.238	178.981	0.023
11	272459.8257	3698037.097	178.9254	0.023
12	272463.8976	3698040.883	178.8098	0.023
13	272465.9231	3698042.866	178.7212	0.023
14	272471.7283	3698048.61	178.476	0.023
15	272474.6876	3698051.646	178.1928	0.023
16	272477.3278	3698054.154	177.975	0.023
17	272479.8004	3698056.471	177.8599	0.023
18	272486.6997	3698063.34	177.3938	0.023
19	272500.6062	3698076.983	177.0172	0.023
20	272504.0368	3698080.267	176.9952	0.023
21	272506.8167	3698083.021	176.9822	0.023
22	272508.6096	3698084.853	176.9606	0.023
23	272511.1516	3698087.376	176.9698	0.023
24	272515.4932	3698089.297	176.8671	0.023
25	272517.6135	3698088.24	176.8131	0.023
26	272516.6207	3698088.78	176.8279	0.023
…	…	…	…	…
…	…	…	…	…
…	…	…	…	…
60213	272401.73	3698531.52	175.54944	0.5
60214	272403.39	3698514.56	176.354112	0.5
60215	272399.31	3698515.96	175.131864	0.5
60216	272395.4	3698496.41	174.921552	0.5
60217	272386.23	3698481.65	174.58932	0.5

Table 4.3. Mean K_s of horizons of pedons evaluated data.

	Sample Number	Range	Mean	SE[†]
		cm/hr	cm/hr	
Upper Parent Material	5	0.1 - 0.6	0.2 A	0.08
Lithologic Contact[‡]	5	0.1 - 0.4	0.2 A	0.08
Residual Parent Material	5	0.01 - 0.04	0.02 B	0.02

[†]SE = standard error of the mean.

[‡]Horizon immediately overlying the parent material change.

[*]Means with the same letter within the same column showed no statistical difference (multiple t-test adjusted for heterogeneous variances, $\alpha = 0.05$).

Fig. 4.1. Site Map

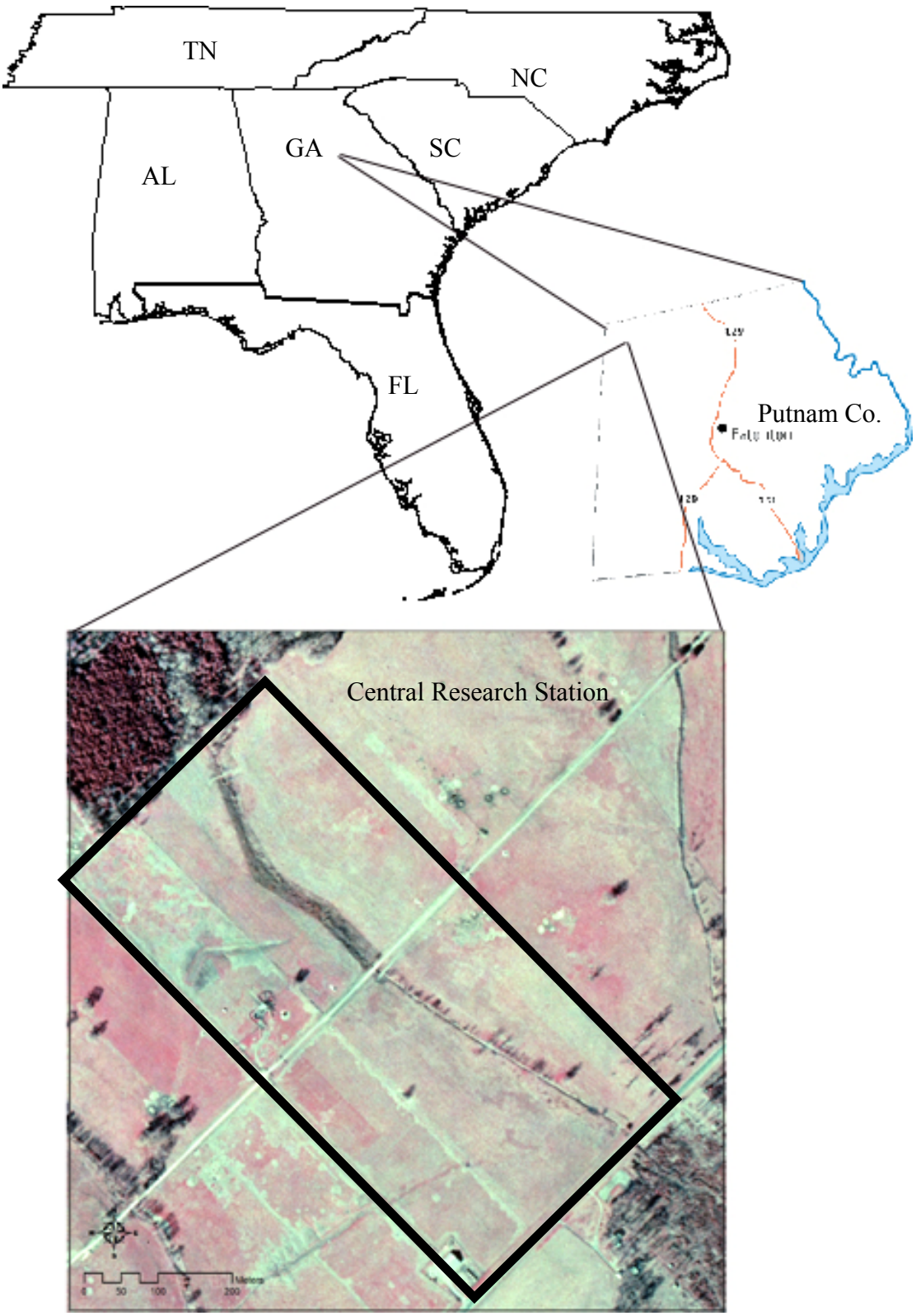

Fig. 4.2. Points taken during surface elevation survey.

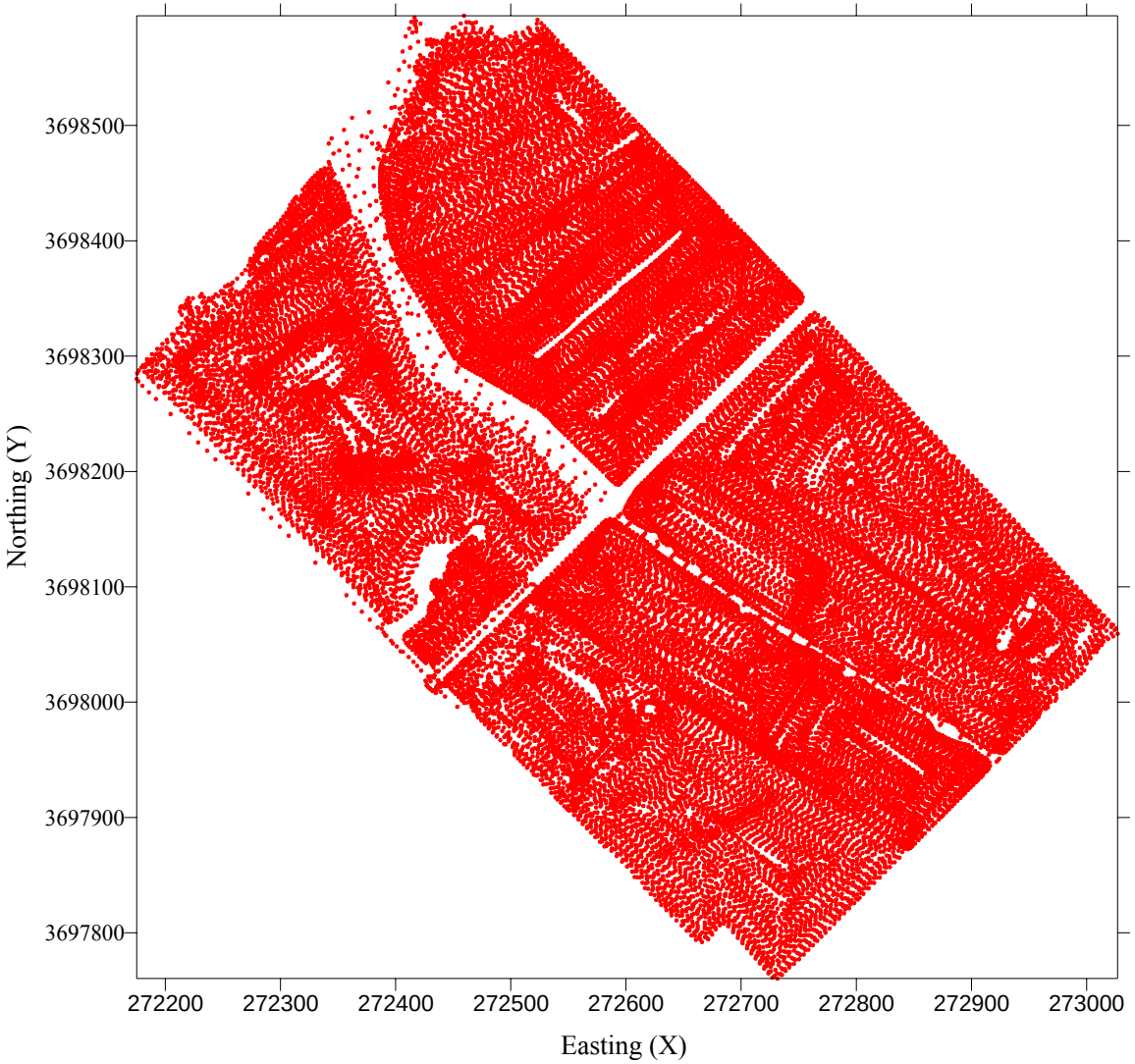

Fig. 4.3. Contour map of ground surface elevations. Contour interval is 0.5 m.

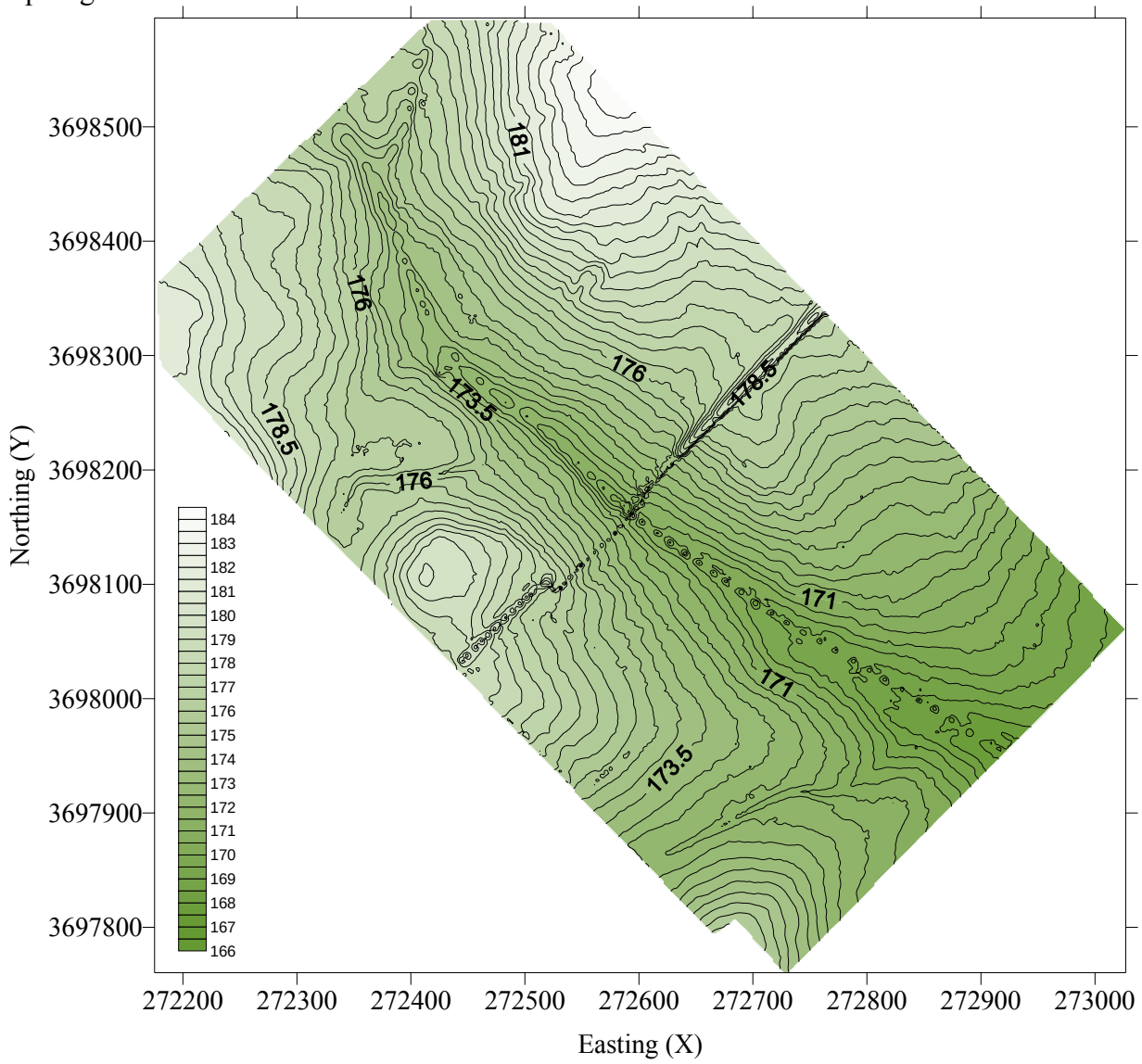

Fig. 4.4. Surface elevation plot of project site (vertical exaggeration 12X). Contour interval is 0.25 m.

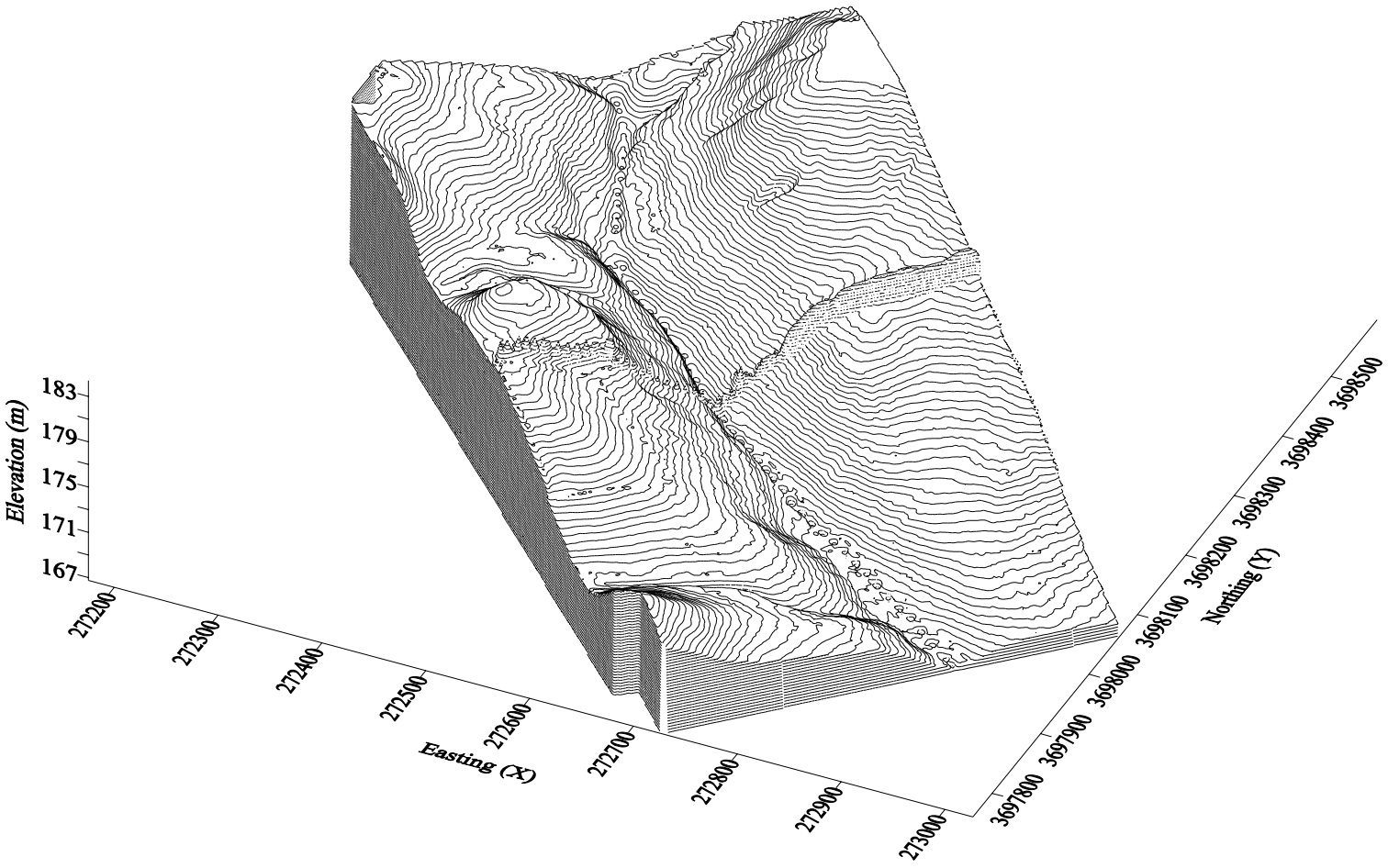

Fig. 4.5. Pedon locations and depth of the lithologic discontinuity contact.

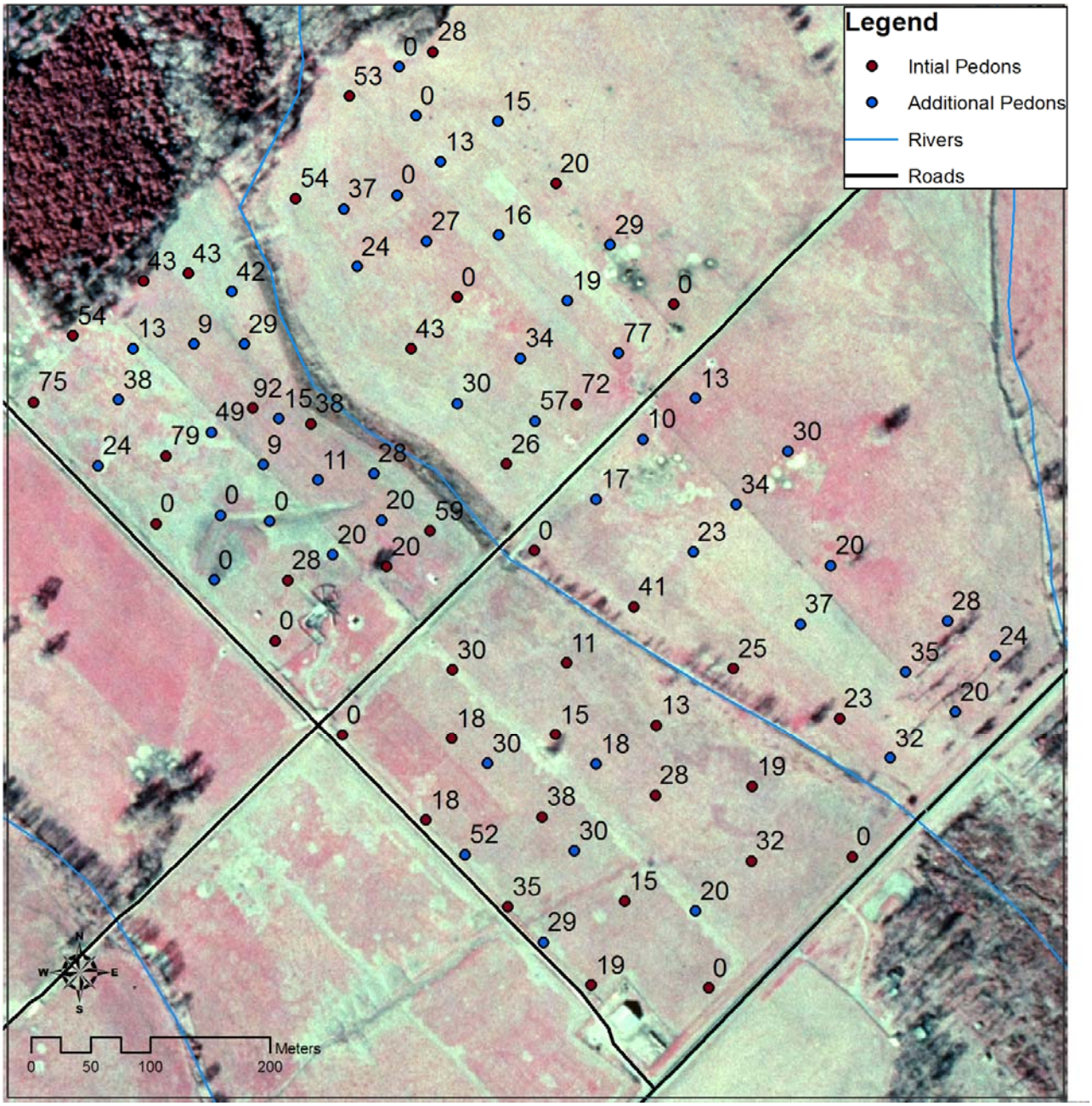

Fig. 4.6. A) Contour map of the depth to the lithologic discontinuity. The contour interval is 0.05 m; B) Contour map of the surface of the lower residual parent material ranging from 166.68 m to 184.05 m, with a contour interval of 0.5 m .

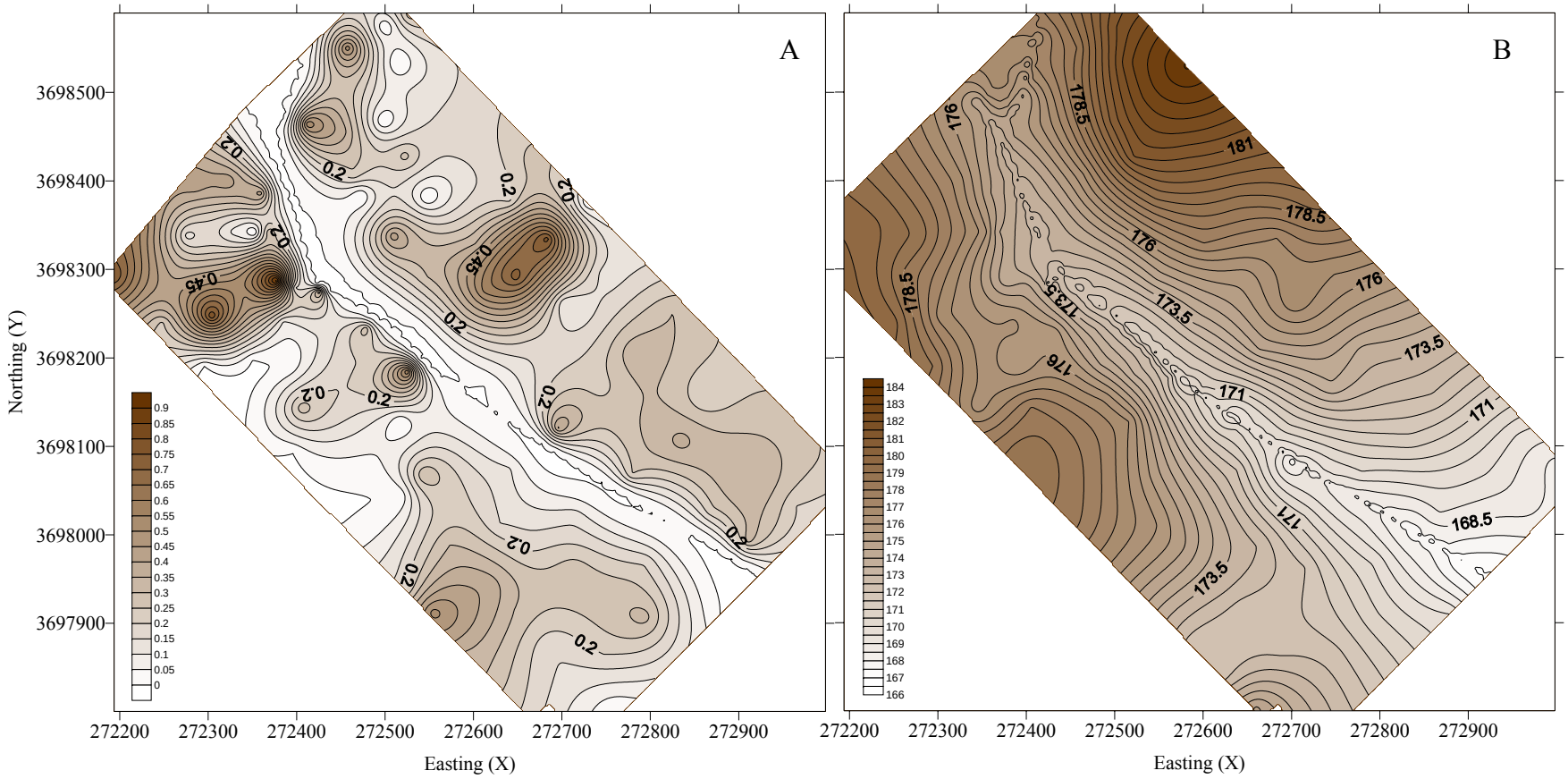

Fig. 4.7. Piezometer locations on project site. Wells 1, 2, 14, 15, and 17 were equipped with data loggers that took daily readings. Remaining wells were manually read weekly.

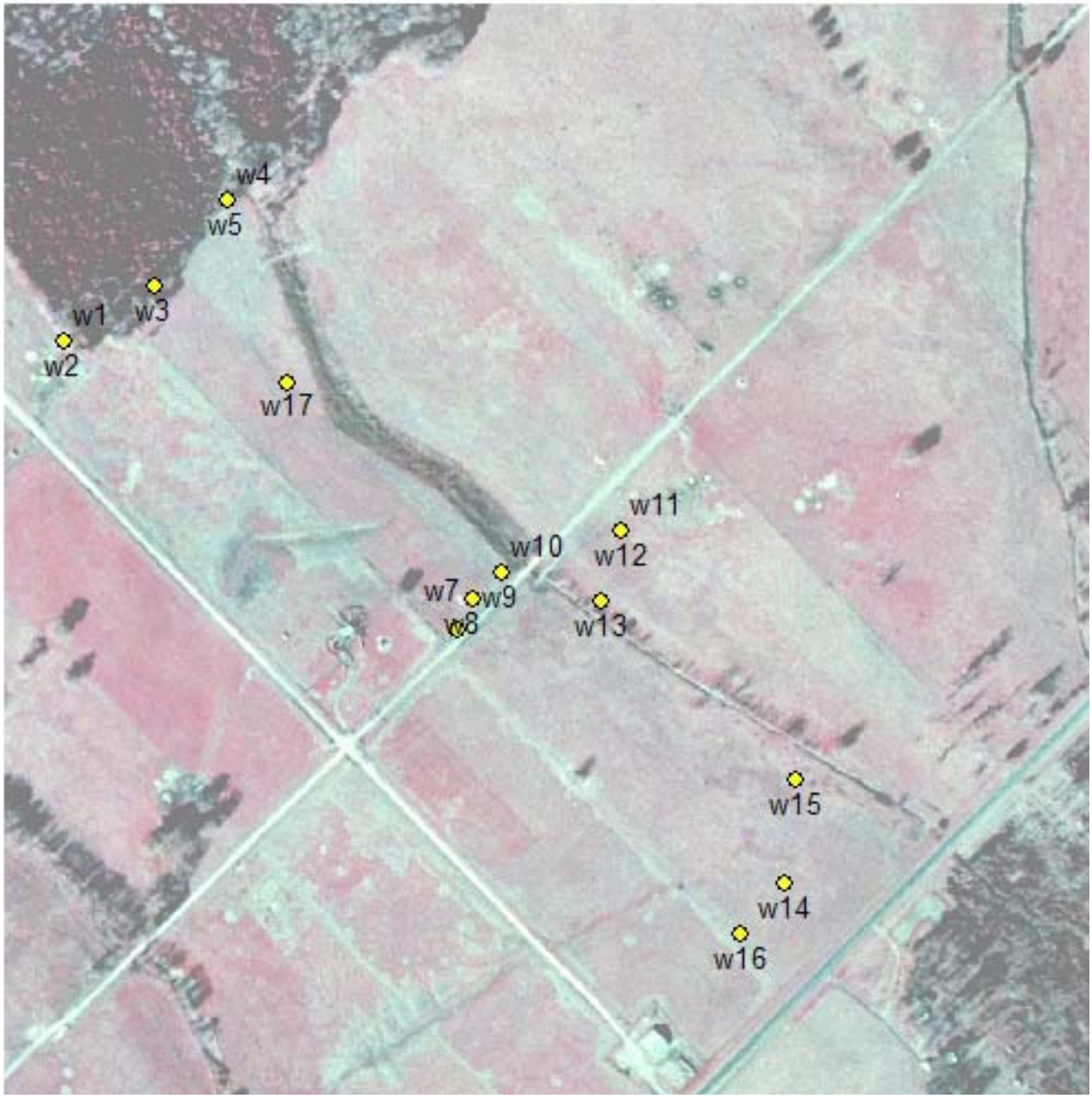

Fig. 4.8. Contour map of upper boundary elevations of the water table levels. A) Data collected on February 2, 2007 representative of highest water table level; B) Data collected on March 15, 2006 representative of the intermediate water table level; C) Data collected on August 25, 2006 representative of lowest water table level. Contour interval is 0.5 m.

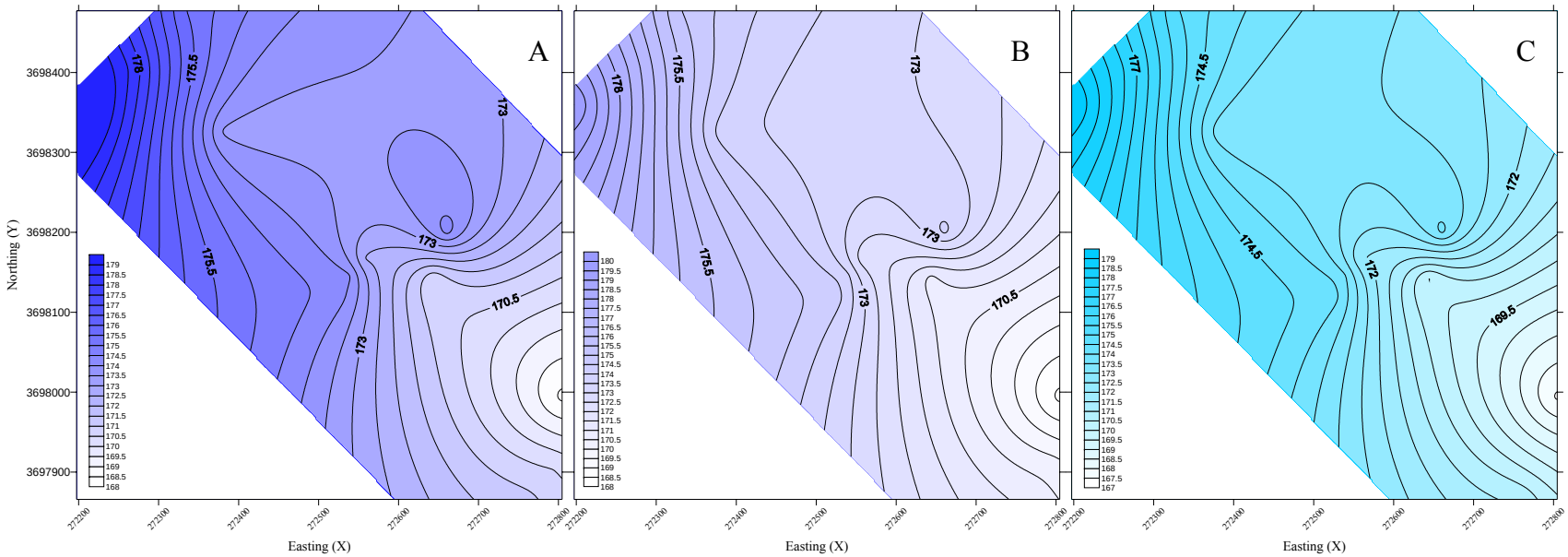

Fig 4.9. Rainfall and contributions to stream flow from the upstream and downstream halves of site for A) 2001; B) 2002; and C) 2003. Watershed segment contributions were based on differences in flow measured at the two ends of the two stream reaches

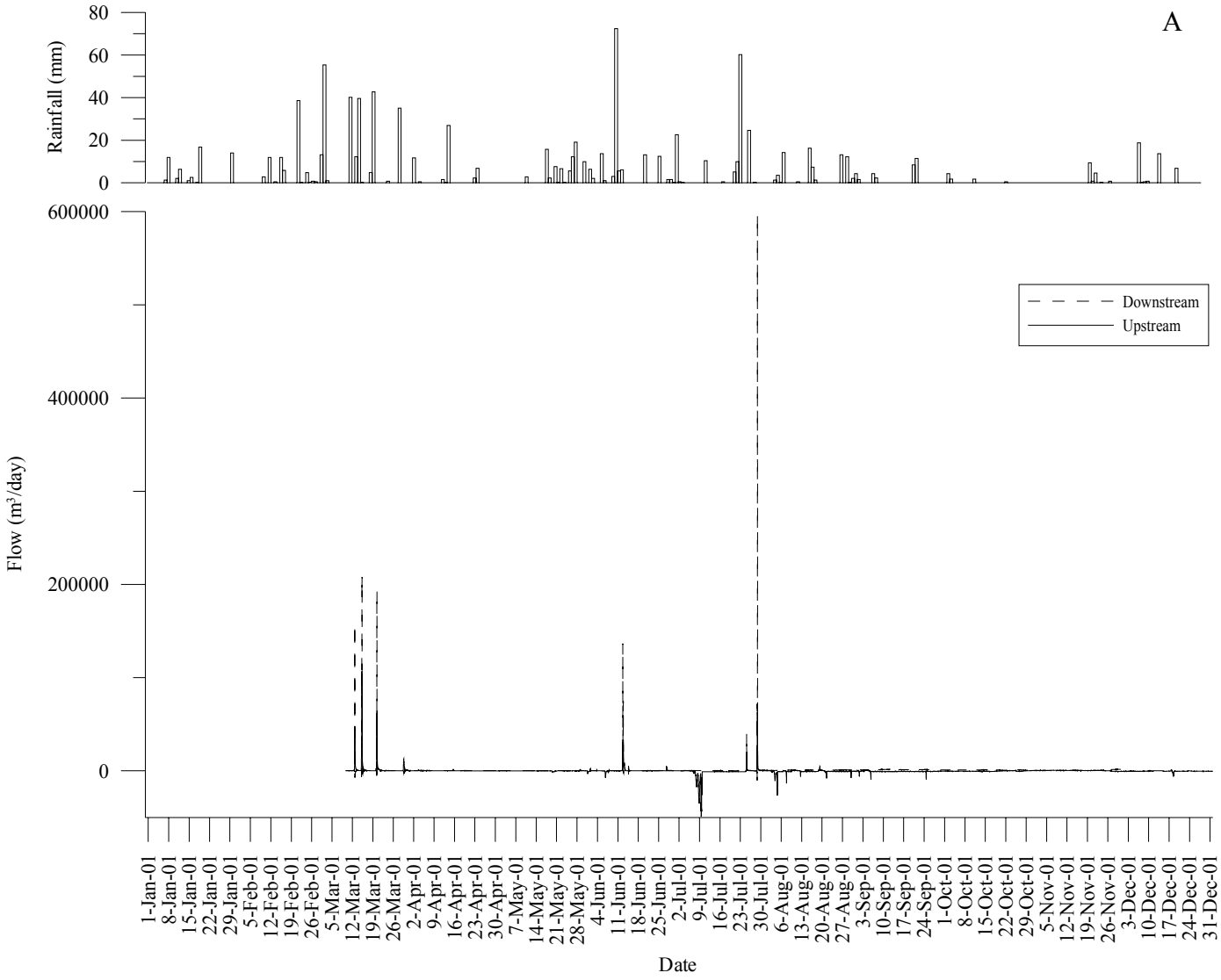

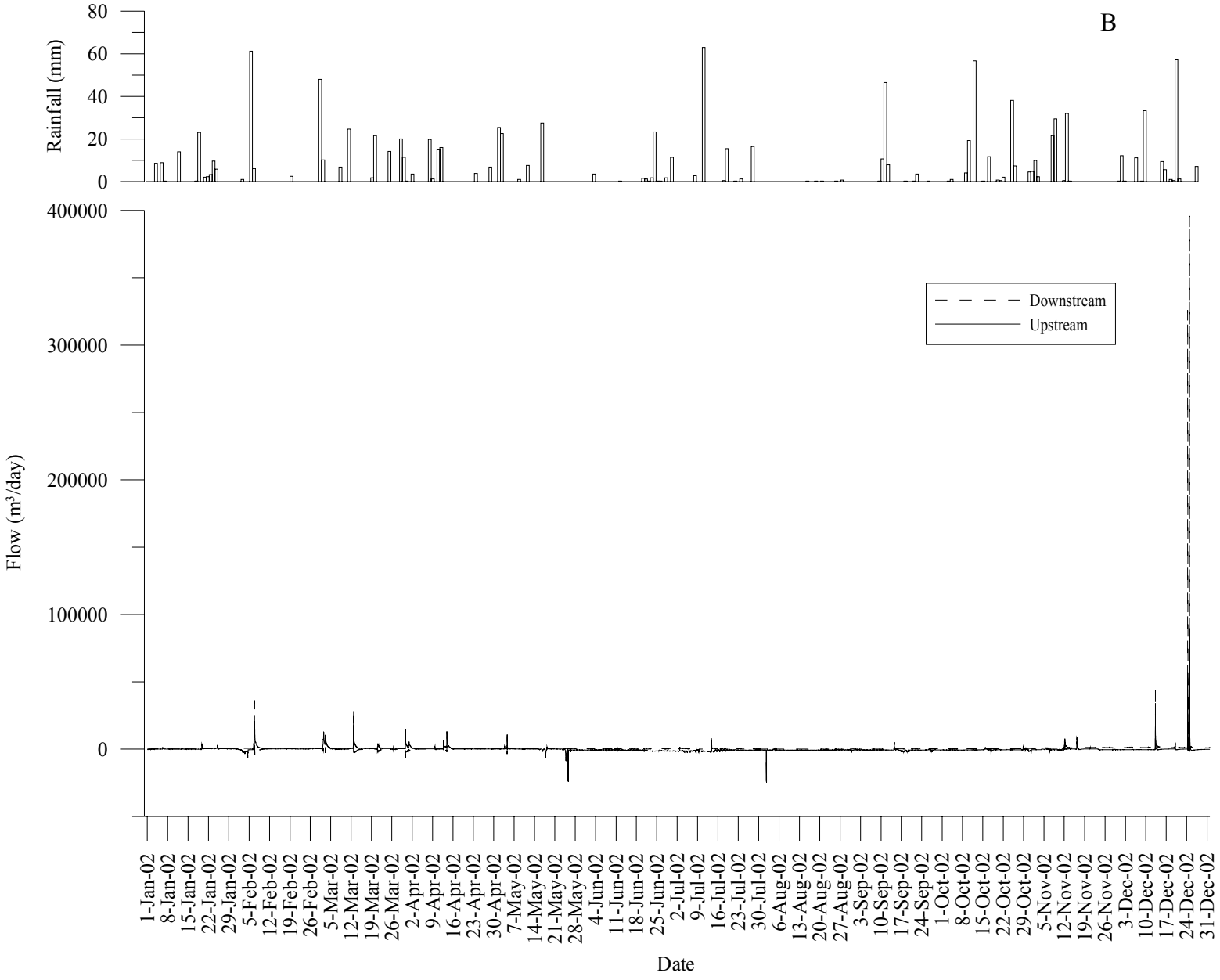
B
Rainfall (mm)
80
60
40
20
0
400000
300000
200000
100000
0
Flow (m³/day)
Downstream
Upstream
1-Jan-02
8-Jan-02
15-Jan-02
22-Jan-02
29-Jan-02
5-Feb-02
12-Feb-02
19-Feb-02
26-Feb-02
5-Mar-02
12-Mar-02
19-Mar-02
26-Mar-02
2-Apr-02
9-Apr-02
16-Apr-02
23-Apr-02
30-Apr-02
7-May-02
14-May-02
21-May-02
28-May-02
4-Jun-02
11-Jun-02
18-Jun-02
25-Jun-02
2-Jul-02
9-Jul-02
16-Jul-02
23-Jul-02
30-Jul-02
6-Aug-02
13-Aug-02
20-Aug-02
27-Aug-02
3-Sep-02
10-Sep-02
17-Sep-02
24-Sep-02
1-Oct-02
8-Oct-02
15-Oct-02
22-Oct-02
29-Oct-02
5-Nov-02
12-Nov-02
19-Nov-02
26-Nov-02
3-Dec-02
10-Dec-02
17-Dec-02
24-Dec-02
31-Dec-02
Date

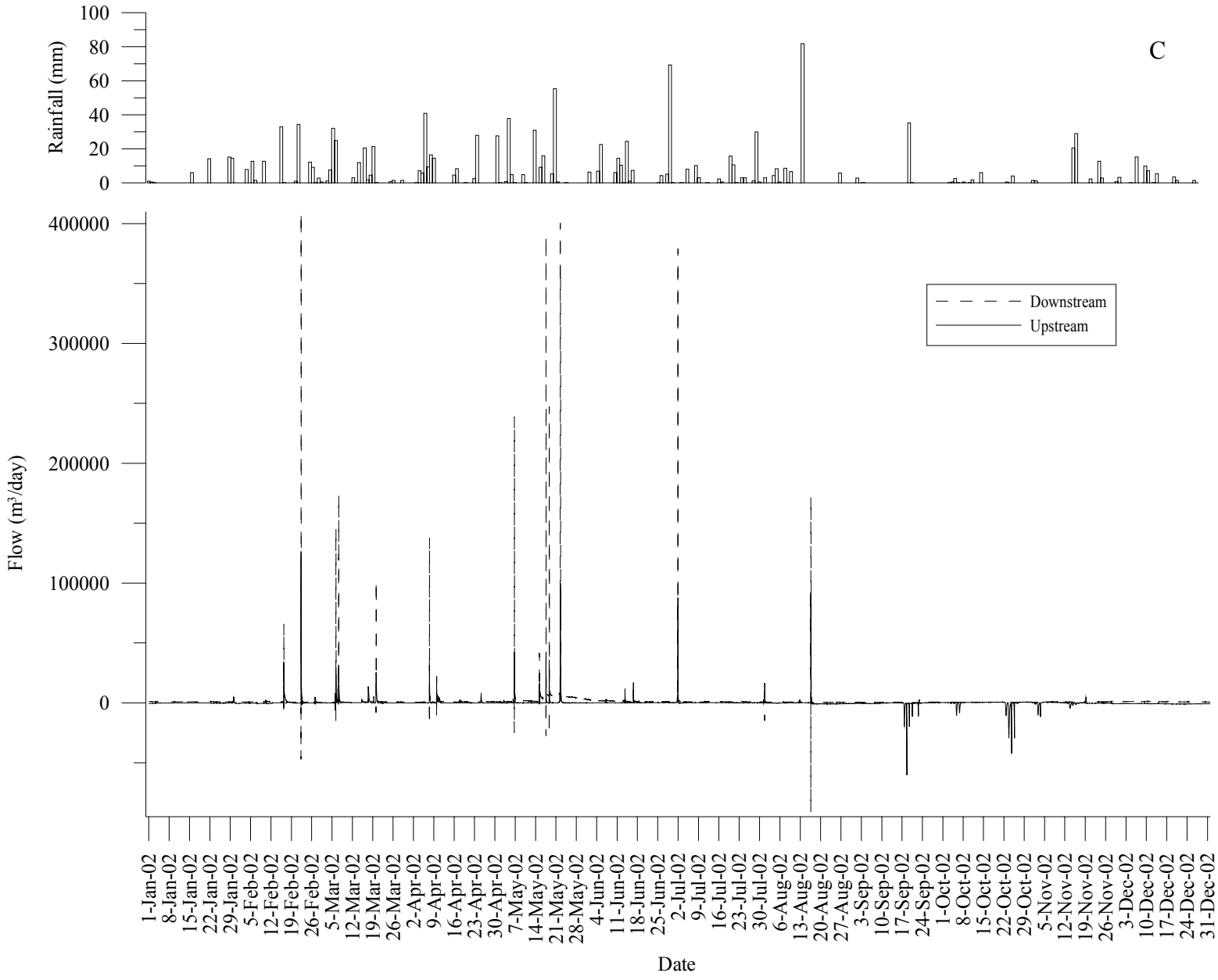
C
Rainfall (mm)
100
80
60
40
20
0
Flow (m³/day)
400000
300000
200000
100000
0
Downstream
Upstream
1-Jan-02
8-Jan-02
15-Jan-02
22-Jan-02
29-Jan-02
5-Feb-02
12-Feb-02
19-Feb-02
26-Feb-02
5-Mar-02
12-Mar-02
19-Mar-02
26-Mar-02
2-Apr-02
9-Apr-02
16-Apr-02
23-Apr-02
30-Apr-02
7-May-02
14-May-02
21-May-02
28-May-02
4-Jun-02
11-Jun-02
18-Jun-02
25-Jun-02
2-Jul-02
9-Jul-02
16-Jul-02
23-Jul-02
30-Jul-02
6-Aug-02
13-Aug-02
20-Aug-02
27-Aug-02
3-Sep-02
10-Sep-02
17-Sep-02
24-Sep-02
1-Oct-02
8-Oct-02
15-Oct-02
22-Oct-02
29-Oct-02
5-Nov-02
12-Nov-02
19-Nov-02
26-Nov-02
3-Dec-02
10-Dec-02
17-Dec-02
24-Dec-02
31-Dec-02
Date

Fig. 4.10. Map showing transect locations on soil surface.

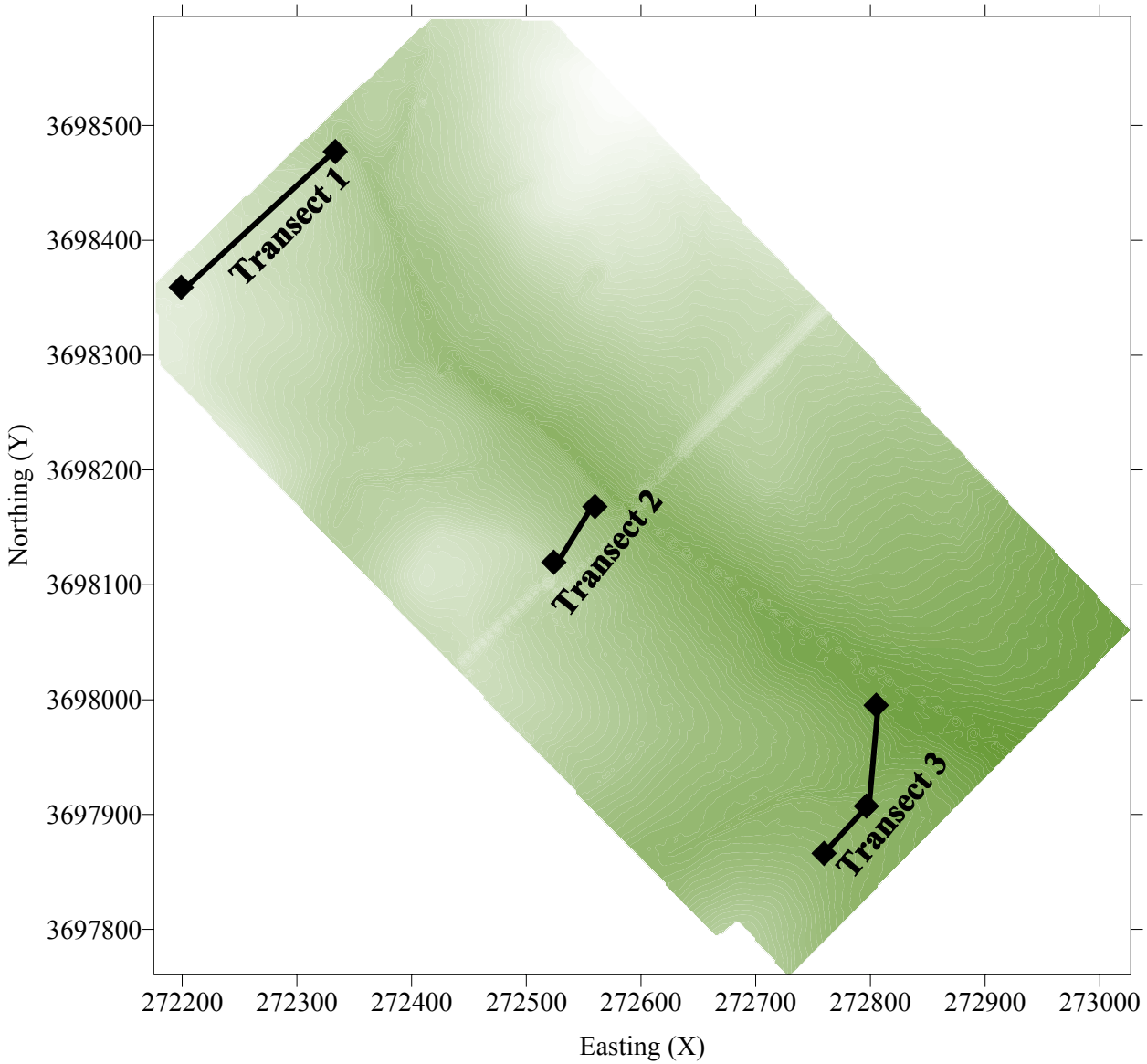

Fig. 4.11. Cross-section of Transect 1 (piezometers 2, 3, and 5) showing surface elevations, surface of lower residual parent material, and water table elevations.

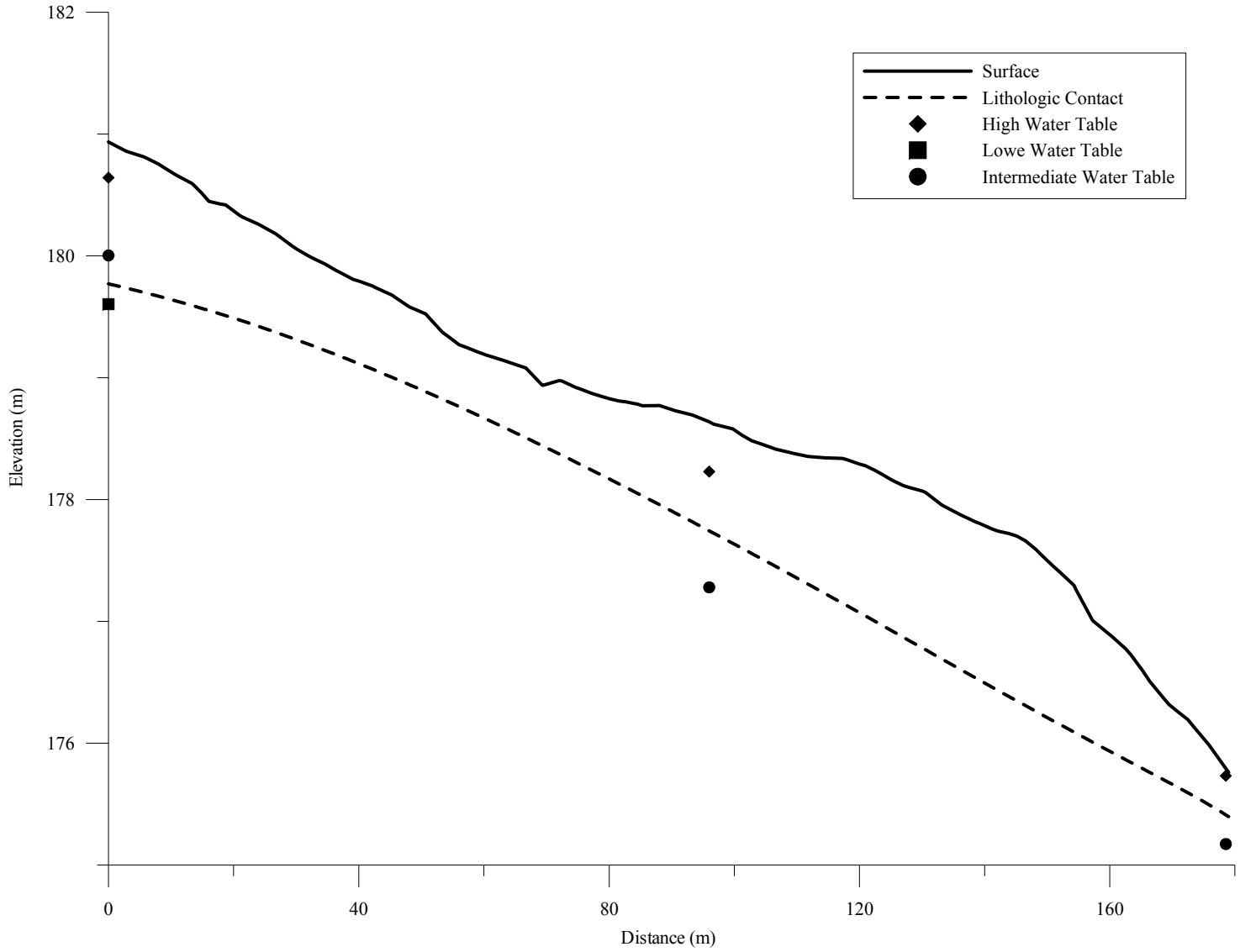

Fig. 4.12. Cross-section of transect 2 (piezometers 6, 8, and 10) showing surface elevations, surface of lower residual parent material, and water table elevations.

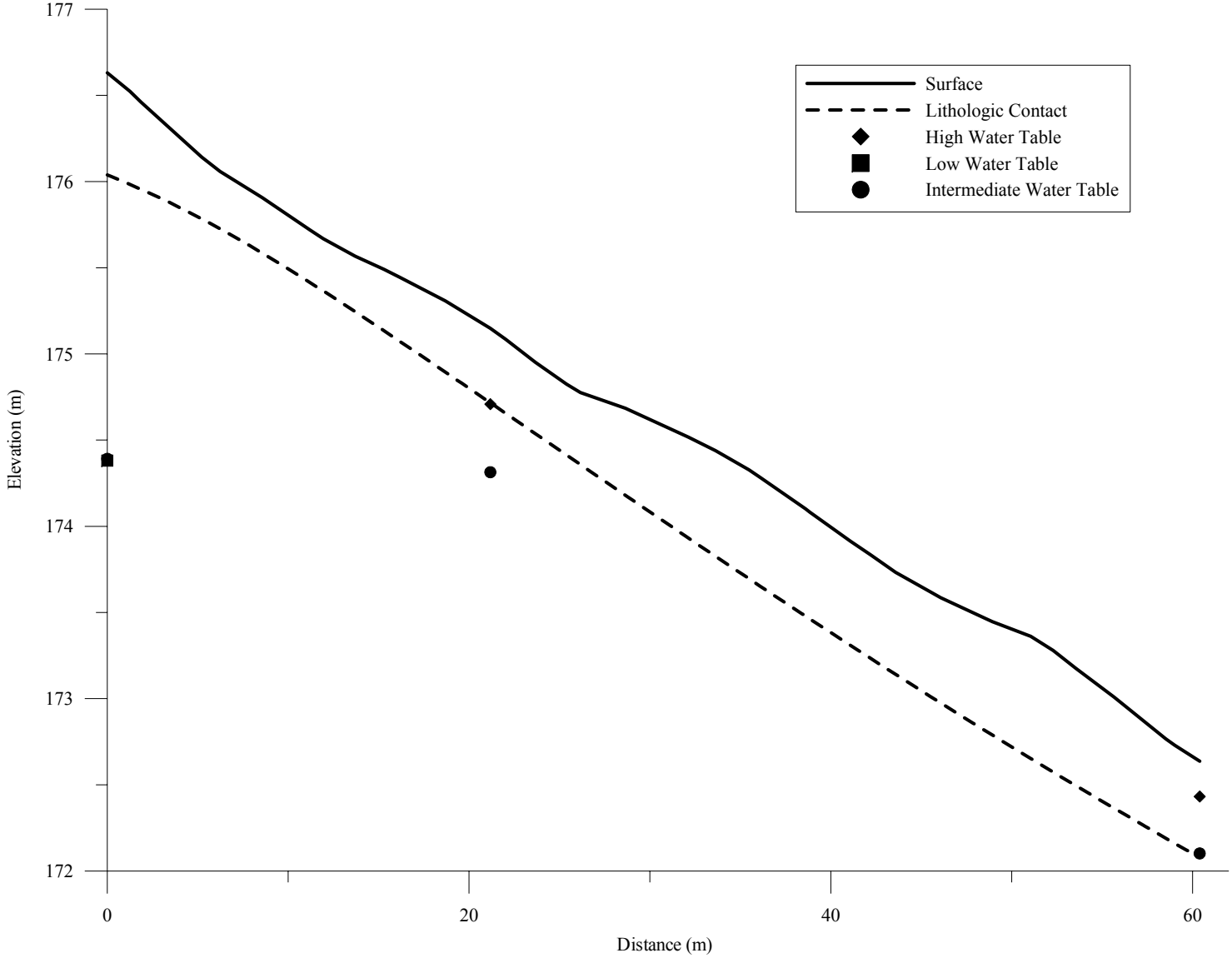

Fig. 4.13. Cross-section of transect 3 (piezometers 14, 15, and 16) showing surface elevations, surface of lower residual parent material, and water table elevations.

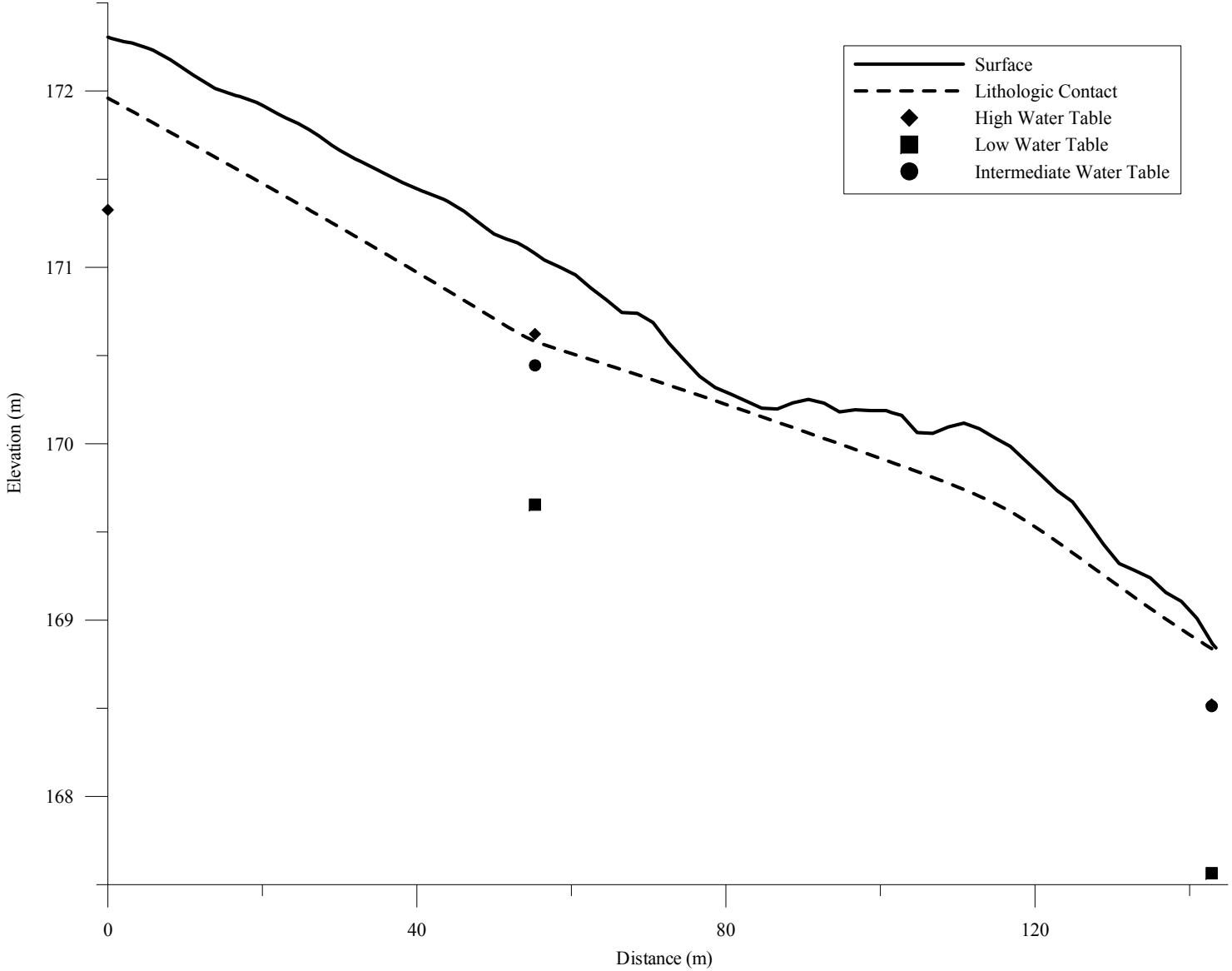

Chapter Five

Conclusions

Soil derived from mafic parent materials effect the movement of soil water differently than other soils due to their unique characteristics. The shrink-swell risks associated with mafic-derived subsoils tend to correlate with the low K_s exhibited by these clayey residual horizons. The loamy colluvial horizons have a higher K_s, sufficiently moving water through the soil. The adjacent layering of these two K_s contrasting soil types, however, causes a perching of water at their lithologic contact. An accumulation of black redox concentrations at the lithologic discontinuity provides further evidence of perching water.

The thickness of horizons with loamy textures dictates the water storing capacity of the soil. The upstream half of the site, with twice the amount of loamy colluvial parent material, has nearly twice the amount of water storing capacity as that of the downstream half, allowing less flow into the stream. The thinner colluvial parent material on the downstream half causes saturated induced flow to occur sooner than on the upstream half, thereby increasing the amount of runoff and decreasing the amount of infiltration and potential for evapotranspiration.

For soils in the southeast US, the lag time between saturation and the onset of reduction has been reported to be 14 to 30 days and to vary with organic C content as related to depth of the horizon. Redox data at this site suggest $\leq$ 14 day lag between saturation and Fe reduction. IRIS tubes were found to be reliable indicators of reduction in mafic soils. Horizons with greater than 30% of the FH removal are considered to be reducing. This study found that when FH loss for subsurface horizons with NSE > 0 were evaluated, a strong correlation between the

percentage of FH loss and number of saturation events (NSE) is shown ($r^2 = 0.9$). Differences are shown between the percentage of time saturated NSE for horizons with no redox features, [concentrations, depletions], and low Munsell chroma (≤2) matrices during field description; the longer a horizon was saturated the more pronounced the redox features. However, there are no statistical difference in the percentage of time saturated and the NSE for horizons with concentrations verses horizons with depletions.

In conclusion, the unique soil characteristics of this site have a definite effect on the movement water on the site. Landscape attributes and soil characteristics at this site strongly affect the frequency and duration of saturation. In turn, evidence suggests the frequency and duration of saturation plays an important role in the type and abundance of redoximorphic features in these mafic soils.

.

Appendices

Appendix A

Series: NSD Pedon: S03GA237-01

Location: Putnam County, GA. University of Georgia Central Research and Education Station.

Slope:3% Aspect: ENE (60°) Slope curvature: convex

MLRA: Piedmont Landform: Upland

Position on slope: backslope

Parent material: Residuum from mafic schist

Drainage class: moderately well

Described by: Soil Mineralogy Class Date: August, 2003

Classification: fine, mixed, active, thermic, Typic Paleudalf

Pedon Description (colors are for moist soil unless otherwise noted):

Ap1 -- 0 to 12 cm; dark brown (10YR 3/3) sandy loam; weak fine granular and subangular blocky structure; very friable; few fine black concretions; few coarse fragments of quartzite; clear smooth boundary.

Ap2 -- 12 to 25 cm; dark brown (10YR 3/3) sandy clay loam; weak fine subangular blocky structure; friable; few fine black concretions; few medium faint dark yellowish brown (10YR 4/4) mottles; abrupt smooth boundary.

Bt -- 25 to 50 cm; strong brown (7.5YR 4/6) clay; weak medium prismatic parting to moderate fine subangular blocky structure; friable; few thin clay films on ped faces; common fine black concretions; lower part of horizon has coarse concretions; clear smooth boundary.

Btss1 -- 50 to 63 cm; strong brown (7.5YR 4/6) clay; moderate very fine subangular blocky structure; friable; few thin clay films on ped faces; common medium black concretions; many pressure faces; few small slickensides; clear wavy boundary.

Btss2 -- 63 to 89 cm; strong brown (7.5YR 4/6) clay; common medium distinct brown (7.5YR 5/2) redox depletions; moderate medium subangular and angular blocky structure; firm; few thin clay films on ped faces; common medium black concretions; many pressure faces; few small slickensides; lowest 5 cm of horizon has many depletions; abrupt wavy boundary.

CB -- 89 to 107 cm; strong brown (7.5YR 5/6) loamy sand; massive; friable; many fine Fe-Mn masses; few 2-5 cm thick gray (7.5YR 6/1) foliations inclined 30 degrees from horizontal; gray seams are more clayey than brown sandy parts.

Comments: Described and sampled from a pit wall.

Series: NSD Pedon: S03GA237-02

Location: Putnam County, GA. University of Georgia Central Research and Education Station

Slope: 1% Aspect: ENE (68°) Slope curvature: linear

MLRA: Southern Piedmont Landform: Stream terrace

Parent material: Alluvium over residuum from mafic schist

Drainage class: moderately-well

Described by: Soil Mineralogy Class Date: August, 2003

Classification: coarse-loamy, mixed, superactive, thermic, Typic Dystrudept

Pedon Description (colors are for moist soil unless otherwise noted):
Ap -- 0 to 12 cm; dark reddish brown (5YR 3/3) silt loam; moderate fine granular and subangular blocky structure; very friable; few fine black concretions; abrupt smooth boundary.

Bw -- 12 to 37 cm; brown (7.5YR 4/2) silty clay loam; moderate fine subangular blocky structure; friable; common medium black concretions; abrupt smooth boundary.

Ab -- 37 to 50 cm; very dark grayish brown (10YR 3/2) sandy loam; common coarse distinct dark brown (7.5YR 3/2) mottles; moderate fine granular structure; friable; common medium black concretions; clear smooth boundary.

B'w1 -- 50 to 78 cm; brown (10YR 4/3) sandy clay loam; weak medium subangular blocky structure; friable; many coarse black concretions up to 3 mm diameter; gradual smooth boundary.

B'w2 -- 78 to 96 cm; dark grayish brown (10YR 4/2) sandy loam; massive; very friable; many coarse black concretions; black concretions are up to 30 mm diameter and irregularly shaped; clear smooth boundary.

B’sm -- 96 to 120 cm; dark grayish brown (10YR 4/2) sandy loam; massive; extremely firm; many coarse black concretions; concretions are up to 30 mm diameter and irregularly shaped; in about 60% of horizon, nodules have been cemented together; abrupt smooth boundary.

2Bss -- 120 to 160 cm; strong brown (7.5YR 5/8) clay; common fine prominent dark gray (10YR 4/1) redox depletions; moderate fine subangular and angular blocky structure; very firm; few dark gray (10YR 4/1) slickensides; upper part of horizon has many medium black concretions; gradual boundary.

2C -- 160 to 226 cm; olive brown (2.5Y 4/4) sandy loam; friable; gradual boundary.

2Cr -- 226 to 246 cm; dark olive brown (2.5Y 3/3) sand; friable.
Comments: Ap-2Bss horizons were described and sampled from pit wall. 2C1 and 2Cr horizons were sampled from bucket auger. Water was seeping into pit at Bsm/2Bss boundary.

Soil Series: NSD Pedon: S07GA237-01

Location: Putnam County, GA. University of Georgia Central Research and Education Station (N 33°24.024, W 83°26.965)

Landform: Upper Backslope Elevation (m): 152.968

Parent materials: colluvium over residuum

Physiography: Piedmont Land use: pasture

Described by: Coleman, West, Bradshaw Date: 5/30/2007

Classification: fine, mixed, active, thermic, Typic Paleudalf

Soil Description: (colors for moist soil unless otherwise noted)

Ap - 0 to 13 cm; dark reddish brown (5YR 3/3) medium sandy loam; medium fine granular structure; friable; many fine roots; abrupt boundary.

Btc1 - 13 to 35 cm; dark brown (7.5YR 3/4) clay loam; weak fine subangular blocky structure; friable; common fine roots; 5% Mn nodules up to 5mm in diameter; clear boundary.

Btc2 - 35 to 60 cm; brown (7.5YR 4/4) clay loam; common fine distinct yellowish red (5YR 4/6) redox concentrations; moderate medium subangular blocky structure; friable; few roots; 10% Mn nodules (increasing at lower boundary); clear boundary.

Btcg1 - 60 to 88 cm; dark reddish brown (10YR 4/2) clay loam; common fine prominent yellowish red (5YR 4/6) redox concentrations; moderate fine subangular blocky structure; friable; 35% Mn nodules up to 5mm in diameter; clear boundary.

Btcg2 - 88 to 120 cm; dark grayish brown (10YR 4/2) clay loam; common medium prominent yellowish red (5YR 4/6) redox concentrations; moderate fine subangular blocky structure; friable; 15% Mn nodules up to 5mm in diameter; abrupt boundary.

2Btss - 120 to 129 cm; dark yellowish brown (10YR 4/6) clay; moderate medium subangular and angular blocky structure; slickensides; firm; clear boundary.

2Bt - 129 to 173 cm; dark yellowish brown (10YR 4/6) clay; many coarse distinct reddish gray (10YR 5/2) redox depletions; moderate medium subangular and angular blocky structure; firm; clear boundary.

2BC - 173 to 182+ cm; brown (7.5YR 4/4) clay loam; many course distinct strong brown (7.5YR 5/8) redox concentrations; many medium prominent gray (10YR 6/1) redox depletions; weak medium subangular blocky structure; friable; probe refusal at 182cm.

Soil Series: NSD Pedon: S07GA237-02

Location: Putnam County, GA. University of Georgia Central Research and Education Station. (N 33°24.051, W 83°26.918)

Landform: Backslope Elevation (m): 150.794

Parent materials: colluvium over residuum

Physiography: Piedmont Land use: pasture

Described by: Coleman, West, Bradshaw Date: 5/30/2007

Classification: fine, mixed, active, thermic, Typic Paleudalf

Soil Description: (colors for moist soil unless otherwise noted)

Apc - 0 to 22 cm; dark brown (7.5YR 3/2) clay loam; moderate medium granular structure; friable; few fine roots; 2% Mn nodules up to 5mm in diameter; abrupt boundary.

2Btc - 22 to 65 cm; reddish brown (5YR 4/4) clay; moderate medium subangular blocky structure; friable; 1% Mn nodules up to 5mm in diameter; gradual boundary.

2BCc1 - 65 to 86 cm; brown (7.5YR 4/4) clay loam; common fine distinct reddish brown (5YR 4/4) redox concentrations; moderate medium subangular blocky structure; friable; 15% soft Mn concentrations; few soft rock fragments; gradual boundary.

2BCc2 - 86 to 122 cm; brown (10YR 5/3) clay loam; common medium distinct brown (7.5YR 4/4) redox concentrations; weak medium subangular blocky structure; friable; 10% soft Mn concentrations; gradual boundary.

2C1 - 122 to 165 cm; brown (10YR 5/3) sandy clay loam; common medium distinct brown (7.5YR 4/4) redox concentrations; massive structure; friable; 10% weathered grains; weathered mica flakes; feldspar/kaolinitic pockets; friable; clear boundary.

2C2 - 165 to 232+ cm; very pale brown (10YR 7/3) loam; common fine prominent yellowish red (5YR 5/6) redox concentrations; few medium faint light gray (10YR 7/2) redox depletions; massive structure; friable; kaolinitic; highly weathered.

Soil Series: NSD Pedon: S07GA237-03

Location: Putnam County, GA. University of Georgia Central Research and Education Station. (N 33°24.090, W 83°26.879)

Landform: Footslope Elevation (m): 147.798

Parent materials: colluvium over residuum

Physiography: Piedmont Land use: pasture

Described by: Coleman, West, Bradshaw Date: 5/30/2007

Classification: fine, mixed, active, thermic, Typic Hapludalf

Soil Description: (colors for moist soil unless otherwise noted)

Ap - 0 to 6 cm; dark reddish brown (5YR 3/2) loam; weak medium granular structure; friable; many fine roots; abrupt boundary.

BAc - 6 to 42 cm; dark reddish brown (7.5YR 3/4) clay loam; few medium distinct yellowish red (5YR 5/6) redox concentrations; moderate medium subangular blocky structure; friable; common fine roots; 4% soft Mn concentrations; gradual boundary.

2Btc - 42 to 73 cm; brown (10YR 4/3) clay; common fine prominent strong brown (7.5YR 5/6) redox concentrations; few medium distinct grayish brown (10YR 5/6) redox depletions; moderate medium subangular blocky structure; firm; 4% soft Mn concentrations; gradual boundary.

2Btssc - 73 to 110 cm; dark yellowish brown (10YR 4/4) clay ; many fine faint yellowish brown (10YR 5/6) redox concentrations; common medium distinct dark grayish brown (10YR 4/2) redox depletions; weak fine angular blocky structure; firm; 10% soft Mn concentrations; weak slickensides; gradual boundary.

2Btsscg - 110 to 133 cm; dark gray (2.5Y 4/1) clay; many medium prominent yellowish brown (10YR 5/6) redox concentrations; weak fine angular blocky structure; very firm; 5% soft Mn concentrations; slickensides; clear boundary.

2Btg - 133 to 150 cm; dark gray (N 4/) clay; few medium prominent yellowish brown (10YR 5/4) redox concentrations; weak medium angular and massive structure; very firm; gradual boundary.

2BCg - 150 to 186 cm; dark gray (N 4/) sandy clay; few medium prominent yellowish brown (10YR 5/6) redox concentrations; massive; firm; few siliceous fragments; gradual boundary.

2Cg - 186 to 210+ cm; dark gray (2.5Y 4/1) sandy loam; few medium prominent yellowish brown (10YR 5/4) redox concentrations; massive structure; friable.

Soil Series: NSD Pedon: S07GA237-04

Location: Putnam County, GA. University of Georgia Central Research and Education Station. (N 33°23.009, W 83°26.845)

Landform: Footslope Elevation (m): 146.523

Parent materials: colluvium over residuum

Physiography: Piedmont Land use: pasture

Described by: Coleman, Bradshaw Date: 5/30/2007

Classification: fine, mixed, active, thermic, Oxyaquic Hapludalf

Soil Description: (colors for moist soil unless otherwise noted)

Ap - 0 to 8 cm; dark brown (7.5YR 3/2) fine sandy loam; weak medium granular structure; friable; many fine roots; abrupt boundary.

ABc - 8 to 23 cm; dark brown (7.5YR 3/2) sandy loam; few fine distinct brown (7.5YR 4/4) redox concentrations; weak medium subangular blocky structure; friable; common fine roots; 5% Mn nodules and soft concentrations; few irregular rose quartz fragments up to 10mm in diameter; gradual boundary.

Btc - 23 to 49 cm; brown (10YR 4/3) clay loam; common medium distinct brown (7.5YR 4/4) redox concentrations; moderate medium subangular blocky structure; friable; 5% soft Mn concentrations; gradual boundary.

BC - 49 to 74 cm; mottled sandy clay loam; many fine distinct yellowish red (5YR 4/6) redox concentrations; many fine prominent dark gray (10YR 4/1) redox depletions; massive structure; friable; kaolinitic; weathered grains; gradual boundary.

CB- 74 to 101+ cm; mottled sandy clay loam; few fine distinct yellowish red (5YR 4/6) redox concentrations; few fine prominent dark gray (10YR 4/1) redox depletions; massive structure; friable; kaolinitic/feldspar pockets; very weathered grains; probe refusal at 101 cm.

Soil Series: NSD Pedon: S07GA237-05

Location: Putnam County, GA. University of Georgia Central Research and Education Station. (N 33°23.899, W 83°26.751)

Landform: Shoulder Elevation (m): 148.699

Parent materials: colluvium over residuum

Physiography: Piedmont Land use: pasture

Described by: Coleman, Bradshaw, Newsome Date: 5/30/2007

Classification: fine, mixed, active, thermic, Typic Paleudalf

Soil Description: (colors for moist soil unless otherwise noted)

Ap - 0 to 5 cm; dark reddish brown (5YR 3/3) fine sandy loam; weak medium granular structure; friable; many fine roots; abrupt boundary.

Ac - 5 to 21 cm; dark reddish brown (5YR 3/3) fine sandy loam; weak medium granular structure; friable; common fine roots; 5% Mn nodules; few irregular quartz fragments less than 5mm in diameter; gradual boundary.

Btc - 21 to 46 cm; dark reddish brown (2.5YR 3/4) clay loam; weak medium subangular blocky structure; friable; few fine roots; 10% soft Mn nodules; gradual boundary.

2Btc1 - 46 to 68 cm; red (2.5YR 4/6) clay; moderate medium subangular blocky structure; firm; clay films; 10% soft Mn concentrations; clear boundary.

2Btc2- 68 to 92 cm; red (2.5YR 4/6) clay; common medium prominent red (10YR 4/8) redox concentrations; common medium prominent light red (10YR 6/8) redox concentrations; moderate medium subangular blocky structure; firm; clay films; <5% soft Mn concentrations; clear boundary.

2Bt- 92 to 130 cm; red (2.5YR 4/6) clay; few fine prominent pink (10YR 8/4) redox concentrations; common medium prominent light red (10YR 6/8) redox concentrations; moderate medium subangular blocky structure; firm; clay films; gradual boundary.

2BCc- 130 to 187 cm; red (2.5YR 4/8) sandy clay loam; few medium prominent red (10YR 4/6) redox concentrations; few fine prominent light red (10YR 6/8) redox concentrations; weak medium subangular blocky structure; friable; 5% soft Mn concentrations; gradual boundary.

Soil Series: NSD Pedon: S07GA237-06

Location: Putnam County, GA. University of Georgia Central Research and Education Station. (N 33°23.913, W 83°26.743)

Landform: Backslope Elevation (m): 146.777

Parent materials: colluvium over residuum

Physiography: Piedmont Land use: pasture

Described by: Coleman, Bradshaw, Newsome Date: 5/30/2007

Classification: coarse-loamy, mixed, active, thermic, Typic Hapludalf

Soil Description: (colors for moist soil unless otherwise noted)

Ap - 0 to 6 cm; dark brown (5YR 3/3) fine sandy loam; weak medium granular structure; friable; many fine roots; abrupt boundary.

Ac - 6 to 24 cm; dark reddish brown (5YR 3/3) fine sandy loam; weak medium granular structure; friable; common fine roots; 5% Mn nodules and soft concentrations; few irregular quartz fragments less than 5mm in diameter; clear boundary.

BAc - 24 to 50 cm; dark reddish brown (2.5YR 3/4) sandy clay loam; weak medium subangular blocky structure; friable; few fine roots; 10% soft Mn nodules; gradual boundary.

Btc - 50 to 66+ cm; dark reddish brown (5YR 3/4) clay loam; moderate medium subangular blocky structure; friable; 20% Mn nodules up to 2 cm in diameter; few irregular quartz rocks; probe refusal at 66 cm.

Soil Series: NSD Pedon: S07GA237-07

Location: Putnam County, GA. University of Georgia Central Research and Education Station. (N 33°23.924, W 83°26.725)

Landform: Toeslope Elevation (m): 146.151

Parent materials: colluvium over residuum

Physiography: Piedmont Land use: pasture

Described by: Coleman, Bradshaw, Newsome Date: 5/30/2007

Classification: coarse-loamy, mixed, active, thermic, Aquic Paleudalf

Soil Description: (colors for moist soil unless otherwise noted)

Ap - 0 to 8 cm; dark brown (7.5YR 3/2) fine sandy loam; weak medium granular structure; friable; many fine roots; abrupt boundary.

Ac - 8 to 42 cm; dark brown (7.5YR 3/2) fine sandy loam; moderate medium subangular blocky structure; friable; common fine roots; 30% Mn concentrations; gradual boundary.

BA- 42 to 60 cm; dark yellowish brown (10YR 4/4) fine sandy loam; few fine distinct yellowish brown (10YR 5/8) redox concentrations; moderate medium subangular blocky structure; friable; few fine roots; clear boundary.

Btg- 60 to 74 cm; dark grayish brown (2.5Y 4/2) sandy clay loam; common fine prominent yellowish brown (10YR 5/8) redox concentrations; few medium distinct dark reddish gray (10YR 4/1) redox depletions; moderate medium subangular blocky and massive structure; friable; few fine mica flakes; weathered feldspar grains; clear boundary.

Ccg - 74 to 83+ cm; dark grayish brown (2.5Y 4/2) fine sandy loam; common fine prominent yellowish brown (10YR 5/8) redox concentrations; common medium prominent dark reddish gray (2.5YR 4/1) redox depletions; massive structure; friable; few soft Mn concentrations; fine mica flakes; weathered grains; probe refusal at 83 cm.

Soil Series: NSD Pedon: S07GA237-08

Location: Putnam County, GA. University of Georgia Central Research and Education Station. (N 33°23.945, W 83°26.664)

Landform: Upper Backslope Elevation (m): 146.473

Parent materials: colluvium over residuum

Physiography: Piedmont Land use: pasture

Described by: Coleman, Bradshaw, Newsome Date: 5/31/2007

Classification: fine, mixed, active, thermic, Typic Paleudalf

Soil Description: (colors for moist soil unless otherwise noted)

Ap - 0 to 6 cm; dark brown (7.5YR 3/2) fine sandy loam; weak medium granular structure; friable; many fine roots; abrupt boundary.

Ac - 6 to 23 cm; dark brown (7.5YR 3/3) fine sandy loam; weak medium granular structure; friable; common fine roots; 5% Mn nodules; 2% irregular quartz fragments less than 5mm in diameter; clear boundary.

Btc1 - 23 to 44 cm; brown (7.5YR 4/3) clay loam; few fine prominent red (2.5YR 5/8) redox concentrations; moderate medium subangular blocky structure; friable; 20% Mn nodules and soft concentrations; gradual boundary.

Btc2 - 44 to 55 cm; brown (7.5YR 4/4) clay loam; common fine prominent red (2.5YR 5/8) redox concentrations; weak medium subangular blocky structure; friable; 35% Mn nodules and soft concentrations; 2% irregular quartz fragments up to 5mm in diameter; clear boundary.

2Btss- 55 to 78 cm; yellowish brown (10YR 5/6) clay; common fine faint red (10YR 4/8) redox concentrations; common fine distinct dark grayish brown (10YR 4/2) redox depletions; moderate medium angular blocky structure; firm; clay films; slickensides; clear boundary.

2CB- 78 to 89+ cm; mottled sandy clay loam; massive structure; friable; kaolinitic; siliceous fragments; very weathered light colored grains; probe refusal at 89 cm.

Soil Series: NSD Pedon: S07GA237-09

Location: Putnam County, GA. University of Georgia Central Research and Education Station. (N 33°23.913, W 83°26.674)

Landform: Toeslope Elevation (m): 143.002

Parent materials: colluvium over residuum

Physiography: Piedmont Land use: pasture

Described by: Coleman, Bradshaw, Newsome Date: 5/31/2007

Classification: coarse-loamy, mixed, superactive, thermic, Udollic Albaqualf

Soil Description: (colors for moist soil unless otherwise noted)

Ap - 0 to 10 cm; dark brown (7.5YR 3/2) loam; weak medium granular structure; friable; many fine roots; abrupt boundary.

ABg- 10 to 25 cm; very dark grayish brown (10YR 3/2) fine sandy loam; few fine prominent yellowish red (5YR 5/8) redox concentrations; weak medium subangular blocky structure; friable; few fine roots; clear boundary.

2Btcg- 25 to 55 cm; dark gray (N 4/) clay; few fine prominent yellowish red (5YR 5/8) redox concentrations; moderate medium subangular blocky structure; firm; few fine roots; small vein of iron stone concretions up to 2mm in diameter; abrupt boundary.

2Btg1- 55 to 80 cm; dark bluish gray (5B 4/) sandy clay; few fine prominent yellowish red (5YR 5/8); weak medium subangular blocky structure; firm; soft quartz fragments at 60 cm; clear boundary.

2Btg2- 80 to 97 cm; greenish gray (10GY 5/) sandy clay; few fine prominent yellowish red (5YR 5/8) redox concentrations along old root channels; few medium distinct very dark greenish gray (5BG 3/) redox depletions; moderate medium subangular blocky structure; firm; fine black mica flakes; vein of quartz fragments at 88 cm; clear boundary.

2BCg- 97 to 124 cm; mottled (light gray (5Y 7/2), olive yellow (2.5Y 6/6)) sandy clay loam; weak fine subangular blocky structure; friable; siliceous fragments; fine black mica flakes, small distinct greenish gray (10GY 5/) clay pockets; clear boundary.

2CBg- 124 to 146 cm; mottled (light gray (5Y 7/2), olive yellow (2.5Y 6/6), red (2.5YR 4/8), reddish gray (2.5YR 5/1)) sandy clay loam; weak fine subangular blocky structure; friable; siliceous fragments; fine mica flakes; abrupt boundary.

2Cg- 146 to 156+ cm; mottled sandy loam; massive structure; friable; siliceous fragments; very fine mica flakes, very weather dark grains.

Soil Series: NSD Pedon: S07GA237-10

Location: Putnam County, GA. University of Georgia Central Research and Education Station. (N 33°23.788, W 83°26.572)

Landform: Backslope Elevation (m): 143.095

Parent materials: colluvium over residuum

Physiography: Piedmont Land use: pasture

Described by: Coleman, Bradshaw Date: 5/31/2007

Classification: fine, mixed, active, thermic, Oxyaquic Hapludalf

Soil Description: (colors for moist soil unless otherwise noted)

Ap - 0 to 6 cm; very dark grayish brown (10YR 3/2) fine sandy loam; weak medium granular structure; friable; many fine roots; abrupt boundary.

Ac - 6 to 19 cm; dark brown (10YR 3/3) fine sandy loam; weak medium granular structure; friable; common fine roots; 20% Mn nodules; clear boundary.

BA - 19 to 33 cm; brown (10YR 4/3) loam; weak medium subangular blocky structure; friable; few fine roots; clear boundary.

2Btc1 - 33 to 50 cm; dark yellowish brown (10YR 3/4) clay ; moderate medium subangular blocky structure; firm; few fine roots; 5% Mn nodules; clear boundary.

2Btc2- 50 to 62 cm; brown (7.5YR 4/4) clay; few fine prominent red (10YR 5/8) redox concentrations; moderate medium angular blocky structure; firm; few fine roots; 35% Mn nodules; 2% irregular quartz fragments up to 5mm in diameter; clay films; clear boundary.

2Btssc- 62 to 87 cm; light olive brown (2.5Y 5/4) clay; few fine prominent red (10YR 5/8) redox concentrations; moderate medium subangular blocky structure; firm; few fine roots; 3% Mn nodules; slickensides; clear boundary.

2BCcg- 87 to 108 cm; dark grayish brown (2.5Y 4/2) sandy clay; common fine prominent reddish yellow (7.5YR 6/8) redox concentrations; few fine prominent olive (5Y 5/4) redox depletions; moderate medium subangular blocky structure; firm; 5% soft Mn concentrations; gradual boundary.

2Cg- 108 to 137+ cm; mottled (dark grayish brown (2.5Y 4/2), red (2.5YR 4/8), red (10R 4/8), olive (5Y 5/6)) medium sandy loam; massive structure; friable; very fine mica flakes; soft black masses, kaolinitic; probe refusal at 137 cm.

Soil Series: NSD Pedon: S07GA237-11

Location: Putnam County, GA. University of Georgia Central Research and Education Station. (N 33°23.835, W 83°26.568)

Landform: Footslope Elevation (m): 140.930

Parent materials: colluvium over residuum

Physiography: Piedmont Land use: pasture

Described by: Coleman, Bradshaw Date: 5/31/2007

Classification: fine, mixed, active, thermic, Typic Hapludalf

Soil Description: (colors for moist soil unless otherwise noted)

Ap - 0 to 5 cm; dark brown (10YR 3/3) fine sandy loam; weak medium granular structure; friable; many fine roots; abrupt boundary.

BA - 5 to 12 cm; very dark grayish brown (10YR 3/2) loam; weak medium subangular blocky structure; friable; common fine roots; 10% Mn nodules; 3% irregular quartz fragments 2 – 5mm in diameter; clear boundary.

2Btc1 - 12 to 29 cm; brown (7.5YR 4/4) clay; few fine distinct strong brown (7.5YR 5/8) redox concentrations; moderate medium subangular blocky structure; firm; 3% soft Mn concentrations; clear boundary.

2Btc2 - 29 to 50 cm; brown (7.5YR 4/4) clay; few medium distinct strong brown (7.5YR 5/8) redox concentrations; moderate medium subangular blocky structure; firm; 5% soft Mn concentrations; kaolinitic; gradual boundary.

2Cc- 50 to 89+ cm; strong brown (7.5YR 5/6) sandy loam; massive structure; friable; weathered grains; soft Mn concentrations; siliceous; kaolinitic; fine mica flakes; probe refusal at 89 cm.

Soil Series: NSD Pedon: S07GA237-12

Location: Putnam County, GA. University of Georgia Central Research and Education Station. (N 33°23.765, W 83°26.595)

Landform: Backslope Elevation (m): 144.330

Parent materials: colluvium over residuum

Physiography: Piedmont Land use: pasture

Described by: Coleman, Bradshaw Date: 5/31/2007

Classification: fine, mixed, active, thermic, Typic Paleudalf

Soil Description: (colors for moist soil unless otherwise noted)

Ap - 0 to 5 cm; dark brown (7.5YR 3/2) fine sandy loam; weak medium granular structure; friable; many fine roots; abrupt boundary.

Ac - 5 to 18 cm; dark brown (7.5YR 3/3) fine sandy loam; weak medium granular structure; friable; common fine roots; 10% Mn nodules; clear boundary.

2Btc - 18 to 53 cm; red (2.5YR 4/6) clay; few fine faint red (2.5YR 5/8) redox concentrations; moderate medium subangular blocky structure; firm; 5% soft Mn concentrations; clay films; clear boundary.

2BCc - 53 to 104 cm; reddish brown (2.5YR 4/4) sandy clay loam; common fine prominent reddish yellow (5YR 6/8) redox concentrations; weak medium subangular blocky structure; friable; 15% soft Mn concentrations; kaolinitic; weathered grains; gradual boundary.

2Cc- 104 to 141 cm; mottled (reddish yellow (5YR 6/7), yellow (10YR 7/6) fine sandy loam; massive structure; friable; weathered grains; 25% soft Mn concentrations; kaolinitic; clear boundary.

2Ccg- 141 to 229+ cm; mottled (reddish yellow (7.5YR 6/8), olive yellow (2.5Y 6/6), gray (2.5Y 5/1), light gray (2.5Y 7/1) fine sandy loam; massive structure; friable; weathered grains; 40% soft Mn concentrations; kaolinitic.

Appendix B

A brief recount of the construction of Pt electrodes with modifications from the original method discussed by Vepraskas (2002) follows:

Platinum wire, cut into 13 mm pieces, was fused into 1 mm holes drilled in the tips of brass-brazing rods. Heat shrink tubing was placed around the tip, leaving enough of the platinum exposed for proper contact with the soil (approximately 5 mm). The rest of the rod was wrapped with heat shrink tubing; 5 cm on the opposite end was left exposed for the attachment of mV leads (18 gauge copper wire). The copper wire was soldered to the brass rod; a second layer of heat shrink tubing was applied, making sure to cover the soldered connection and approximately 15 cm up the copper wire. To ensure a waterproof seal at the tip, several coats of multi purpose rubber coating were applied. The electrodes were then standardized using the quinhydrone method described by Dirasian (1968).

Reference:

Dirasian, H.A. 1968. Electrode potentials – significance in biological systems, Part 1: fundamentals of measurement. Water and Sewage Works 115:420-425.

Vepraskas, M.J. 2002. Redox potential measurements [Online]. Available at http://www.soil.ncsu.edu/wetlands/wetlandsoils/RedoxWriteup.pdf (accessed 9 Sept. 2005; verified 27 Sept. 2005). Dept. of Soil Science at North Carolina State University.

Appendix C

IRIS tube construction

Ferrihydrite paint was prepared by dissolving 16 g ferric chloride salt ($FeCl_3$) in 0.5 L deionized (DI) water in a 2 L beaker. While stirred with magnetic stirrer, monitor the pH wile adding approximately 370 mL one molar KOH until a pH of 12 is reached. Allow the suspension to stand for approximately 30 minutes, then restart the stirring and check the pH. If it has dropped below 12, add additional KOH dropwise to bring it back to the target pH. At this point the total volume of suspension should be approximately 900 mL. Transfer the suspension into for 250mL nalgene bottles and centrifuge at approximately 1000 rpm for 5 minutes to concentrate the Fe oxides, discard the supernatant. Transfer the contents of the four bottles into two bottles and centrifuge was the precipitated Fe oxides two additional times with DI water, discarding the supernatant each time. After the third centrifugation, resuspend the Fe oxides with DI water and transfer to 30 cm pieces of dialysis tubing, filling the tubes half full. Place dialysis tubing into basins filled with DI water and replace water at six hour intervals during the first day and then twelve hour intervals for a total of three days. Transfer the Fe oxides from the dialysis tubing to a nalgene storage bottle and keep in the dark. The suspension should be suitable for painting one week after the initial synthesis of the Fe oxides. Once paint was suitable, polyvinyl chloride tubes (one-half inch schedule 40 PVC tubing) were cleaned with acetone and lightly sanded using coarse grit sand paper. Three coats of ferrihydrite (FH) paint were applied to the sanded portions of the tubes.

Estimating Loss of FH from Surface of IRIS Tubes

The appearance of the IRIS surface can be evaluated qualitatively by determining whether or not some FH was removed or it can be evaluated semi-quantitatively (Jenkinson and Franszmeier, 2006). After IRIS tubes were left over the winter wet season, they were removed, rinsed with water, dried, and photographed with a digital camera. Segments of the IRIS tubes corresponding with soil horizons at each site were photographed at three 120° rotations and then combined into a composite photo using Adobe Photoshop software. Using that software, a semi-quantitative evaluation of the loss of FH paint from IRIS tubes was conducted using the following procedure adapted from Hans-Anton, et al. (1997) and Jenkinson and Franszmeier (2006). Using the Magic Wand tool of Photoshop, an area that showed some FH depletion was selected. Using the Similar command in the Select menu, all areas of showing FH depletion were automatically selected. The areas should then be compared to the actual IRIS tubes to make sure they should be included. At this point, areas can be added or subtracted using the Magic Wand tool. The tolerance level of the Magic Wand tool was adjusted so that only depleted areas were included in the selection. The Histogram tool generates a graph, in which each vertical line represents the number of pixels associated with the color spectrum. This tool also reports the number of pixels represented by the chosen selection. Thus, the number of pixels representing the total depleted area and the number of pixels representing the surface of the IRIS tube were obtained. From these two measurements, the percentages of FH loss from the IRIS tubes were calculated. The average loss of FH paint from the IRIS tubes is shown in Table below. IRIS tubes were grouped according to their locations within the project site.

Estimation of FH depletion on IRIS tubes generated with Adobe Photoshop software.

Horizon	Lower Boundary	Texture	FH Loss
	Cm		%
Site 1			
Ap	13	Sandy Loam	N/A*
Btc1	35	Clay Loam	14
Btc2	60	Clay Loam	23
Btcg1	88	Clay Loam	15
Btcg2	100+	Clay Loam	25
Site 3			
Ap	6	Loam	N/A*
BAc	42	Clay Loam	22
2Btc	73	Clay	21
2Btssc	110	Clay	25
Site 4			
Ap	8	Sandy Loam	N/A*
ABc	23	Sandy Loam	40
Btc	49	Clay Loam	15
BC	74	Clay Loam	16
Site 6			
Ap	6	Sandy Loam	N/A*
Ac	24	Sandy Loam	38
BAc	50	Sandy Clay Loam	9
Btc	66	Clay Loam	19
Cr	125+	N/A	20
Site 7			
Ap	8	Sandy Loam	N/A*
Ac	42	Sandy Loam	40
BA	60	Sandy Loam	10
Btg	74	Sandy Clay Loam	29
Ccg	83	Sandy Loam	22
Cr	109+	N/A	38
Site 8			
Ap	6	Sandy Loam	N/A*
Ac	23	Sandy Loam	6
Btc1	44	Clay Loam	13
Btc2***	55	Clay Loam	25
2Btss***	62+	Clay	28
Site 10			

Ap	6	Sandy Loam	N/A*
Ac	19	Sandy Loam	26
BA	33	Loam	17
2Btc1	50	Clay	12
2Btc2	62	Clay	9
2Btssc	87	Clay	10
Site 11			
Ap	5	Sandy Loam	N/A*
BA	12	Loam	25
2Btc1	29	Clay	9
2Btc2	50	Clay	16
2Cc	80+	Sandy Loam	26
Site 12			
Ap	5	Sandy Loam	N/A*
Ac	18	Sandy Loam	25
2Btc	53	Clay	36
2BCc	104	Sandy Clay Loam	22

* Due to Bentonite applied at surface.
**At time of soil characterization, the probe would not penetrate past 66 cm (Site 6) and 83 cm (Site 7).
***Iris tubes in Btc2 and 2Btss horizons showed 5% and 10%, respectively, iron concentrations (determined with by visual estimation).

Reference:

Hans-Anton L., D.A. Mankoff, D. Corwin, G. Santeusanio, and A.M. Gown. 1997. Application of Photoshop-based Image Analysis to Quantification of Hormone Receptor Expression in Breast Cancer. J. Histochem. and Cytochem. 45:1559–1565.

Jenkinson, B.J., and D.P. Franzmeier. 2006. Development and evaluation of Fe-coated tubes that indicate reduction in soils. Soil Sci. Soc. Am. J. 70:183–191.

Appendix D

A. Saturation depths measured with piezometers at site 2.

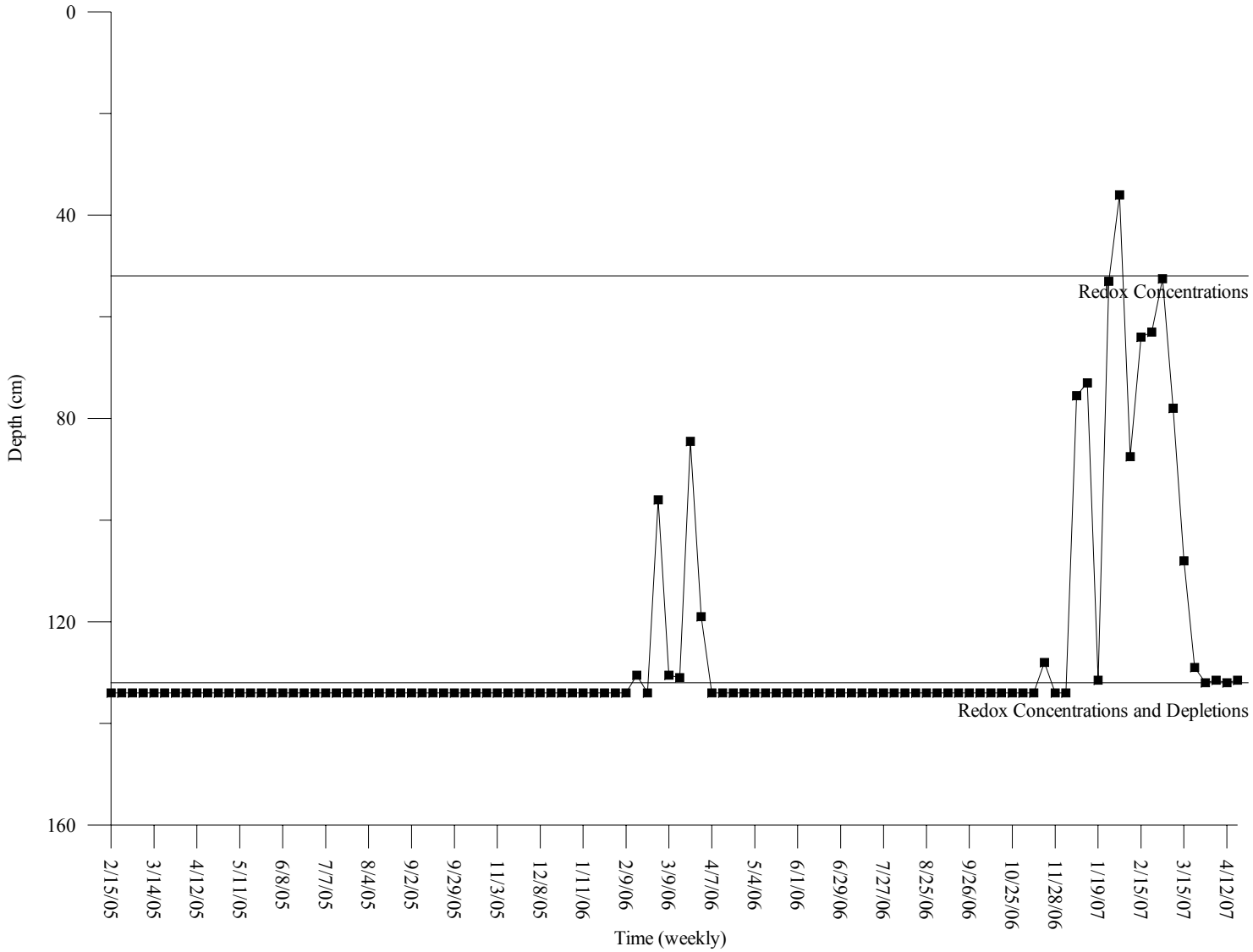

C. Saturation depths measured with piezometers at site 3.

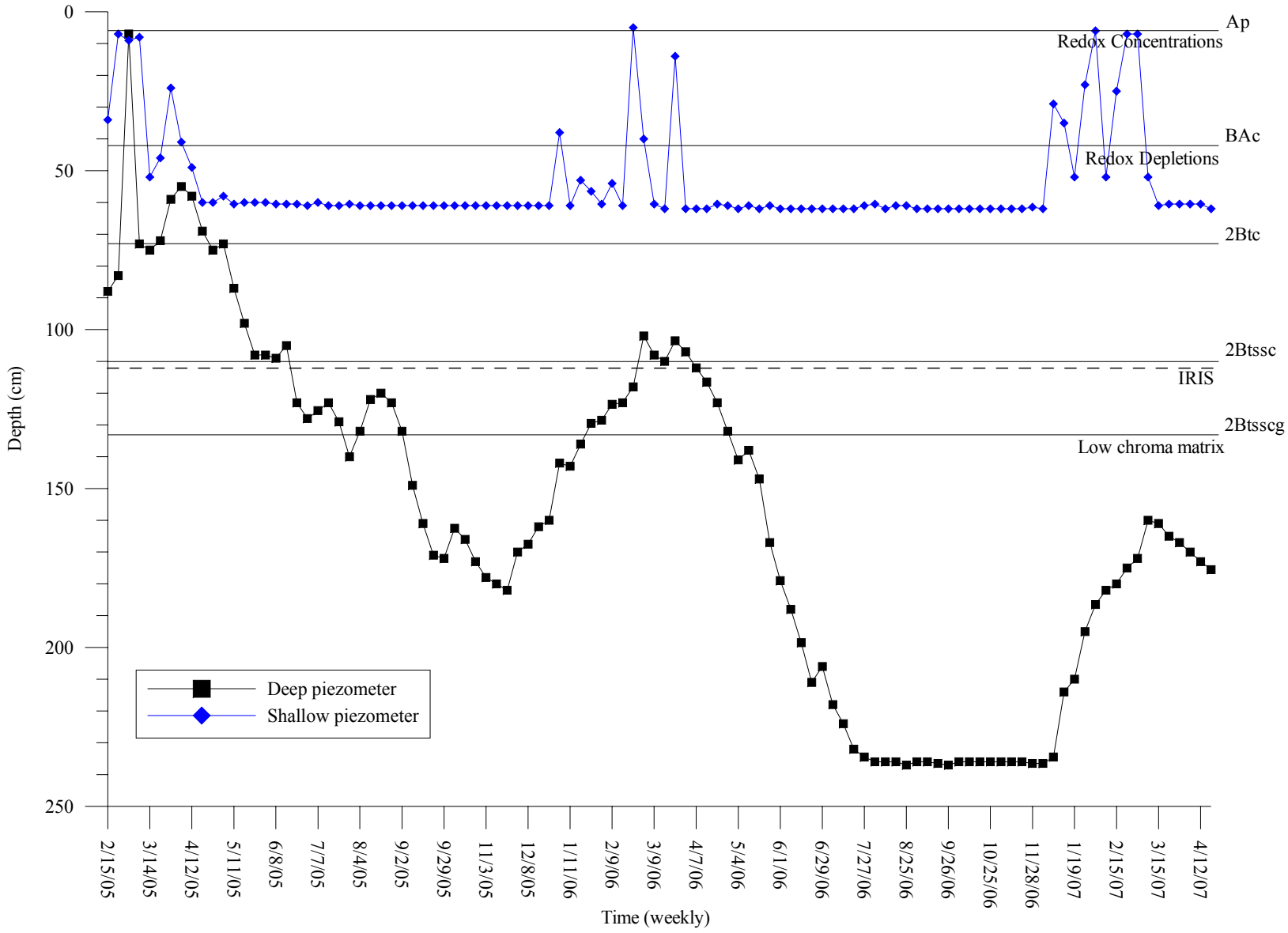

D. Saturation depths measured with piezometers at site 4.

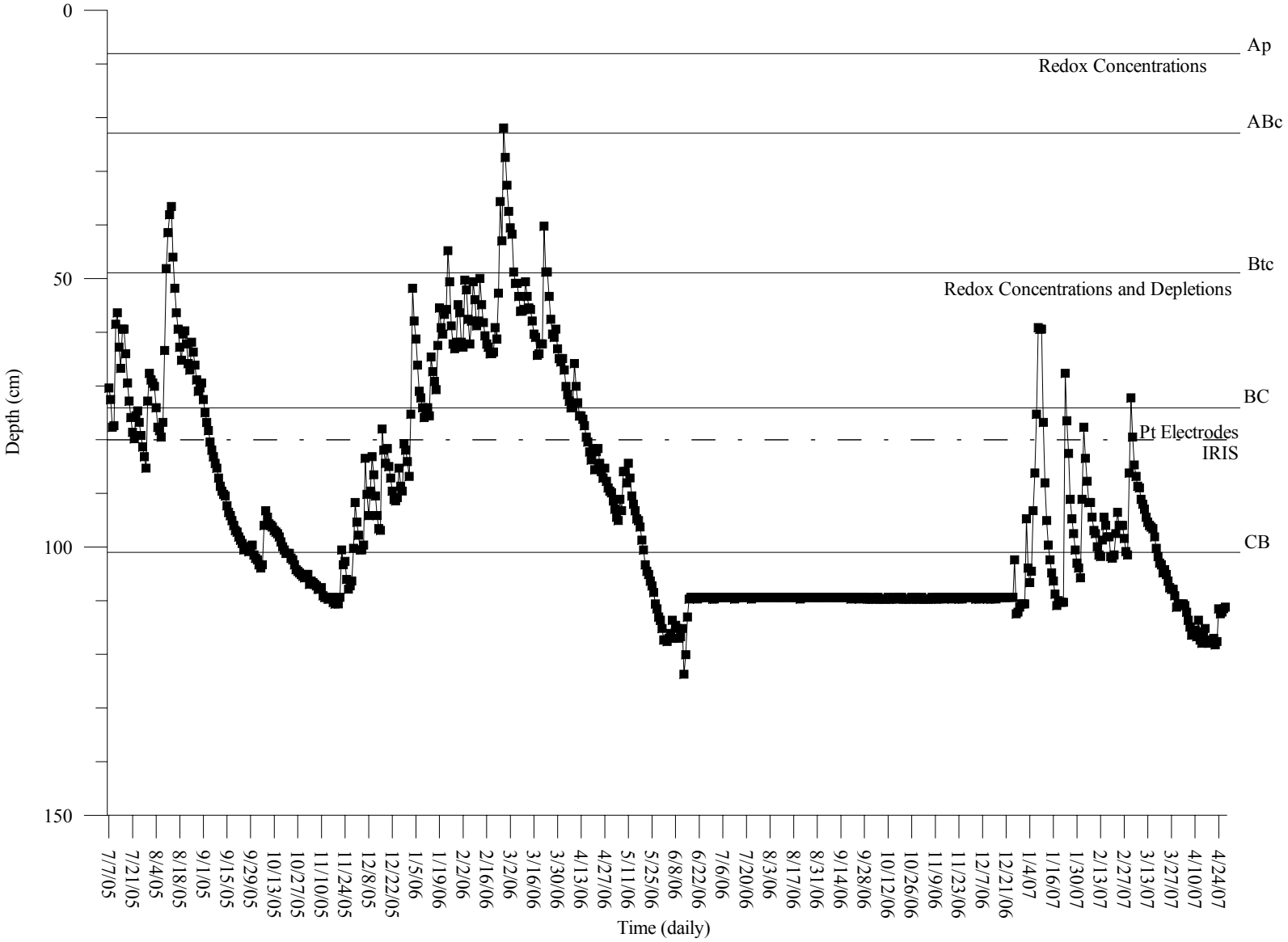

E. Saturation depths measured with piezometers at site 5.

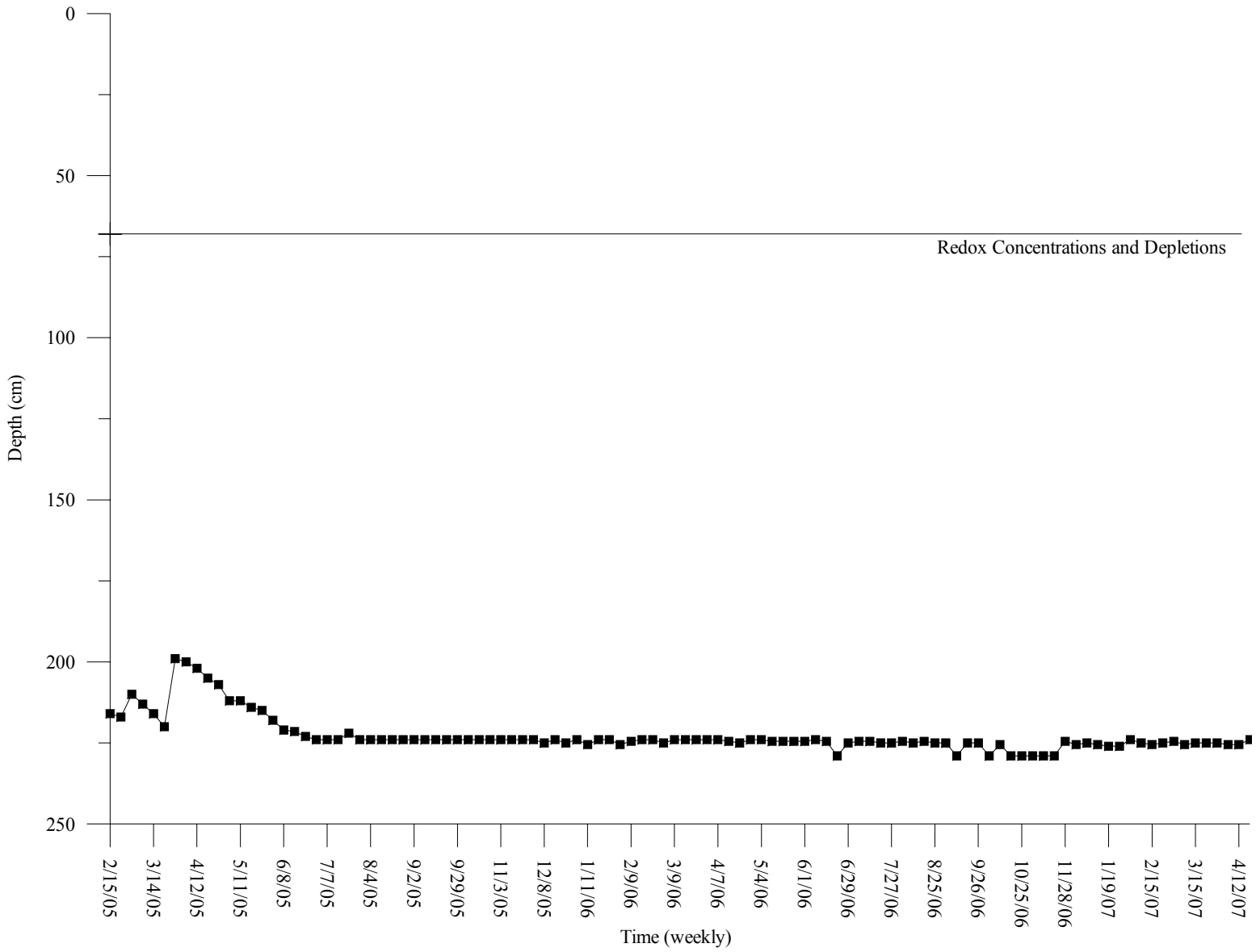

F. Saturation depths measured with piezometers at site 6.

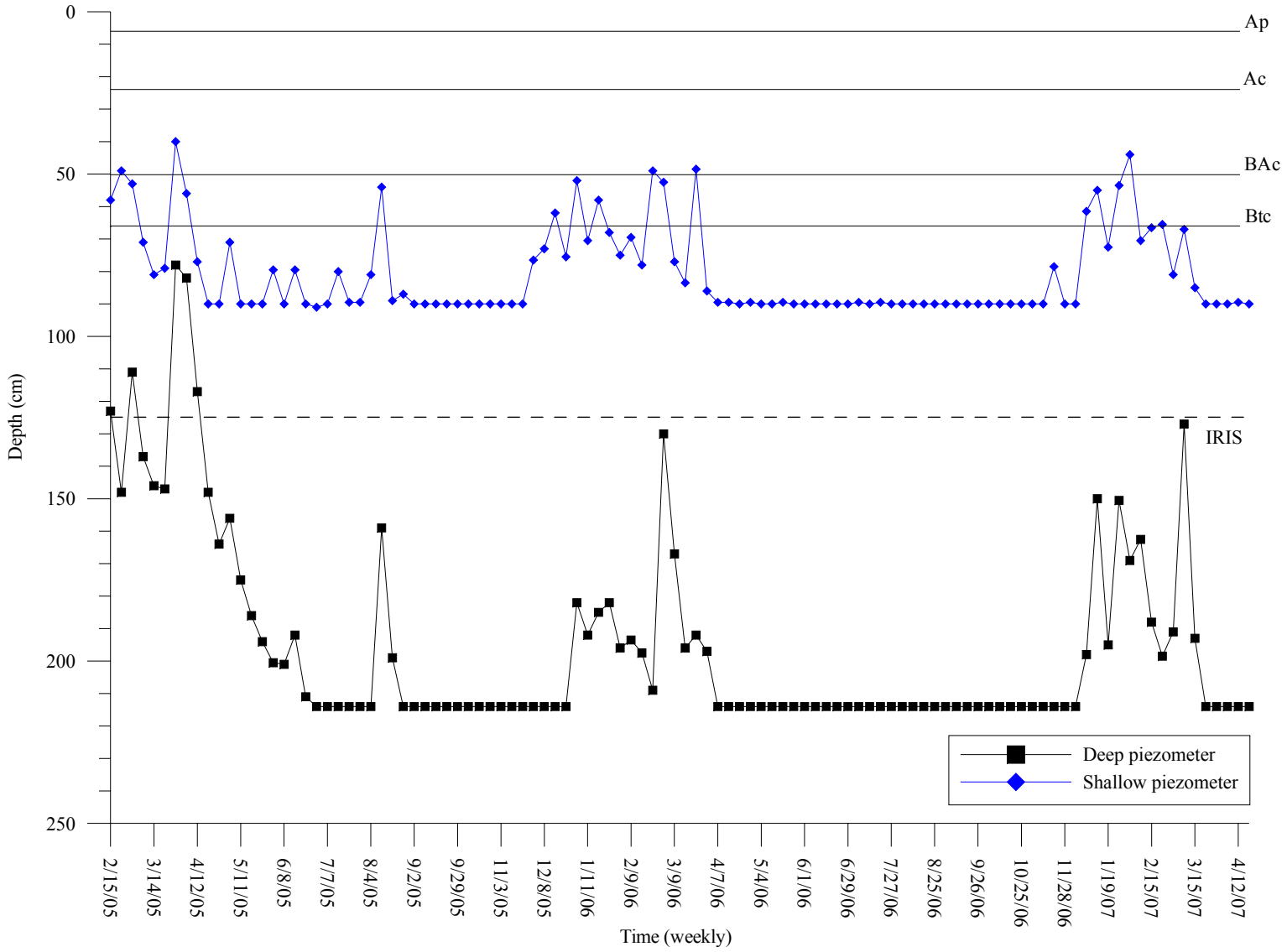

G. Saturation depths measured with piezometers at site 7.

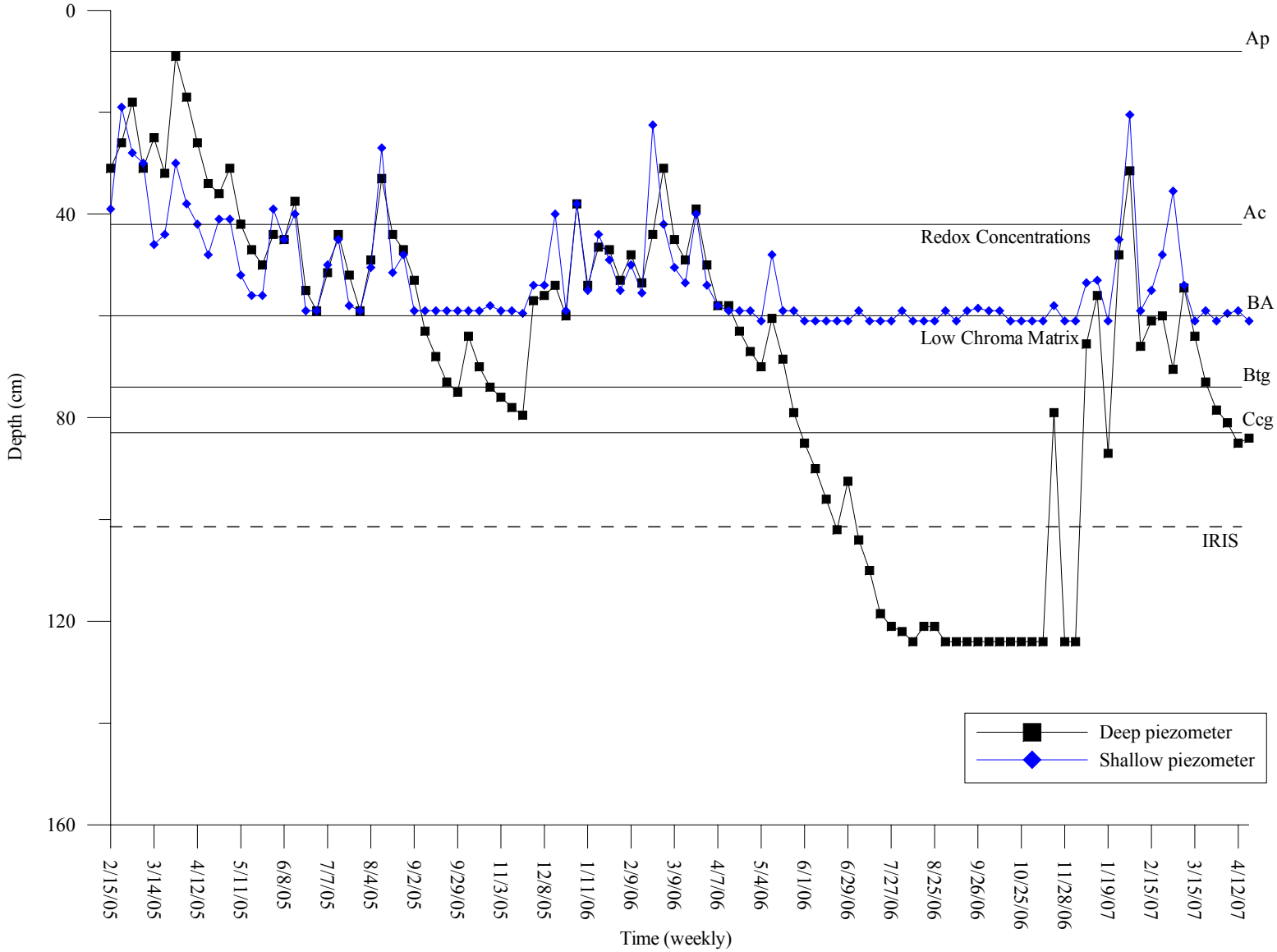

H. Saturation depths measured with piezometers at site 8.

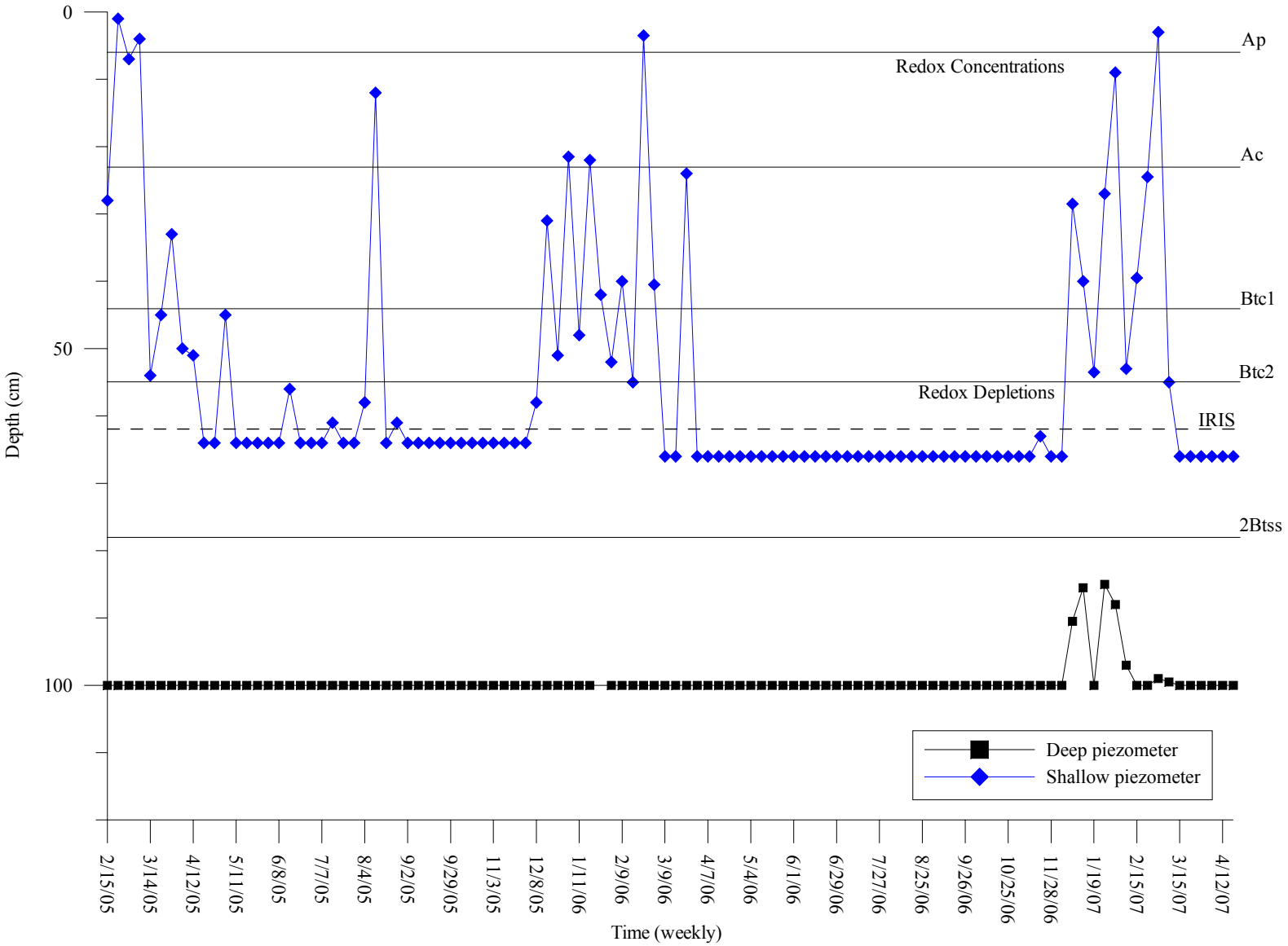

I. Saturation depths measured with piezometers at site 9.

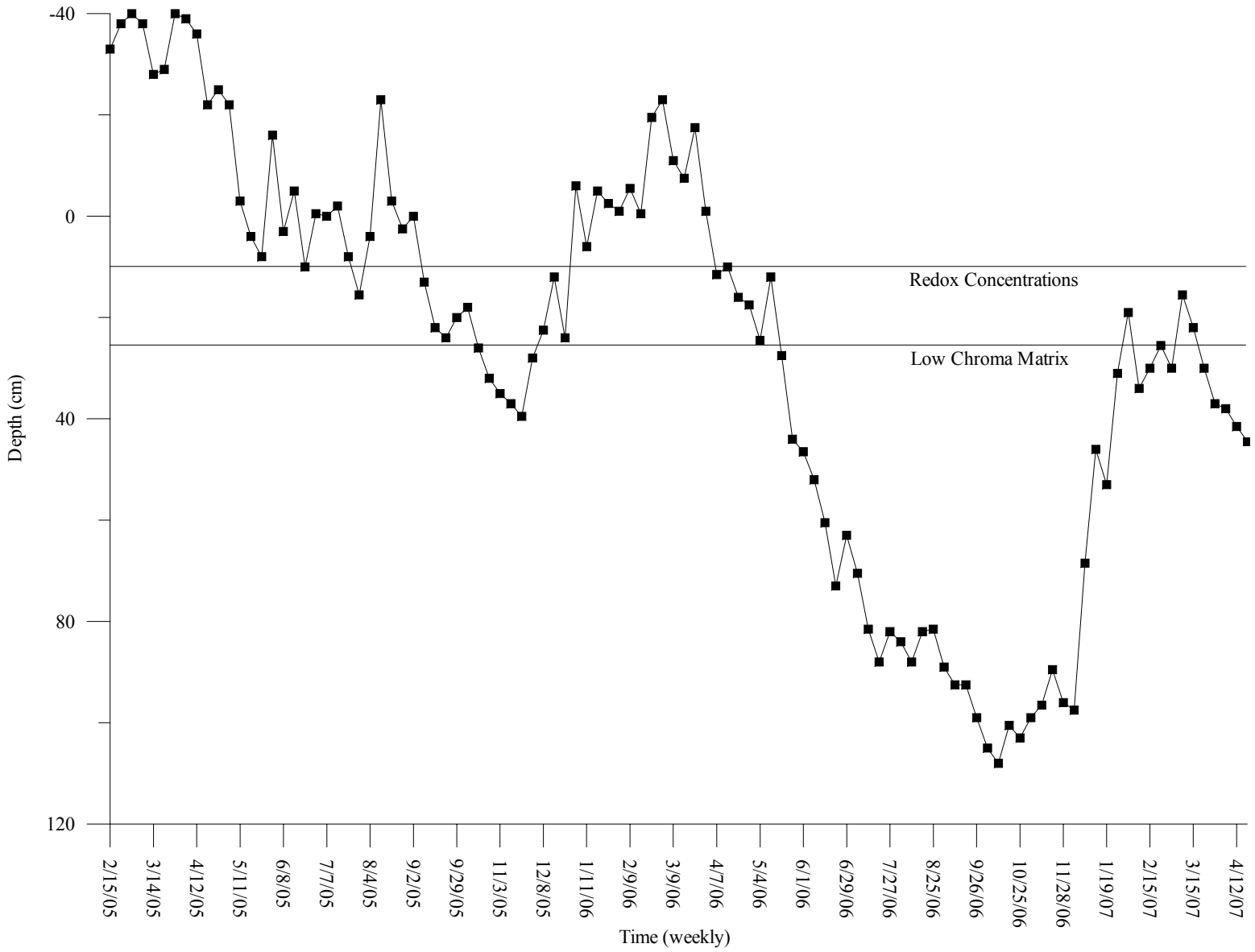

J. Saturation depths measured with piezometers at site 10.

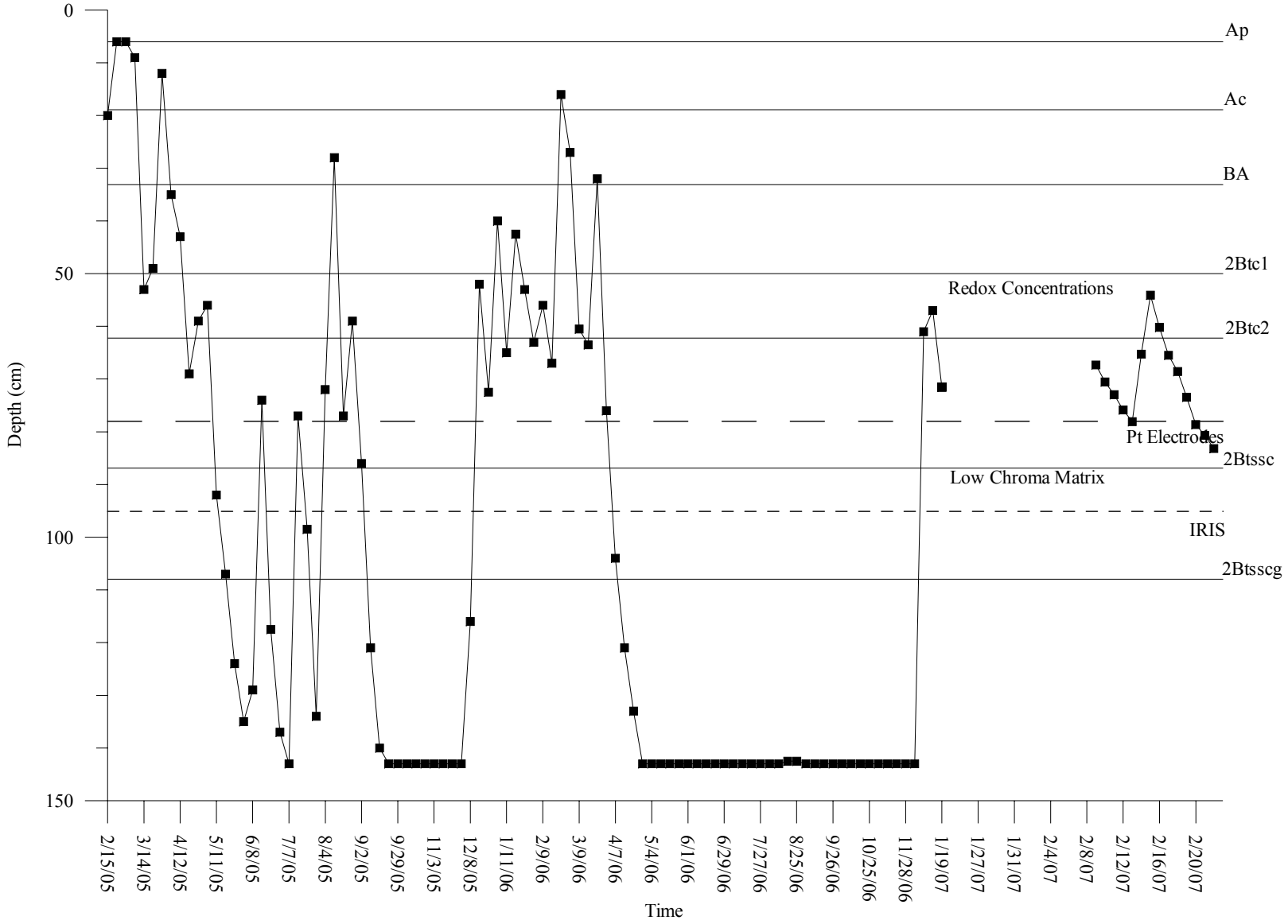

K. Saturation depths measured with piezometers at site 11.

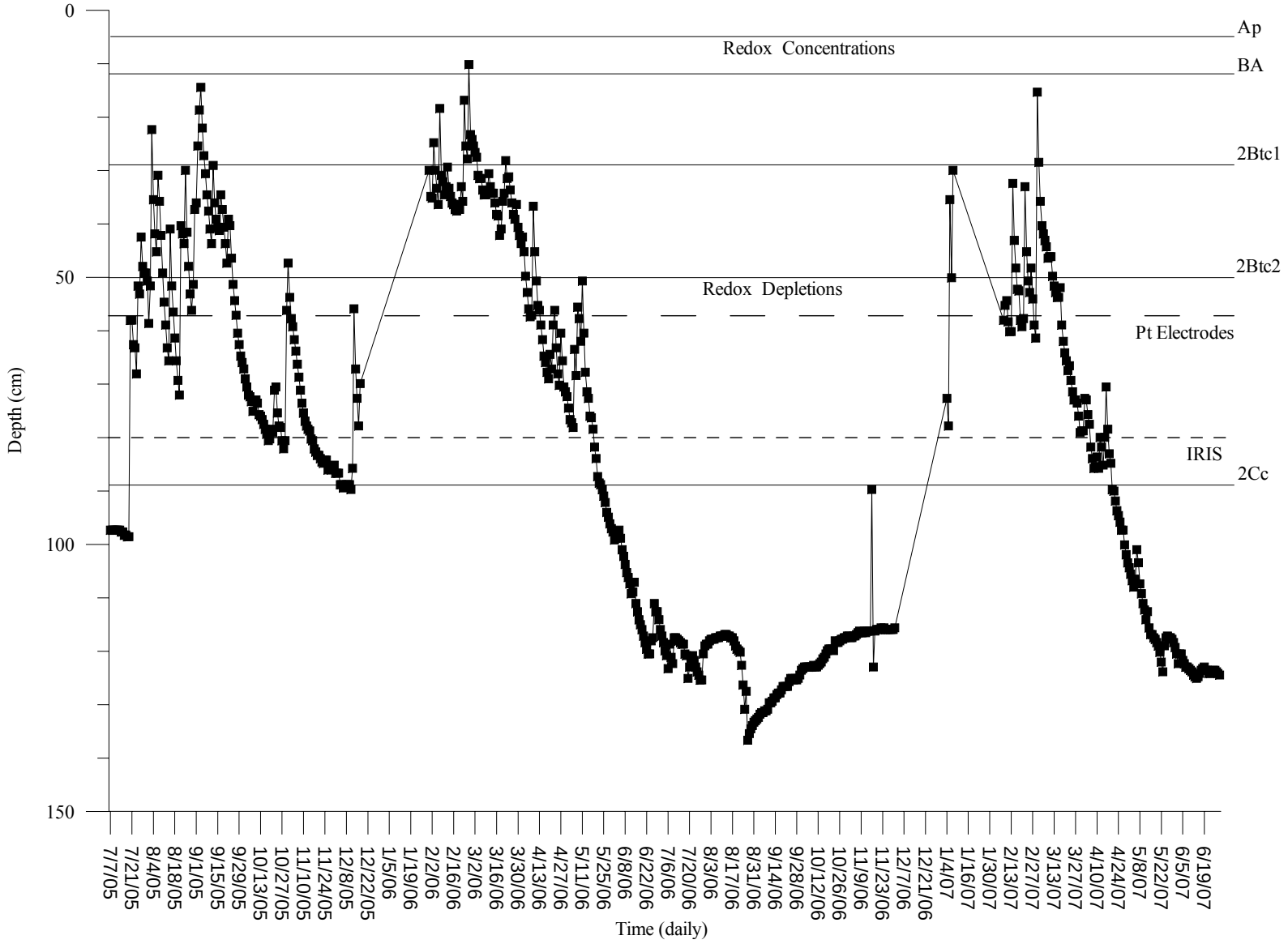

L. Saturation depths measured with piezometers at site 12.